

INVESTIGATION ON THE OCCURRENCE OF
TLES ASSOCIATED POSITIVE CLOUD TO
GROUND (+CG) LIGHTNING IN UMP PEKAN



CHAN HWEE GEEM

UMP

MASTER OF SCIENCE

UNIVERSITI MALAYSIA PAHANG

UNIVERSITI MALAYSIA PAHANG

DECLARATION OF THESIS AND COPYRIGHT

Author's Full Name : CHAN HWEE GEEM

Date of Birth : 01/04/1990

Title : INVESTIGATION ON THE OCCURRENCE OF TLES

ASSOCIATED POSITIVE CLOUD TO GROUND (+CG)

LIGHTNING IN UMP PEKAN

Academic Session : SEM I 2018/2019

I declare that this thesis is classified as:

- CONFIDENTIAL (Contains confidential information under the Official Secret Act 1997)*
- RESTRICTED (Contains restricted information as specified by the organization where research was done)*
- OPEN ACCESS I agree that my thesis to be published as online open access (Full Text)

I acknowledge that Universiti Malaysia Pahang reserves the following rights:

1. The Thesis is the Property of Universiti Malaysia Pahang
2. The Library of Universiti Malaysia Pahang has the right to make copies of the thesis for the purpose of research only.
3. The Library has the right to make copies of the thesis for academic exchange.

Certified by:

(Student's Signature)

(Supervisor's Signature)

900401-01-6710
New IC/Passport Number
Date: 11 January 2019

DR. AMIR IZZANI BIN MOHAMED
Name of Supervisor
Date: 11 January 2019

NOTE : * If the thesis is CONFIDENTIAL or RESTRICTED, please attach a thesis declaration letter.

SUPERVISOR'S DECLARATION

We hereby declare that we have checked this thesis and in our opinion, this thesis is adequate in terms of scope and quality for the award of the degree of Master of Science.

(Supervisor's Signature)

Full Name : DR. AMIR IZZANI BIN MOHAMED

Position : SENIOR LECTURER

Date : 11 JANUARY 2019

(Co-supervisor's Signature)

Full Name : DR. NURUL HAZLINA BINTI NOORDIN

Position : SENIOR LECTURER

Date : 11 JANUARY 2019

STUDENT'S DECLARATION

I hereby declare that the work in this thesis is based on my original work except for quotations and citations which have been duly acknowledged. I also declare that it has not been previously or concurrently submitted for any other degree at Universiti Malaysia Pahang or any other institutions.

(Student's Signature)

Full Name : CHAN HWEE GEEM

ID Number : MEE14005

Date : 11 JANUARY 2019



UMP

INVESTIGATION ON THE OCCURRENCE OF TLES ASSOCIATED
POSITIVE CLOUD TO GROUND (+VE) LIGHTNING
IN UMP PEKAN

CHAN HWEE GEEM

Thesis submitted in fulfillment of the requirements
for the award of the degree of
Master of Science

UIMP
Faculty of Electrical & Electronics Engineering

UNIVERSITI MALAYSIA PAHANG

JANUARY 2019

ACKNOWLEDGEMENTS

Praise to God, the Most Gracious Sakyamuni Buddha,

Who has created the creatures with life, mankind with knowledge, and ability to carry on tasks. Being the greatest creation of God, author still has to depend on others for guidance and teaching in order to have a better understanding of the knowledge. During the research, it is received lot of help, co-operation and encouragement that need to be duly acknowledged. First and foremost wishes to express gratitude and thank to supervisor, Dr. Amir Izzani Bin Mohamed. His guidance and advice along the period of research is peerless. Dr. inspired researcher to work in this project. Dr's dedication, guidance, and willingness to motivate researcher has contributed tremendously to the project.

Acknowledgements are due to UMP Pekan Campus members for the help, advise, guidance and opinion given during the whole study period. Gratitude is also extended to the technical staff of the Building laboratory at Faculty of Electrical and Electronic Engineering (FKEE). Appreciation is extended to the FKEE, for providing equipment to use in research during the period of study at the university and also providing financial on components electrical. An honourable mention goes to her parents and relatives for their countless blessing which have always and forever will be a source of inspiration in achieving success.

Finally, a very special gratitude is reserved for the researcher's friends, for their understanding, helping, and support towards the accomplishment of the study. To them, this thesis earnestly dedicated.



UMP

ABSTRAK

Kilat merupakan suatu fenomena yang berlaku di atas kawasan atmosfera. Kejadian cahaya transien merupakan satu jenis kejadian kilat yang melebihi kelajuan kilauan kilat dalam suatu kejadian rebut petir. Ia adalah kejadian yang sukar dilihat dan berlaku dalam masa yang singkat. Maka, suatu alat foto dengan kadar bingkai tinggi adalah diperlukan. Projek ini mengkaji tentang kebarangkalian berlakunya kejadian transien cahaya di sekelilingi Universiti Malaysia Pahang (UMP) Kampus Pekan dengan menggunakan alat yang ringkas dan sesuai untuk mengesan kejadian ini. Fenomena cahaya transien terbahagi kepada beberapa jenis seperti “*Elves*”, “*Sprites*”, “*Halos*”, “*Blue Jets*”, dan “*Gigantic Jets*”. Kejadian ini dikesan dengan menggunakan satu kamera monokrom dalam jejari 100 km dari UMP Pekan berserta ketinggian 20 km agar kejadian tersebut dapat direkod dengan jelas dan ciri-cirinya dapat dianalisa secara kategori dengan video dan bingkai yang direkod. *Sprites* adalah keruntuhan dielektrik dalam lingkungan ketinggian 20 km hingga 95 km dan sentiasa berlaku disebabkan oleh berlakunya kilat positif dari awan ke tanah (+CG). Setiap proses penjejakan menetapkan kebarangkalian berlakunya TLEs di sekelilingi UMP Pekan. Keputusan dihadkan dalam jejari 100 km dari kawasan UMP Pekan sahaja. Daripada kajian ini, transien cahaya susah dapat dikesan. Numun begitu, satu jenis kilat baru dapat dijumpa. Kilat baru adalah serupa dengan ciri-ciri *Carrot Sprite* selepas semua ciri-cirinya dibandingkan dengan Jabatan Meteorologi Malaysia (MMD). Kesimpulannya, transien cahaya dapat dijumpa di sekelilingi UMP Kampus Pekan terutamanya *Sprites*.

The logo of Universiti Malaysia Pahang (UMP) is a large, stylized letter 'V' shape. The left side of the 'V' is light blue, the right side is light purple, and the bottom point is a darker blue. The letters 'UMP' are written in white, bold, sans-serif font across the center of the 'V'.

ABSTRACT

Lightning is one of the phenomena that occur around the area above the atmosphere. Transient Luminous Events (TLEs) is a type of lightning events which take place above the flash of lightning in a thunderstorm cloud. It is a very fast event that is hardly seen and happens in a very short period of time. So, a high frame-rate capturing device is required to record it. This project studies about the possibility of TLEs occurrences around Universiti Malaysia Pahang (UMP) Pekan campus area by selecting a simple and suitable device to detect the event. There are various types of transient luminous such as Elves, Sprites, Halos, Blue Jets, and Gigantic Jets. By setting a distance radius of 100 km from UMP Pekan with a minimum altitude height of 20 km, the event was traced using a monochrome camera. This allowed the event to be clearly recorded and analysed, namely by the characteristic of categories captured with the video and frame. Sprites are dielectric breakdown at an approximate altitude of 20 km to 95 km and are normally triggered by +CG lightning events. Each of the tracking process results in the possibility of TLE occurrences in the atmosphere of UMP Pekan campus. This result was limited to only a radius of 100 km away from UMP Pekan campus. The study revealed that, TLEs cannot be easily captured. However, an unknown discharge lightning event was found. The unknown event detected was possibly a Carrot Sprite upon comparing all the data obtained with those available in Malaysian Meteorological Department (MMD). Hence, TLEs can be observed around UMP Pekan campus, especially Sprites.

The logo of Universiti Malaysia Pahang (UMP) is a large, stylized letter 'V' shape. The left side of the 'V' is light blue, the right side is light purple, and the bottom point is a darker shade of purple. The letters 'UMP' are written in white, bold, sans-serif font across the center of the 'V'.

TABLE OF CONTENT

DECLARATION	
TITLE PAGE	
ACKNOWLEDGEMENTS	ii
ABSTRAK	iii
ABSTRACT	iv
TABLE OF CONTENT	v
LIST OF TABLES	viii
LIST OF FIGURES	ix
LIST OF SYMBOLS	xii
LIST OF ABBREVIATIONS	xiii
CHAPTER 1 INTRODUCTION	1
1.1 Introduction	1
1.2 Background Study	1
1.3 Problem Statement	3
1.4 Objectives of the Study	5
1.5 Project Scope	5
1.6 Definition of Terms	5
1.7 Outline of Thesis	6
1.8 Summary	6
CHAPTER 2 LITERATURE REVIEW	7
2.1 Introduction	7
2.2 Lightning Generation	8

2.3	Return Stroke	8
2.4	Types of Lightning	9
2.4.1	Negative Cloud to Ground (-CG) Lightning	10
2.4.2	Positive Cloud to Ground (+CG) Lightning	11
2.5	Types of TLEs	12
2.5.1	Sprites	13
2.5.2	Halos	14
2.5.3	Elves	15
2.5.4	Gigantic Jets	16
2.5.5	Blue Jets	17
2.6	Camera	18
2.6.1	Waterc Ultimate 902H2 Specification	19
2.7	Frames Rate	20
2.8	Field of View (FOV)	20
2.9	Summary	21
CHAPTER 3 METHODOLOGY		22
3.1	Introduction	22
3.2	Data Collection	24
3.2.1	Malaysian Meteorological Department (MMD)	24
3.3	Image Capture	30
3.3.1	Camera Lens	32
3.3.2	Digital Video Recorder (DVR)	32
3.3.3	Video Record Control Panel	34
3.3.4	Frames Extraction	36
3.3.5	Frames Rate Calculation	40

3.3.6	Angle of View (AOV) Calculation	40
3.3.7	Camera Setting Calculation (Degree)	41
3.4	Summary	43
CHAPTER 4 RESULTS AND DISCUSSION		44
4.1	Introduction	44
4.2	2015 Lightning Data Analysis from MMD	44
4.2.1	Occurrence of +CG Lightning and –CG Lightning from MMD	45
4.2.2	Monthly +CG Lightning Events	45
4.3	Lightning Map Analysis for 2015	49
4.3.1	Day and Night Lightning Map for 2015	50
4.3.2	2015 Lightning Map Obtained from MMD Data	57
4.4	Image Capture Analysis	59
4.4.1	Unknown Discharge Lightning Event	59
4.4.2	Unknown Discharge Lightning Event Data Analysis	62
4.4.3	Unknown Discharge Lightning Calculation	63
4.4.4	Horizon Distance	68
4.5	Summary	70
CHAPTER 5 CONCLUSION AND RECOMMENDATION		71
5.1	Conclusion	71
5.2	Recommendation	72
REFERENCES		73
APPENDIX A LIST OF PUBLICATION		79
APPENDIX B TECHNICAL DATA SHEET		80

LIST OF TABLES

Table 3.1	Components used during the research.	31
Table 3.2	Comparison of DVR.	34
Table 3.3	Initial condition for FOV calculation.	40
Table 3.4	Angle of view with different lenses.	40
Table 3.5	Camera setting's calculated result.	42
Table 4.1	Percentage of +CG lightning and -CG lightning for the year 2015.	45
Table 4.2	Percentage of +CG lightning for day time and night-time in Pekan for 2015.	48
Table 4.3	Lightning event information.	62
Table 4.4	Initial condition for image calculation.	63
Table 4.5	Calculated horizontal and vertical size in cm.	66
Table 4.6	Calculated size of the unknown discharge lightning.	68

The logo for UIMP (Universiti Malaysia Perlis) is a large, stylized shield shape. It is divided into four quadrants by a white cross. The top-left and bottom-right quadrants are light blue, while the top-right and bottom-left quadrants are light purple. The letters 'UIMP' are written in white, bold, sans-serif font across the center of the shield.

UIMP

LIST OF FIGURES

Figure 1.1	Different TLEs occur below ionosphere.	3
Figure 2.1	(a) Upward-moving positively charged leaders; (b) Upward-moving negatively charged leaders.	10
Figure 2.2	(a) Inter-cloud lightning; (b) Intra-cloud lightning.	10
Figure 2.3	Downward-moving negatively charged leaders.	11
Figure 2.4	Downward-moving positively charged leaders.	12
Figure 2.5	Global occurrence of most TLEs: (a) Sprite and Gigantic Jets, (b) Elves, (c) Halos.	13
Figure 2.6	Different types of Sprites: (a) Carrot Sprits, (b) Column Sprite, (c) Jellyfish Sprite	14
Figure 2.7	Halos associated with Sprites.	15
Figure 2.8	Elves.	16
Figure 2.9	Gigantic Jets.	17
Figure 2.10	Blue Jets.	18
Figure 2.11	Watec Ultimate 902H2 camera.	19
Figure 3.1	Flow diagram of the research tasks.	23
Figure 3.2	Process of data collection.	24
Figure 3.3	Localisation with radius 100 km.	25
Figure 3.4	Covered area within 100 km radius.	26
Figure 3.5	Microsoft Excel sort function.	27
Figure 3.6	Lightning map for 100 km radius.	27
Figure 3.7	Origin Lab data booklet.	28
Figure 3.8	Column properties.	29
Figure 3.9	PolarXrYTheta type.	29
Figure 3.10	A block diagram of image captured.	30
Figure 3.11	(a) Camera setup panel; (b) Camera locate beside window.	31
Figure 3.12	Explanation to capture a Sprite.	31
Figure 3.13	Two different of lens: (a) Nikon lens 50 mm focal length with aperture f1.4; (b) Brinno Lens 24 mm – 70 mm focal length with aperture f 1.4.	32
Figure 3.14	Three types of DVRs (a) HD USB 2.0 DVR; (b) Jovision (JVS C300Q DVR); (c) UU-DVR.	33
Figure 3.15	Recording control panel.	35
Figure 3.16	System setting.	35
Figure 3.17	Video setting.	36

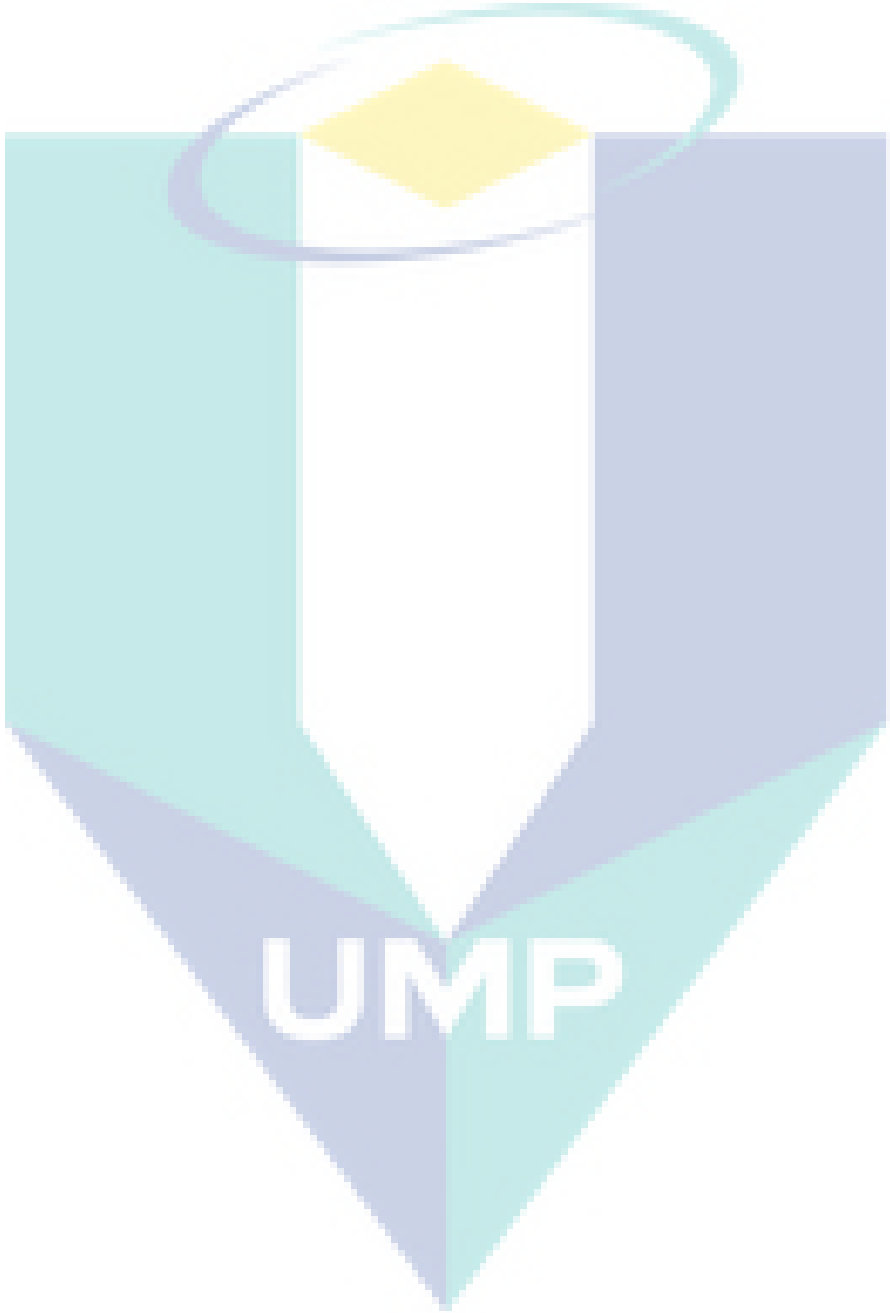
Figure 3.18	Channel 1 was enlarged by double-clicking the channel screen.	36
Figure 3.19	Steps to invoke “Frame Extraction”.	38
Figure 3.20	Format selection of image frames extracted.	38
Figure 3.21	Method selection of image frames extracted.	39
Figure 3.22	“Frame Extraction” setting and control panel.	39
Figure 3.23	FOV coverage of Nikon lens.	41
Figure 3.24	FOV coverage of Brinno lens.	41
Figure 3.25	Camera condition.	41
Figure 3.26	The setting of camera shooting upward at 11 °	42
Figure 4.1	Number of +CG lightning for each month in 2015.	46
Figure 4.2	Comparison of total lightning events and rainfall quantity in Pekan in Year 2015.	47
Figure 4.3	Percentages of +CG lightning in the day and night times.	49
Figure 4.4	Vastu directions.	49
Figure 4.5	Day and night lightning map for January.	50
Figure 4.6	Day and night lightning map for February.	51
Figure 4.7	Day and night lightning map for March.	51
Figure 4.8	Day and night lightning map for April.	52
Figure 4.9	Day and night lightning map for May.	53
Figure 4.10	Day and night lightning map for June.	53
Figure 4.11	Day and night lightning map for July.	54
Figure 4.12	Day and night lightning map for August.	54
Figure 4.13	Day and night lightning map for September.	55
Figure 4.14	Day and night lightning map for October.	56
Figure 4.15	Day and night lightning map for November.	56
Figure 4.16	Day and night lightning map for December.	57
Figure 4.17	Daytime lightning map for 2015.	58
Figure 4.18	Night-time lightning map for 2015.	59
Figure 4.19	An unknown discharge activity event observed on 2 nd July 2015 at 21:19 pm.	61
Figure 4.20	Location of unknown discharge lightning event in the lightning map.	61
Figure 4.21	Illustration of the camera setup.	64
Figure 4.22	Camera sensor size.	64
Figure 4.23	Actual object size displayed on the monitor screen with distance, d_2 from camera.	65

Figure 4.24 Demonstrated location of the unknown discharge lightning. 67

Figure 4.25 Demonstrated camera lens and the actual field. 67

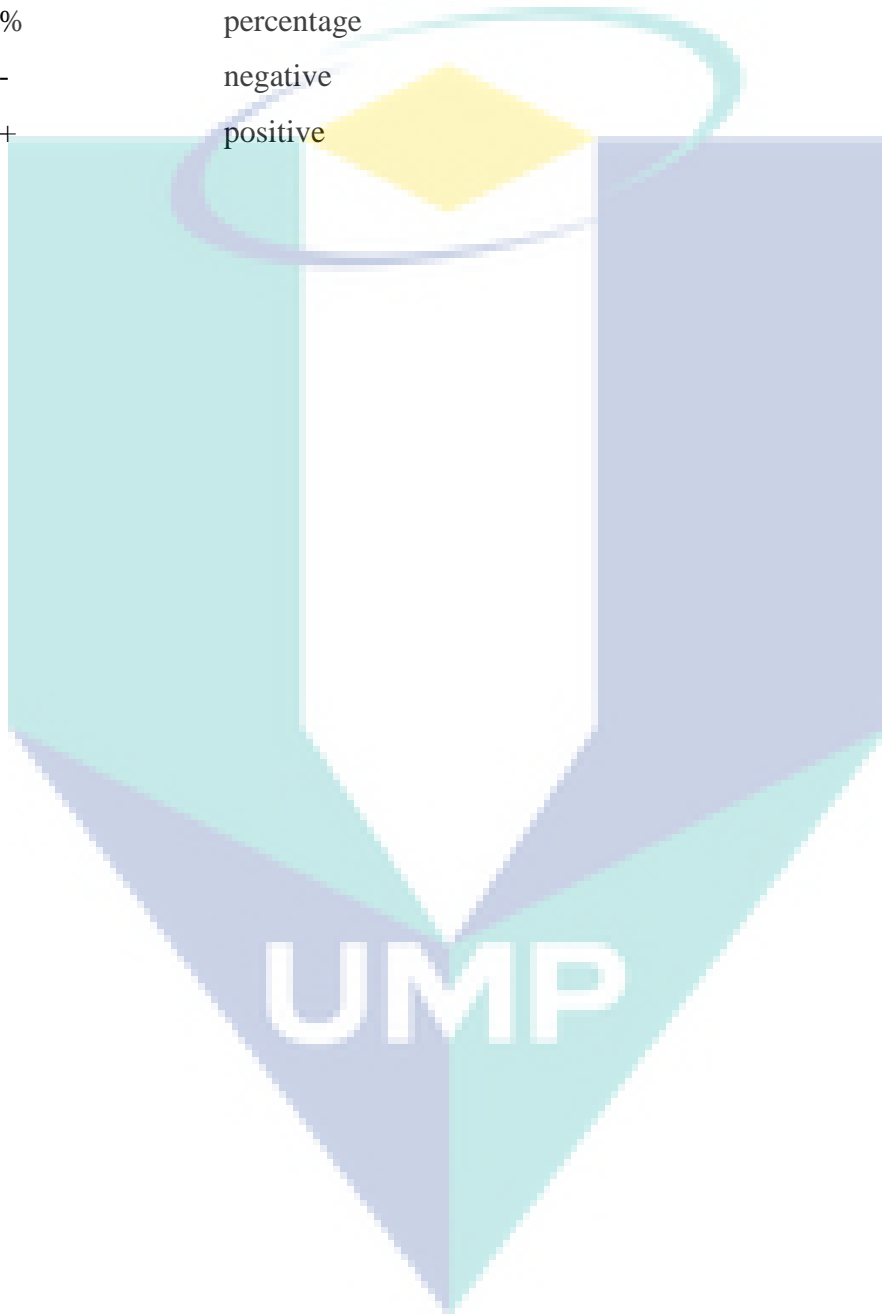
Figure 4.26 Actual view of the +CG lightning event from the PC monitor. 68

Figure 4.27 Condition of the unknown discharge lightning on the horizon distance. 69




LIST OF SYMBOLS

α	alpha
β	beta
$^{\circ}$	degree
%	percentage
-	negative
+	positive

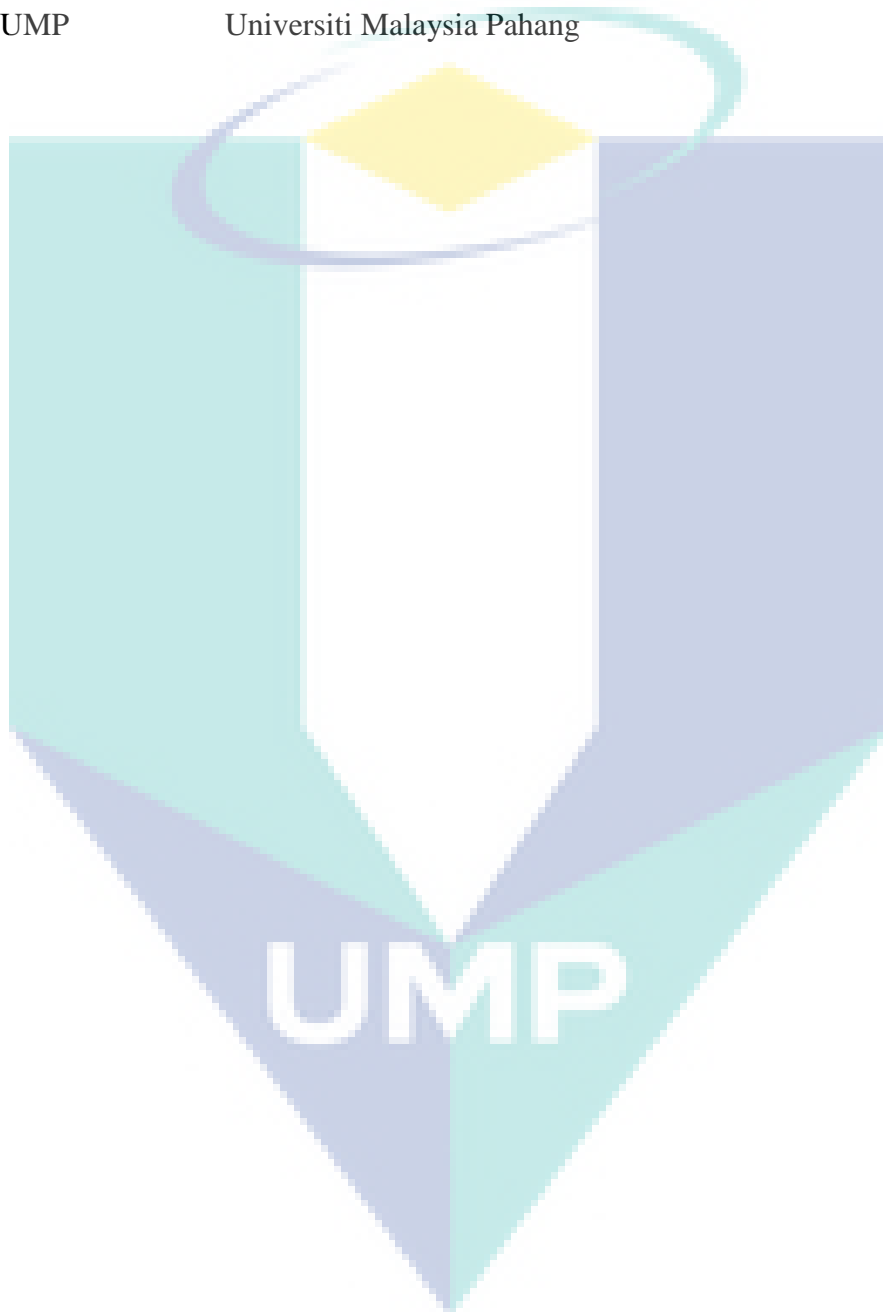


LIST OF ABBREVIATIONS



AOV	Angle of view
CG	Cloud to Ground
-CG	Negative Cloud to Ground
+CG	Positive Cloud to Ground
-GC	Negative Ground to Cloud
+GC	Positive Ground to Cloud
CC	Cloud to Cloud
cm	centimeters
CCD	Charge-coupled device
CCIR	Committee Consultatif International Radiotelecommunique
DSLR	Digital single-lens reflex
DVR	Digital video recorder
E-field	Electromagnetic field
EIA	Electronics Industry Association
ELF	Extremely Low Frequency
FKEE	Faculty of Electrical and Electronics Engineering
FOV	Field of view
fps	Frame per second
GEC	Global Electric Circuit
H-field	Magnetic field
IC	Intra-cloud
IR	Infrared
kA	kilo amperes
km	kilometers
LLTV	Low-light level television
m	meters
mm	millimeters
ms	milli second
MW	Mega Watt
MMD	Malaysian Meteorological Department
nm	nanometers

PAL	Phase Alternation by Line
PC	Personal Computer
s	seconds
TLEs	Transient Luminous Events
UK	United Kingdom
UMP	Universiti Malaysia Pahang



CHAPTER 1

INTRODUCTION

1.1 Introduction

Recently, research on Transient Luminous Events (TLEs) has attracted much interest around the world. It began in 1989 and the findings can be considered as new in studies related to the field of lightning over the last 27 years (Franz et al., 1990). In this chapter, the background of study, research motivation, objectives, significance of study, project scope, definition of terms, and intro to the project flow related to the study are discussed.

1.2 Background Study

Global Electric Circuit (GEC) is described as an active system in the atmosphere. The research in this area is numerous and mostly focus on theoretical and experimental investigation into the phenomena. Scientists have long been interested to discover numerous parts of the GEC although the system changes over time and space (Singh et al., 2014). Lightning is one of the contributors to the GEC system. It is one of the natural phenomena found on Earth and occurs between a thundercloud and the ground. TLEs are also active during the thunderstorm (Ebert, 2012). At the beginning, Franz, Nemzek, and Winckler (1990) intended to carry out research on lightning activities. However, they recorded a unique lightning activity which occurred in the upper atmosphere. The lightning recorded by Franz et al. (1990) at the upper atmosphere was named Sprites. In the following years, there has been a growing research on TLEs by William, Rukov, Uman, Pasko, Lynos, Yair, Wescott, and other researchers, as stated in M. Hayakawa, Y. Hobara, and T. Suzuki

(2012). Serge Soula et al. (2009) found that +CG lightning has the ability to trigger the happening of TLEs, especially Sprites.

Lightning does not only occur in the lower atmosphere but also on the upper atmosphere which is located at the altitude of 40 km to 100 km above the earth's surface (Luque and Ebert, 2010). TLEs are flashes of light which occur at the upper atmosphere or in the D region (60 km to 100 km) of the ionosphere. TLEs occur when reaction in excited gas molecules results in electrical breakdown.

Some of the TLEs occur at the lower region of the ionosphere area which is located at the altitude of 80 km from earth's surface while some of them are located at the altitude of approximately 100 km above ground (Passas et al., 2014). The types of TLEs include Sprites, Elves, Gigantic Jets, Blue Jets, and Halos. Figure 1.1 shows that there are several types of TLEs that can be observed. Each of them happen independently at a specific altitude in the upper atmosphere. This research however focuses on Sprites as to it can be triggered by +CG lightning (Lyons et al., 2003b).

The main purpose of this project is to investigate +CG lightning and to verify the occurrences of different TLEs within a height limit of 80 km. A monochrome camera was used to record data on the image captured. This is to observe their shape and time of occurrence. After that, a group of data for the image captured was obtained through the data recorded by Malaysian Meteorological Department (MMD) to determine the height of the event and the distance between the camera panel setup and the event. In addition, the size can be calculated by using specific equation. Further discussion on calculation is presented in Chapter 4. Lastly, the characteristics and localisation of the specific event are determined from the data recorded by MMD. Further discussion on methodology is presented in Chapter 3.

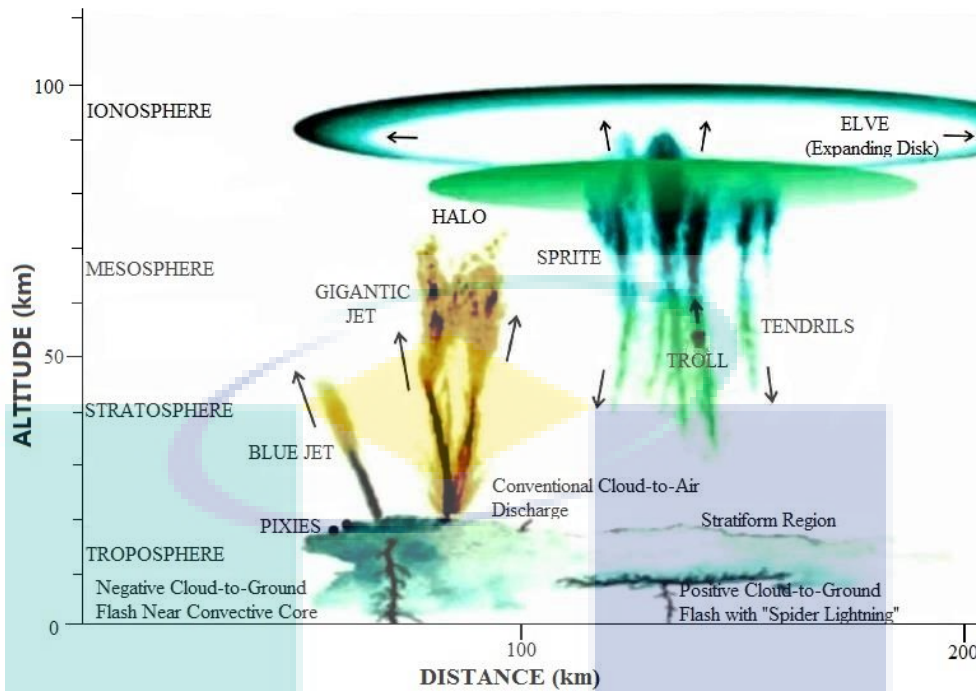


Figure 1.1 Different TLEs occur below ionosphere.

Source: Luque & Ebert (2010).

1.3 Problem Statement

Lightning refers to a natural phenomenon that happens frequently during thunderstorms (Williams, 1987); (Martin A. Uman, 1972). This phenomenon was described as an event of electrical discharge at the rate where the discharge process will deliver a large quantity of current and voltage. A large quantity of radio frequency made up of electromagnetic field (E-field and H-field) is emitted during lightning. TLEs are also known as a part of a lightning event that happened in the upper atmosphere where the electrical discharge is visible as colourful lightning strikes with a series of form.

In addition, lightning is categorized under visible light and its wavelength ranges from 400 nm to 700 nm which can be seen by the human eye easily. However, the wavelength for TLEs is 600 nm to 900 nm (Thomas Ashcraft, 2011). This, wavelength of TLEs falls under the Infrared (IR) range with a wavelength from 750 nm to 1 mm, hence, it is hardly visible to the human eye. Therefore, a low light condition monochrome camera is required to observe TLEs as it is capable to highlight the flashes of the light clearly.

The survey and observation on TLEs have progressed frequently in other countries since 1989, when the first Sprites is recorded (Franz et al., 1990). These studies classified TLEs by the differences of colours and stroke patterns. Sprites and Elves were commonly known TLEs in research studies. Yet, there are lesser specific characteristics that justify the occurrence patterns of Sprites and Elves. Observation results from the past decades are just merely event capturing and data analysis that required justification on the varying attributes of the findings obtained from the capture site.

In addition, the result by Dan Robinson (1995), Lyons et al. (2003), Serge Soula et al. (2009), and V. P. Pasko, Yair, and Kuo (2012) highlight that +CG triggers Sprites within a stratiform cloud region. According to Rocha, Diniz, Carvalho, and Filho (1999), Pettegrew, Market, Holle, and Demetriades (2003), and Arnone et al. (2008), most occurrence of +CG lightning take place during the winter season in northern countries such as Italy, US, UK, and Japan and southern countries such as Brazil. The winter month for northern countries starts from December to February while for southern countries from June until August. However, the four-season climate does not exist in Malaysia. Instead, Malaysia only experiences monsoon seasons such as the Southwest Monsoon season and Northeast Monsoon season. Hence, the occurrences of +CG lightning during these monsoon seasons make an interesting topic to be discovered.

National Lightning Safety Institute (NLSI) (1988) reported that Malaysia is ranked the third in having the most thunderstorms in the world. With the notion that TLEs are a part of the lightning event, there is a high possibility that TLEs do occur in Malaysian atmosphere based on the NLSI report. Thus, this studies seeks to observe +CG lightning and the possibility of TLEs occurrence in Malaysia.

Nevertheless, observation of TLEs requires a wide view to ensure that the capturing process can be done smoothly. The location of UMP Pekan campus fulfils the requirement of TLE image capturing event where the site is located near seashores. Therefore, the university can be considered as a suitable base station for TLEs image capturing. Besides, these observations also assist in validating the data collected by researchers from abroad who observes TLEs from satellite.

1.4 Objectives of the Study

The main objectives of this research are:

- i. To investigate the occurrences of positive cloud to ground (+CG) lightning from Malaysian Meteorological Department (MMD).
- ii. To investigate TLEs in UMP Pekan campus area in Pahang.

1.5 Project Scope

This project includes the following scope:

- i. The project was limited to the area within 100 km radius from UMP Pekan campus.
- ii. The occurrence of lightning is recorded at an altitude of 20 km above the earth's surface.
- iii. Frame rate is at 25 fps.

1.6 Definition of Terms

For the purpose of explanation, the main terms used in this study have been defined. The terms are the following:

Transient Luminous Events (TLEs). Refer to the lightning occurring at the upper atmospheres region such as Sprites, Elves, Halos, Blue Jets, and Gigantic Jets.

Positive Cloud to Ground (+CG) Lightning. Refers to milliseconds of flashes of light occurring at the upper part of a thundercloud which are positively charged and downward-moving to the ground.

Sprites. Refer to types of TLEs that are red in colour and shaped like a jellyfish, carrot, and column.

Frame Rate. Denotes the number of frames or images that are displayed per second throughout the video recording.

Frame per Second (fps). Expresses the unit of frame rate.

1.7 Outline of Thesis

This thesis consists of five chapters, organized as Chapter 1, Chapter 2, Chapter 3, Chapter 4, and Chapter 5 to discuss and conclude the research on +CG lightning and TLEs. The next chapter, Chapter 2 presents the background of the research as well as details and information on lightning, TLEs characteristics, and explanation of camera specification. Chapter 3 details on the methodology set up for image capturing and the method used to collect the data of lightning events recorded. Chapter 4 presents the result and discussion of the project. The collected data is compared with findings from other studies conducted in the same research field. The characteristics of +CG lightning and TLEs (Sprites) are discuss further in this chapter. Lastly, Chapter 5 presents the conclusions of the research.

1.8 Summary

Throughout this chapter, the basic information on the background and research motivation for the research was presented. Using this information, the research is done to validate the possibility of detecting TLEs in UMP Pekan with the appropriate techniques and equipment.



UMP

CHAPTER 2

LITERATURE REVIEW

2.1 Introduction

Lightning, a sudden powerful flow of electricity, is one of the natural phenomena that occur on earth. A lightning strike carries a current of 10 kA and a voltage of 100 million Volt (Stormwise, 2002). The discharge of lightning can travel between one cloud to another (Cloud to Cloud, CC), between a cloud and Earth's ground (Cloud to Ground, CG), or within a thundercloud (Intracloud, IC). According to Martin A. Uman (2008), when positive charge and negative charge in a thundercloud is equal to each other, a lightning flash occurs where the strikes happen when the flash hits an object on the ground.

There are numerous types and forms of lightning. Some popular terms used to classify it include ball lightning, black lightning, heat lightning, ribbon lightning, bead lightning, coloured lightning, cloud to air lightning, sheet lightning, stratospheric lightning, tubular lightning, silent lightning, meandering lightning, and TLEs. TLEs are described as short lived electrical breakdown phenomena. TLEs are broken down into many types as compared to other types of lightning such as Sprites, Elves, Gigantic Jets, Blue Jets, and Halos, as mentioned in Chapter 1. However, the current chapter focuses only on the descriptions of cloud to ground (CG) lightning and TLEs. A review of literature on lightning formation, the capability of the camera, and the function of all the components used in this project are further discussed, specifically, the function of monochrome camera, digital video recorder (DVR) card, and other related instrumentation for this research.

2.2 Lightning Generation

Typical lightning events are commonly visible to the human eye as the bolts strike from clouds to the earth surface. This instant flash event happens within a second or two before a thunderous sound is heard. In scientific terms, a lightning generation is a form of electrostatic discharge. There are three stages of lightning generation. The first stage is the separation of positive and negative charges within a cloud. A strong static charge builds depending on the strong updrafts in the cloud and causes the ice crystals inside the cloud rub against one another. Positively charged crystals then rise to the top causing the cloud top to build up a positive static charge while negatively charged crystals and hailstones drop to the middle and bottom layers of the cloud building up a negative static charge. The reduced production of ice crystals causes cumulonimbus cloud to fail in creating enough static electricity for the lightning action (Martin A. Uman, 2008).

The second stage is the build-up of positive charge on the ground below the clouds. The earth's ground is normally negatively charged. The negative charge at the bottom layers of cumulonimbus cloud pulls the positive charges from the ground to gather along the surface for a few miles around the storm when the thunderstorm passes over the ground. The charges then concentrate on vertical objects such as trees and tall buildings. This is why during a lightning storm, people are reminded to stay away from pole objects to prevent from being struck by lightning.

The third stage occur when the negative charges and positive charges are equalised and gather together, creating an electrical discharge as a result of which bolt occurs within the clouds or between the clouds and ground. Lastly, the lightning is formed. Thomas Ashcraft (2011) stated that TLEs form after certain lightning bolts are formed. The lightning strikes may result in very high currents that are able to cause death.

2.3 Return Stroke

A lightning flash commonly starts with charge transfer in the cloud. A process of neutralization occurs on small positive charge by the negative charge built from ice or water particles. Then, the process is followed by a stepped leader which transfers the charge from the cloud to the ground step by step. The process is fast

and happens in less than one-millionth of a second ($<10^{-6}$ s) for each step of the stepped leader.

Next, the stepped leader carrying some coulomb charges reaches the ground and connects with an upward-moving discharge which carries a large quantity of positive charge from the ground. The stepped leader builds the step to reach the ground while the upward-moving discharge of 30 m to 50 m long is directed upward to meet it. When both of them meet, a complete connection is built. The discharge from the ground moves up to the leader channel. As a result, a return stroke occurs. The flash of light is produced mainly by the return stroke before it returns to their normal state. Lastly, the process may repeat, starting with a continuous leader called dart leader which has lesser charges than stepped leader. It has the ability to move down the return stroke channel from the previous stroke (Rakov, 2007); (Blaes et al., 2014).

2.4 Types of Lightning

There are 3 types of lightning, namely cloud to ground (CG) lightning, inter-cloud lightning or cloud to air lightning, and intra-cloud (IC) lightning. Previous to this, Uman (1994) informed that CG lightning can be separated into 4 categories which are positive cloud to ground (+CG) lightning, negative cloud to ground (-CG) lightning, positive ground to cloud (+GC) lightning, and negative ground to cloud (-GC) lightning. A +GC lightning and -GC lightning occurrences are caused by an upward-moving leader from the ground, as shown in Figure 2.1. However, both of these are not discussed in this study due to their rarity and as they normally take place at mountain peaks and tall built structures such as transmission towers.

In a review on inter-cloud lightning and intra-cloud lightning by Uman (1994), they were categorised as cloud-to-cloud (CC) lightning and they occur due to the electrical breakdown that takes place within the cloud without contacting the ground. The electrical breakdown generates a weak return stroke within the clouds. Inter-cloud lightning occurs between charges that are centred in two different clouds or sometimes in between the air. Nevertheless, intra-cloud lightning occurs between positively charged and negatively charged centres in the same cloud. Figure 2.2 shows the differences of inter-cloud lightning and intra-cloud lightning.

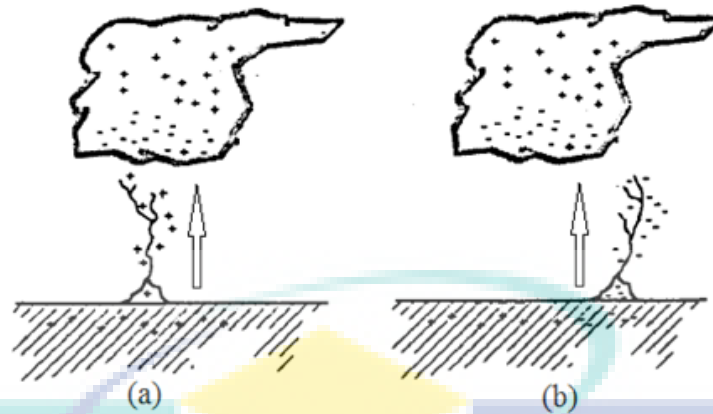


Figure 2.1 (a) Upward-moving positively charged leaders; (b) Upward-moving negatively charged leaders.

Source: Martin A. Uman (2008).



Figure 2.2 (a) Inter-cloud lightning; (b) Intra-cloud lightning.

Source: Martin A. Uman (2008).

2.4.1 Negative Cloud to Ground (-CG) Lightning

As mentioned in the return stroke, lightning occurs due to the connection of positive charges and negative charges between cloud and ground. A sudden connection of positive and negative charges causes a light to be emitted for a few milliseconds called lightning. Furthermore, -CG lightning occurs due to the electrical breakdown that takes place within the lower part of the thundercloud and the ground. Martin A. Uman (2008) claimed that the negative charge at the lower part of the thunderclouds experiences an electrical breakdown and form a downward-moving negative leader travelling to the ground. Then, the electric field around the ground produces a small breakdown and upward-moving discharge to contact the downward-moving negative leader. A -CG lightning occurs when the upward-moving discharge and the downward-moving negative leader meet. According to

Uman (1994), 90% of CG lightning is initiated by downward-moving negative leader while less than 10% of CG lightning is initiated by downward-moving positive leader around the world. Figure 2.3 shows the downward-moving negatively charged leaders.

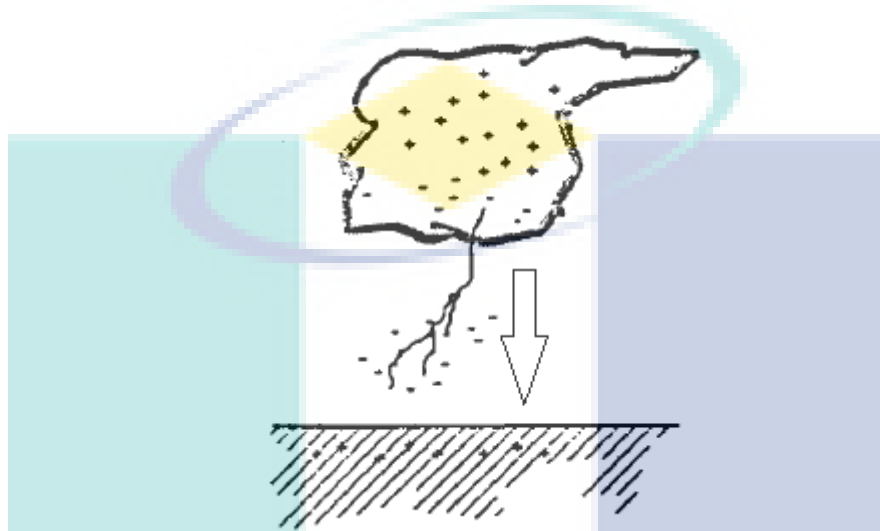


Figure 2.3 Downward-moving negatively charged leaders.

Source: Martin A. Uman (2008).

2.4.2 Positive Cloud to Ground (+CG) Lightning

A review from Uman (1994) reported that +CG lightning occurs at the upper part of a thundercloud which is positively charged. It starts with the electrical breakdown at the upper part of thunderclouds and is initiated by a positively charged downward-moving step leader. Only one return stroke occurs during the +CG lightning event, where -CG lightning does not appear at the same time. In addition, (Pawar and Kamra, 2004) reported that +CG lightning occurs during the last stage of the thunderstorm. The thunderstorm ends after several +CG lightning. Arnone et. al (2008) meanwhile claimed that most of the +CG lightning occurs in winter months. Carey et al. (2003) concluded that the percentage of +CG lightning is less than -CG which is >15% for +CG and >90% for -CG and found that the occurrence of Sprites events are usually related to the strong +CG lightning. Figure 2.4 shows the downward-moving positively charged leaders. Henceforth, it was decided that the focus of the research is to be placed on +CG lightning as it affects the occurrence of TLEs.

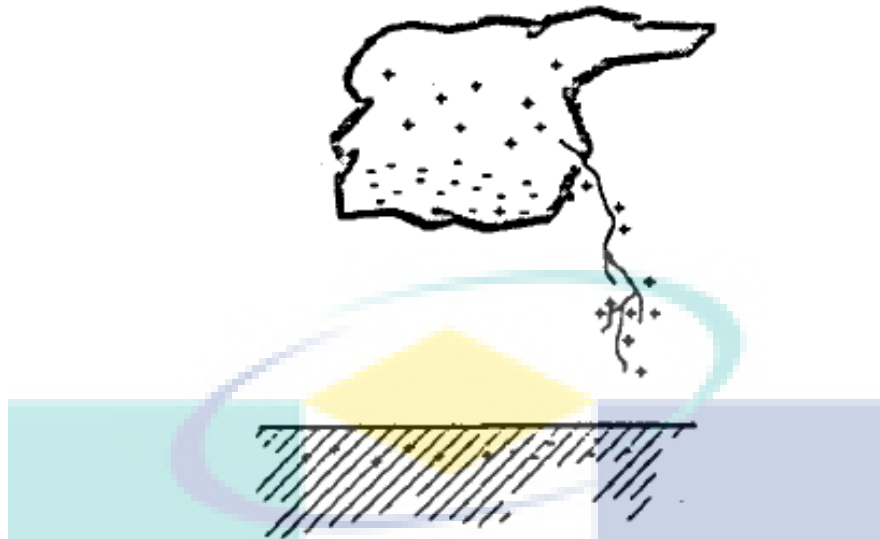


Figure 2.4 Downward-moving positively charged leaders.

Source: Martin A. Uman (2008)

2.5 Types of TLEs

Some TLEs occur at lower altitudes of about 80 km from earth's surface while some of them at approximately 100 km above the ground, as stated by Mar á Passas et al. (2014). It is an electrically induced form that occurs in the upper atmosphere due to the various types of electrical discharge phenomena in the upper atmosphere, which lack several characteristics of tropospheric lightning. They belong to Extremely Low Frequency (ELF) group, as revealed by Bailey (2010). A study on the occurrence rate of TLEs on land, coastal area, and ocean was carried out by Chen et al. (2008). The result showed that Elves dominate most number of TLE events and they are detected frequently above the sea surface compared to above the land surface. Sprites and Halos have almost the same numbers of occurrence, yet they appear more in different places like land surface and above the coastal surface respectively. Sprites and Halos have almost the same number of occurrence probably because Sprites always appear together with Halo. Lastly, Gigantic Jets has the least numbers of events and events often take place above the sea surface. Figure 2.5 indicates global occurrence of most TLEs. Different luminous transient produced at different heights is shown in Figure 1.1.

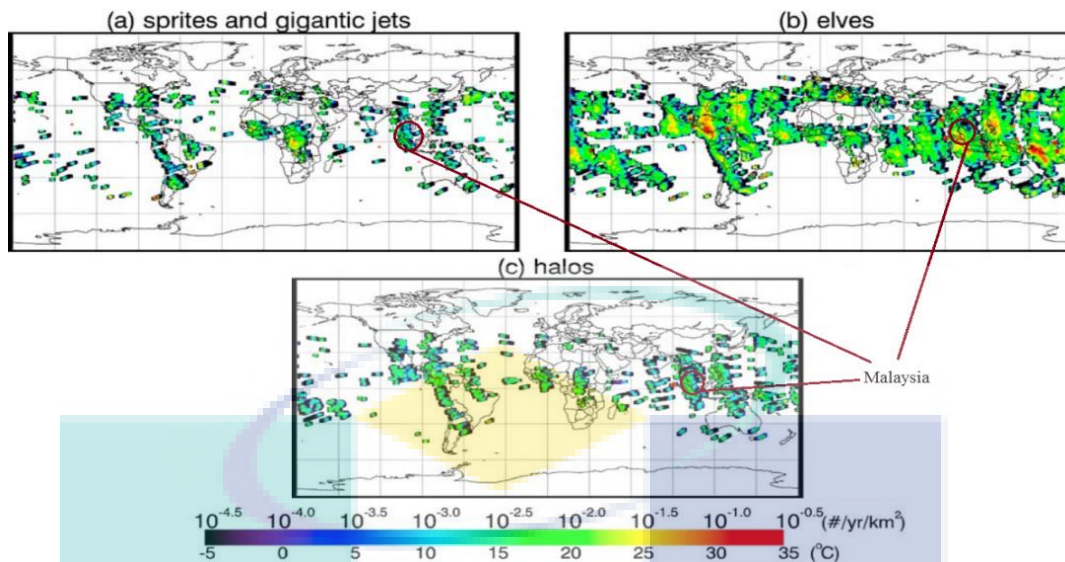


Figure 2.5 Global occurrence of most TLEs: (a) Sprite and Gigantic Jets, (b) Elves, (c) Halos.

Source: Chen et al. (2008).

2.5.1 Sprites

Sprites are the first type of TLEs detected in 1989 by Franz et al. (1990). It was then studied by other researchers who later found different types of Sprites such as Carrot Sprites, Column Sprites, Jellyfish Sprites, and firework, as stated by V. P. Pasko, Yair and Kuo (2012). According to Sentman et al. (1995), Sprite event concludes as a large luminous discharge and its altitude ranges approximately 40 km to 90 km. A large peak current can be detected when the event takes place. The period of Sprites is 0.2 min^{-1} , as explained by S. Soula, van der Velde, and Montanya (2012) and the duration is approximately 5 s to 30 s, as stated by M. Hayakawa, Y. Hobara, and T. Suzuki (2012). Sprites are red in colour due to the excitation of nitrogen gas in the atmosphere (Mende, Rairden, Swenson, & Lyons, 1995); (Franz et al., 1990). Haldoupis et al. (2010) found that second Sprites occurs after the previous event takes place, so, it can last over several frames setting after the first streamer is triggered at about 70 km away from earth's surface. The shape of Sprites can be horizontally displaced from the parent lightning or sometimes oriented towards it. Sprites is triggered by +CG lightning and its flashes within the stratiform region of the storm, as reported by Serge Soula et al. (2009), Lyons et. al (2003), and V. P. Pasko et al. (2012).

The Carrot Sprites have the combination of a bright “head” with a red glow colour as their “hair” (M. Hayakawa et al., 2012). They are able to extend to as high as an 95 km in altitude and their bluish tendrils always reached 20 km from the top clouds with a width of approximately 25 km to 50 km (Sentman et al., 1995; V. P. Pasko, Inan, and Bell, 1996). The Column Sprite was detected by E. M. Wescott, Sentman, M. J. Heavner, and D. L. Hampton (1998) in year 1998 and it was found that they appeared in a group form. The Column Sprite occurs without the hair-like and tendrils structure. It is vertically oriented cylinder-shaped with a height of about 10 km. The diameter is less than 1 km. Yaniv et al. (2014) observed that the Column Sprite might occur due to a weak +CG flashes produced. Thus, the current study seeks to observe Sprites, namely those that are similar to the first TLEs founded in the year 1989 as they are triggered by +CG lightning. Figure 2.6 summarizes the different types of Sprites.

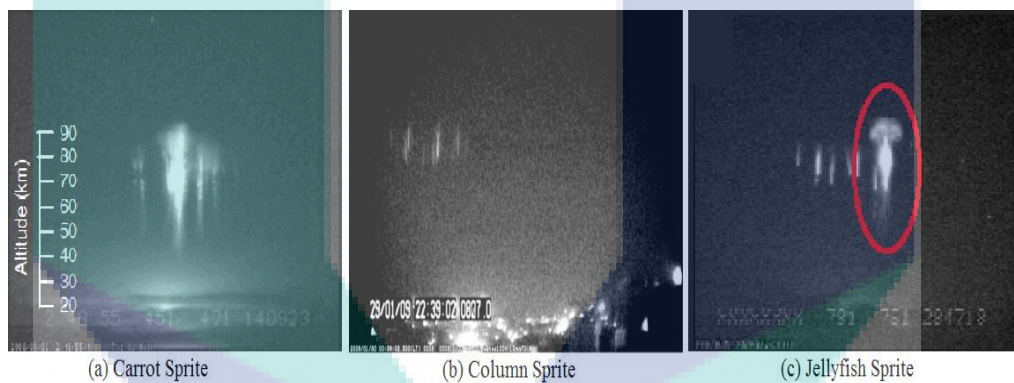


Figure 2.6 Different types of Sprites: (a) Carrot Sprites, (b) Column Sprite, (c) Jellyfish Sprite

Source: (a) S. Soula et al. (2014); (b) Yaniv et al. (2014); (c) S. Soula et al. (2012).

2.5.2 Halos

Halos are defined as the decreasing glow with a side area of 40 km to 70 km and are randomly produced together with Sprites. They are normally located at the tops of Sprites (Barrington-Leigh, Inan, & Stanley, 2001). They were found to escort the occurrence of more structured Sprites. Mar á Passas et al. (2014) claimed that Sprites and Halos happen 25 km across an average horizontal distance source from the first lightning strike. Figure 2.7 shows images of the Halos produced with Sprites.

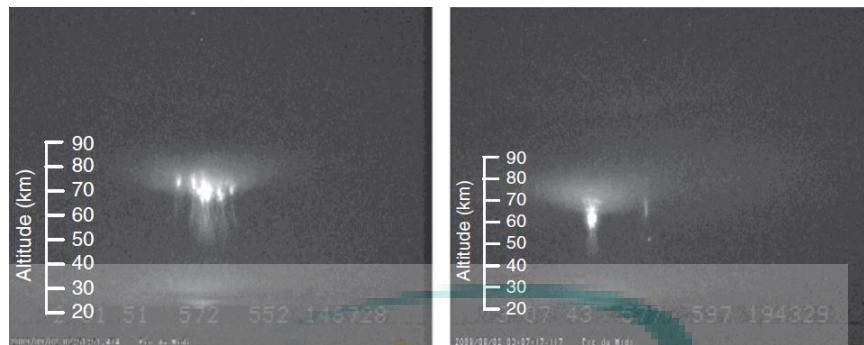


Figure 2.7 Halos associated with Sprites.

Source: S. Soula et al. (2014).

2.5.3 Elves

Elves were first defined by Fukunishi et al. (1996). The speed of Elves is faster than 1 ms while the speed of Elves' downward movement to the ground is 1/10 to 1/3 of the speed of light ($3 \times 10^8 \text{ ms}^{-1}$). They occur at an altitude range of 75 km to 105 km after a large peak current of CG lightning discharge is detected. The rapidly horizontal expansion of Elves is characterized by the shape of luminous rings with a diameter of up to 400 km or larger. Subsequently, Elves expand in a radially outward direction by following the lower edge of the ionosphere which is located at an altitude of about 80 km to 90 km (Newsome & Inan, 2010). They are composed of lights in red colour and are triggered by a +CG lightning or a -CG lightning with a large peak current. This is associated with the major percentage of -CG stroke found by Barrington-Leigh and Inan (1999). Elves have possibly contributed a unique polarity reversal when they produce a flash in a storm, as reported in the research done by S. Soula et al. (2012). Elves' thickness reach 10 km to 20 km and their height can reach up to approximately 95 km, as reported by M. Hayakawa et al. (2012).

The swift duration of Elves made it too hard to see them with the naked eye and it is still difficult to capture them by using a video camera with 25 frames per second (fps). However, a higher performance video camera with 100 fps or above is more suitable to capture Elves event. It is a natural phenomenon that humans are able to predict and prevent earlier because Elves are the type of TLEs that frequently occur across the world. Large storms can produce hundreds of Elves in a few hours. Figure 2.8 shows Elves captured by Van der Velde (2008).



Figure 2.8 Elves.

Source: Van der Velde (2008)

2.5.4 Gigantic Jets

Gigantic Jets appear less frequently compared to Sprites and Elves. It can spread across an altitude of as high as 80 km with upward-directed lightning shooting out of the cloud tops and it is large in size (V. P. Pasko, 2010). S. Soula et al. (2012) recorded the luminosity of Gigantic Jets that appeared blue in colour and the event was estimated to have occurred at the altitude of 80 km to 90 km. However, another new colour of Gigantic Jets was observed by Y. Yair et al. (2013) which comprised of reddish-orange diffused arc and bluish colour at the lower part. Gigantic Jets are mainly caused by intracloud discharges at the lower ionosphere with the thundercloud and without a cloud to ground (CG) flash detected at the same time (V. P. Pasko et al., 2002; Su et al., 2003). Therefore, no charge transfer to the Earth was detected during the occurrences of Gigantic Jets. On the contrary, Jing and GuiLi (2014) found that Gigantic Jets was dominated by -CG lightning during discharging. This shows that Gigantic Jets are one of the TLEs types that are difficult to be determined (V. P. Pasko et al., 2002; Su et al., 2003; & Jing & GuiLi, 2014).

4 structures are needed to produce a huge Gigantic Jets. The first Gigantic Jets structure is the leading jet. Its duration ranges from 33 ms to 167 ms and it propagates at a higher altitude. During the second phase, a tailing jet appears with decreasing luminosity in different parts such as the lower channels and transition region. At the lower channels which are the third structure, it produces blue luminosity at an altitude of approximately 20 km to 40 km. The blue luminosity then diffuses with time as it decreases in altitude. Lastly, the transition region located

around 40 km to 65 km, consisted of bright red luminous beads slowly going up and retracing the initial leading jet channels (Soula et al., 2012). Figure 2.9 presents the images of one of the physical characteristics of Gigantic Jets.

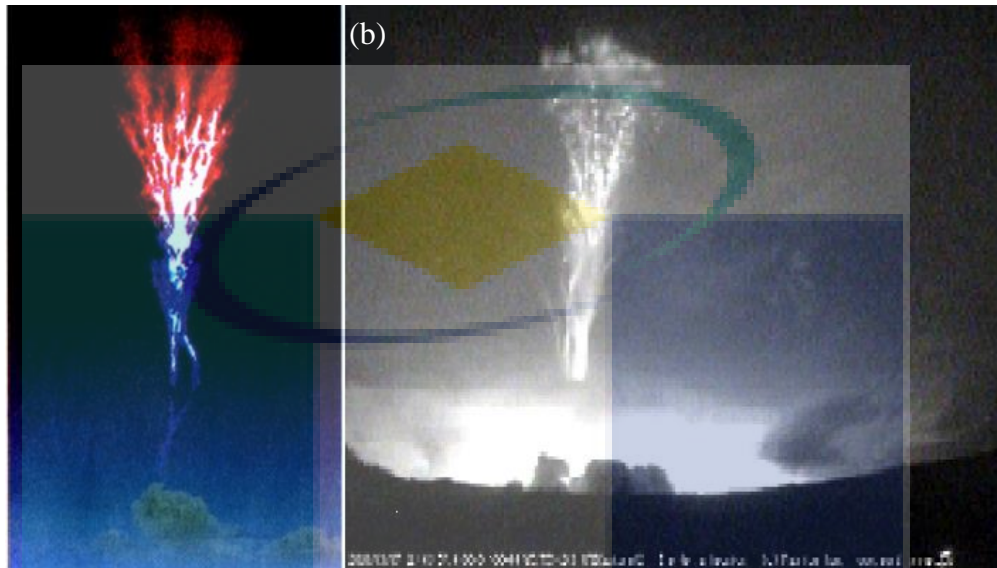


Figure 2.9 Gigantic Jets.

Source: (a) Su et al. (2003); (b) S. Soula et al. (2012)

2.5.5 Blue Jets

Blue Jets is a smaller sized version of Gigantic Jets. They are TLEs with upward-directed lightning shooting out of the cloud tops. Thus, they extend only a few kilometres from the top of thunderclouds up to the clear air above (E. M. Wescott et al., 1996). E. M. Wescott et. al (1998) also emphasized that Blue Jets can spread to an altitude of up to 40 km which is half the distance of Gigantic Jets. It occurs when there is an electrical breakdown in-between the upper storm charge and the screening charge that are attracted across the top of thunderclouds. The phenomenon happens within approximately 5 s to 10 s or less, with the production of a sudden imbalance charge in the storm due to the cloud to ground or intracloud discharging, as indicated by Krehbiel et al. (2008). The duration of Blue Jets is longer than Sprites and their intensity is also larger than Sprites, as reported by M. Hayakawa et al. (2012). Moreover, the upward directed speed of Blue Jets achieved up to 100 km/s (Sentman et. al, 1995). Blue Jets have a blue conical shape with an angular cone at approximately 15°, as discovered by E.M. Wescott, D.D. et. al (2001).

Blue starter is the initial stage of blue jets. It spreads upward from the cloud top at an altitude of 17 km to 18 km, up to the altitude of 25.5 km, as reported by E M Wescott et al. (1996). Gigantic Jets are described to occur as normal intracloud discharge. The discharge process happens in between the dominant level charge and screening-depleted upper level charge. The discharge process for both Blue Jets and Gigantic Jets precedes the propagation on the top of the storm and no polarity is found during the event (Sentman et al., 1995b). Figure 2.10 shows a Blue Jet observed in Kanto, Japan in 2011.

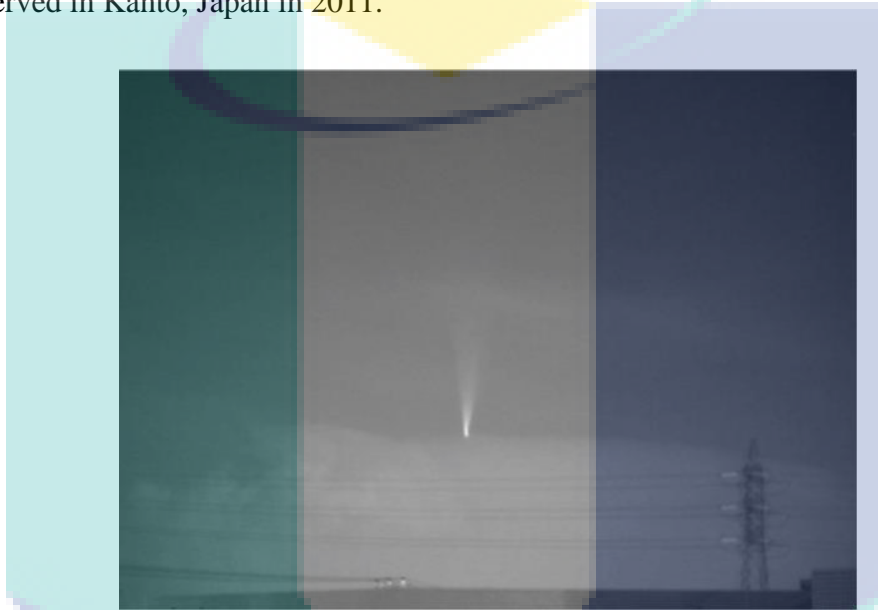


Figure 2.10 Blue Jets.

Source: Suzuki, Hayakawa, Hobara, and Kusunoki (2011).

2.6 Camera

Many types of camera have been used in previous research to capture images of TLEs. Earlier, the low-light level Television (LLTV) camera was used by Franz et al. (1990) and Lyons et al. (2003) to observe TLEs in the year 1990 and year 2003 respectively. In the following year, a Xybion IMC-201 charge-coupled device (CCD) camera was used by the researcher, Y. Yair et al. (2004) to observe the TLE activities in the upper atmosphere.

In the year 2006, other types of low light and high-speed cameras such as Vision Research Phantom 7.1 monochrome were used by Cummer et al. (2006) to capture TLEs images. Later, a new type of camera, namely Watec 902H was used by S. Soula et al. (2012) and S. Soula et al. (2014) in 2012 and 2014, and also Lang

et al. (2010) in 2010. Currently, Watec 902H camera is the most frequently used in the observation of TLEs. Last but not least, another type of camera, namely the high-sensitivity CCD 1/3" camera was also used by Mar á Passas et al. (2014) in 2014.

To conclude, all the cameras used by previous researchers were monochrome and very sensitive to low light conditions. Moreover, Watec 902H has been used to observe meteor and other late night natural phenomena. For the same reason, Watec Ultimate 902H2 camera was chosen by researcher for this research. The camera is shown in Figure 2.11.

2.6.1 Watec Ultimate 902H2 Specification

Watec Ultimate 902H2 camera is a monochrome camera frequently used to observe meteor and other natural phenomena in low light conditions (M. Passas, Madiedo & Gordillo-Vázquez, 2016). The camera type of Committee Consultatif International Radiotelecommunique (CCIR) was chosen instead of Electronics Industry Association (EIA). CCIR is of a black and white television (TV) standard. It is the ancestor of Phase Alternation by Line (PAL) system where PAL system offers automated colour correction and 25 frame rate (Wood, 2004). The sensitivity of Watec Ultimate 902H2 CCIR type camera is 0.0001 lux in aperture F1.4, which means the specific camera can display the image to be captured very clearly under a low light condition (Pillman, 2010). The figure of the full set camera specifications with the parts can be found in the Appendix B.



Figure 2.11 Watec Ultimate 902H2 camera.

2.7 Frames Rate

Frames rate is the frame frequency for a film, video camera, and motion capture system. It is also called as frame per second (fps). Human eyes normally can watch a video at 16 fps to 24 fps (David Neumeyer, 2014). A higher fps produces a clear resolution as more frames are processed within one second. Cummer et al. (2006) used 5000 fps for their research in 2006. The time acquires for each frame is 0.2 ms. Hence, the process of electrical breakdown for TLEs shown in each frame was defined easily. In the same way, Mar á Passas et al. (2014) used 33 frames in their research in 2013. The image captured was blurred yet it was acceptable for review and the TLEs discharge process was able to be concluded. The image captured by Cummer et al. (2006) was clearer compared to Mar á Passas et al.'s (2014). In this research, a camera with 25 fps was used to observe TLEs. The calculation of fps for the current study is further discussed in Chapter 3.

2.8 Field of View (FOV)

Each camera has its own viewing coverage where the field of view is used to describe the cameras' viewing area. Field of View (FOV), also known as Angle of View (AOV), is described as an area that can be observed under a camera's coverage. As explained by Galstian (2013), FOV depicts the image's captured range. It is separated into two sections of description, namely the object space and the image space. Object space is defined as the scope of the captured object. It is measured as an angle and is normally applied toward a faraway object. Image space is defined from the camera sensor size. It measures the FOV that corresponds to the camera sensor dimension such as the width, the height, and the diagonal dimension. In a book written by Corsentino (2013), it was claimed that AOV is the area covered by a lens and is measured in degree type. Moreover, it was found that a camera with a couple of wide-angle lens and set zoom function can capture a wider AOV.

As identified by Robert Hirsch (2012), there are 5 types of angle view which are eye-level angle view, low-angle viewpoint, wide-angle viewpoint, high-angle shot, and bird's eye views. Eye level angle view indicated the AOV covered under human sight. Next, the low-angle viewpoint is described as an image captured by adding wide-angle lenses to the camera and they are used to maximise the image

view. Meanwhile, wide-angle viewpoint refers to the image focus of the viewer's observation in one specific direction. The fourth angle view is a high-angle shot which is defined as the opposite effect of low-angle viewpoint. A high-angle shot focuses on the surrounding environment or a bigger FOV area effective to the portrait situation. Bird's eyes view indicates an image captured from a higher position or above a subject and can be confusing to viewers. Subsequently, oblique angle is another special view angle which demonstrates an unstable camera position on its horizontal line. When applied the oblique angle shot, a suitable position need to be adjusted to capture the photos.

In addition, Kim, Jung, and Paik (2016) confirmed that FOV or AOV are eligible to be changed by substituting them with a different size of focal length to the camera. It was found that the FOV of camera did not change by replacing a normal focal length to the fisheye lens. Hence, only the focal length size affects the performance of FOV.

More importantly, the technique of low-angle and wide-angle viewpoints was chosen for this research. Equation 2.1 explains the relationship between focal length and AOV, where “*d*” represents camera sensor dimension and “*f*” represents effective focal length (Ernest McCollough, 1893). A simplified calculation of AOV is discussed in Chapter 3.

$$AOV, \beta = 2 \tan^{-1} \frac{d}{2f} \tag{2.1}$$

where,

d = camera sensor dimension;

f = effective focal length.

2.9 Summary

From this chapter explained the occurrences of lightning event, and types of TLEs such as Sprites, Halos, Elves, Blue Jets, and Gigantic Jets. In addition, a monochrome camera, Watec Ultimate 902H2, was used as the equipment to record the occurrences of lightning event. Angle of view (AOV) act important role during the research, it will be determined the height of the event. AOV defined by using equation 2.1.

CHAPTER 3

METHODOLOGY

3.1 Introduction

This chapter discusses the research methodology by providing a guideline and step taken to conduct the study by using certain methods, techniques and instruments. The part is separated into two sections comprising the techniques conducted to process the lightning map and the image captured. These two methods were used to categorize the types of TLEs by finding out their unique parent lightning, size, and shape. The function flow diagram of the research is explained in Figure 3.1.

TLEs are natural phenomena located between troposphere and ionosphere. They occur at the height of about 80 km to 100 km above the earth's surface. The data collected by the Malaysian Meteorological Department (MMD) as part of the yearly lightning activities observed as well as to find out the parent lightning of TLEs.

Information for the TLEs would be limited if the research was done only by data collection. Hence, an image captured using a video camera was also analysed simultaneously with the data collected by MMD. Data collected from both methods were found to be more useful in making more reliable conclusions. Lastly, a data comparison was done with results from MMD to perform a final check of the accuracy of the result and to reach the final conclusion on the TLEs observed.

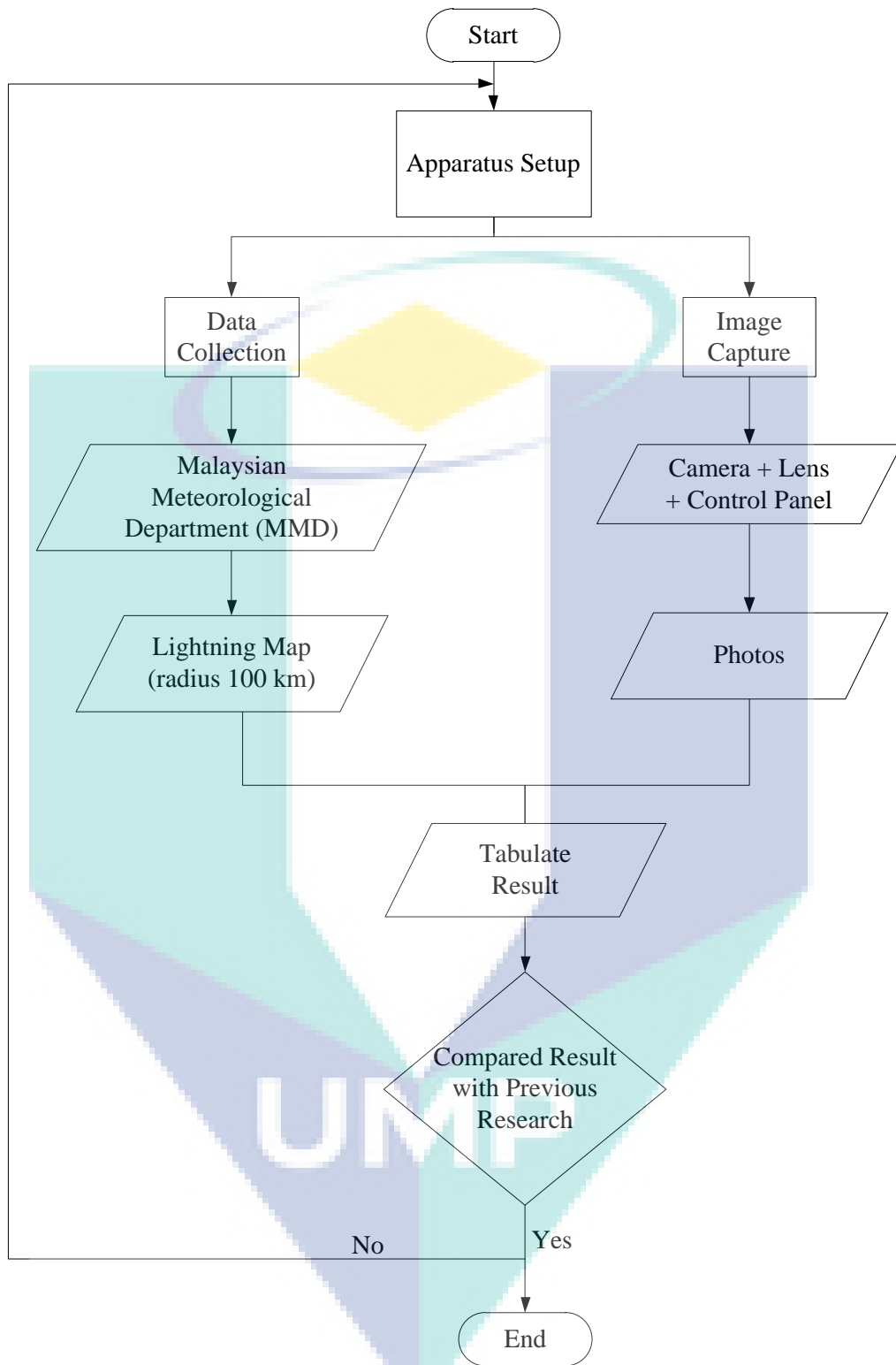


Figure 3.1 Flow diagram of the research tasks.

3.2 Data Collection

Data is from Malaysian Meteorological Department (MMD). The specific function and operation system are explained in the following subtopics.

3.2.1 Malaysian Meteorological Department (MMD)

A set of data collected by Malaysian Meteorological Department (MMD) within an area of 100 km radius coordinated at the centre point of Universiti Malaysia Pahang's (UMP) Pekan campus was requested to find out the parent lightning of the positive cloud to ground (+CG) lightning. Figure 3.2 clarifies the function flow for the process of data collection. In addition, Figure 3.3 explains the localization within the radius of 100 km, whereas Figure 3.4 presents the coverage area of within 100 km radius.

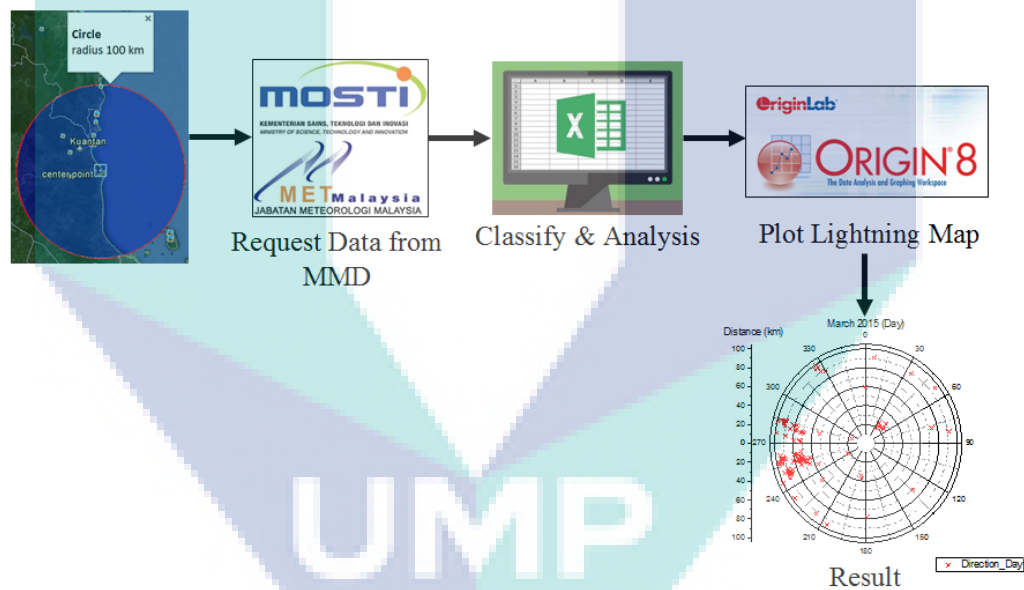


Figure 3.2 Process of data collection.

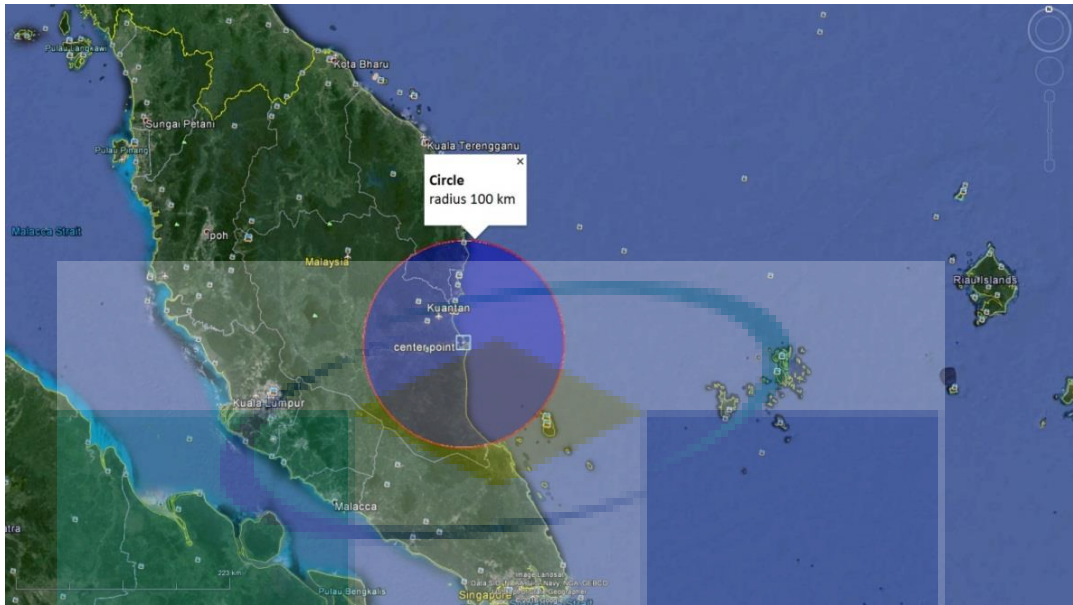
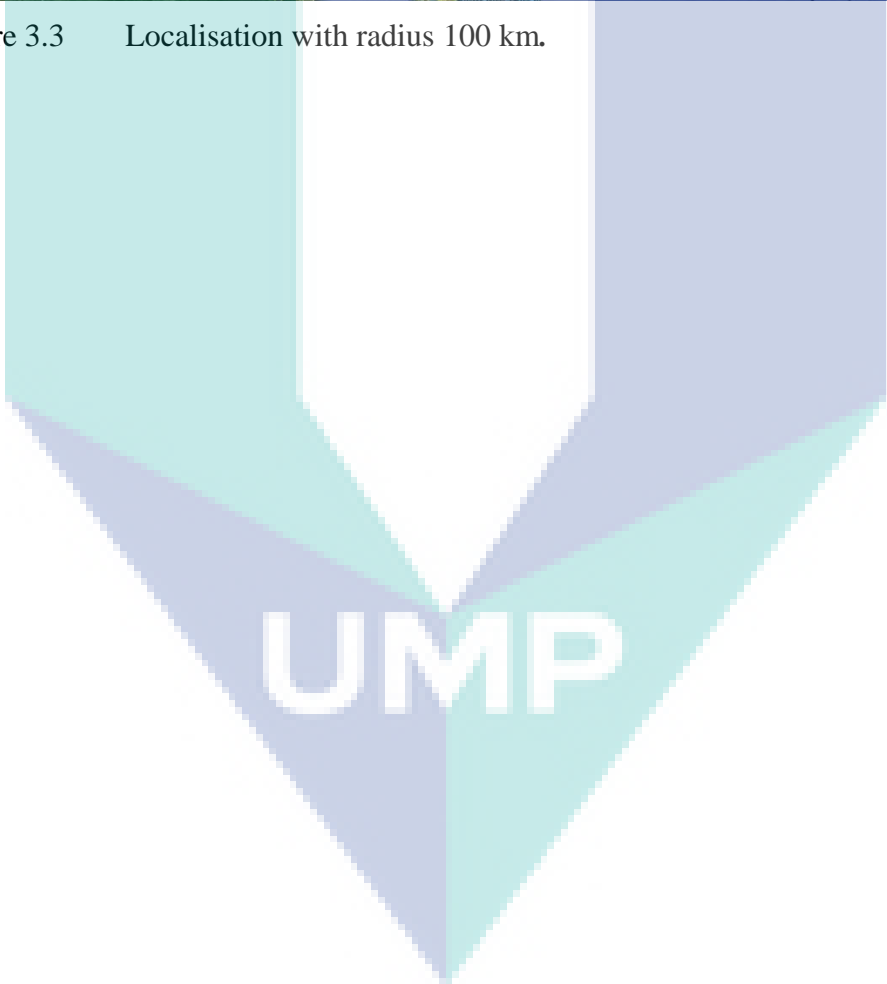


Figure 3.3 Localisation with radius 100 km.



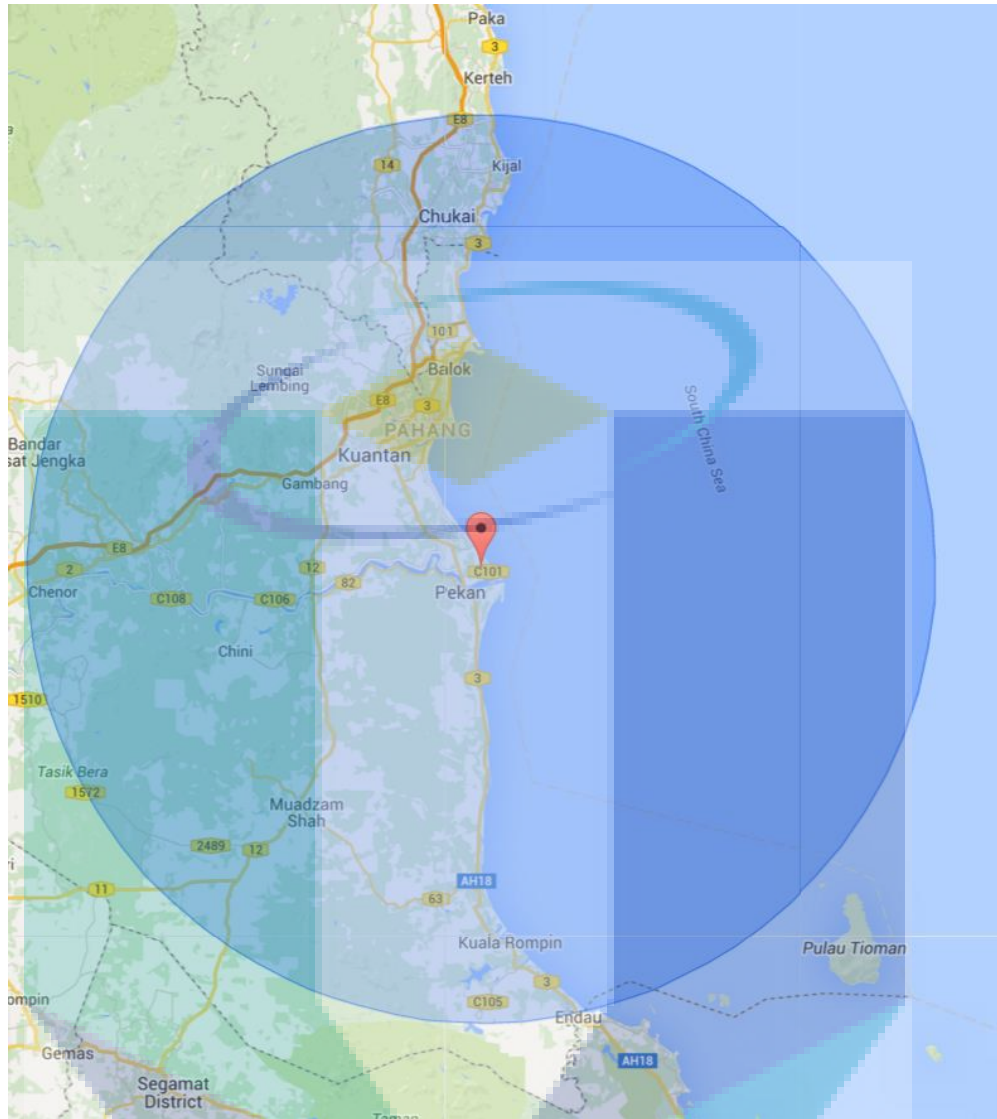


Figure 3.4 Covered area within 100 km radius.

The data was then sorted by using Microsoft Excel's data sorting method based on the highest and the lowest intensity of lightning as shown in Figure 3.5. Then, it was sorted again based on the positive and negative intensity to find out the occurrence frequency of +CG and negative cloud to ground (-CG) lightning. After that, the monthly occurrence of +CG events during the day and the night times were calculated and plotted.

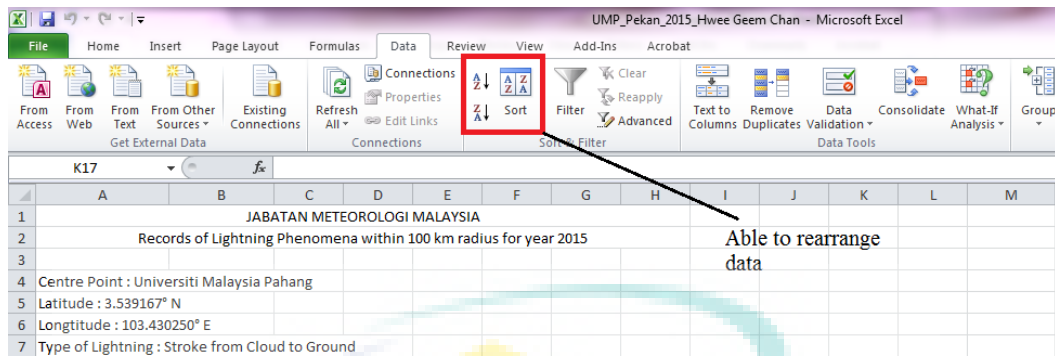


Figure 3.5 Microsoft Excel sort function.

After the calculation section ended, the data was transferred to Origin Lab application to plot the lightning map as shown in Figure 3.6. Data such as lightning direction in degree measurement from the centre point and distance in km from the centre point were copied from Excel and pasted in the Origin Lab booklet, as shown in Figure 3.7. These were copied and pasted separately based on the monthly lightning events and separated into day and night. After being transferred, all the data were selected and set to X1, Y1, X2, Y2 from the column properties to group the data based on day and night occurrences.

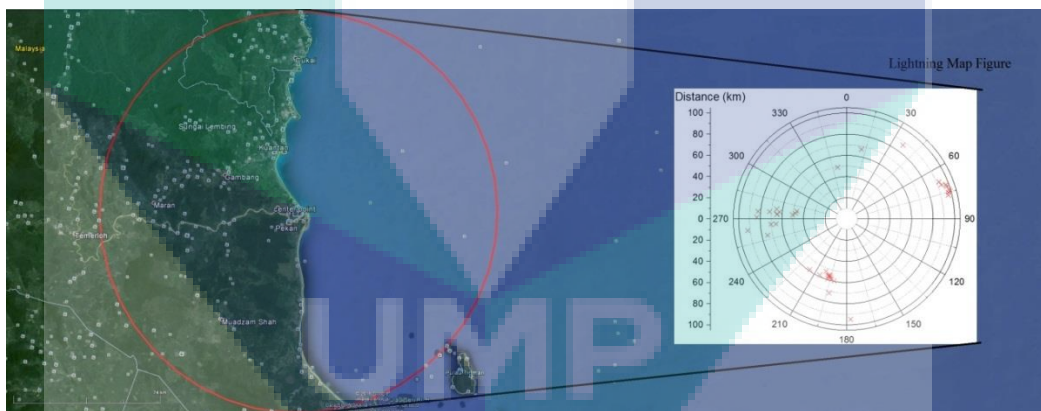


Figure 3.6 Lightning map for 100 km radius.

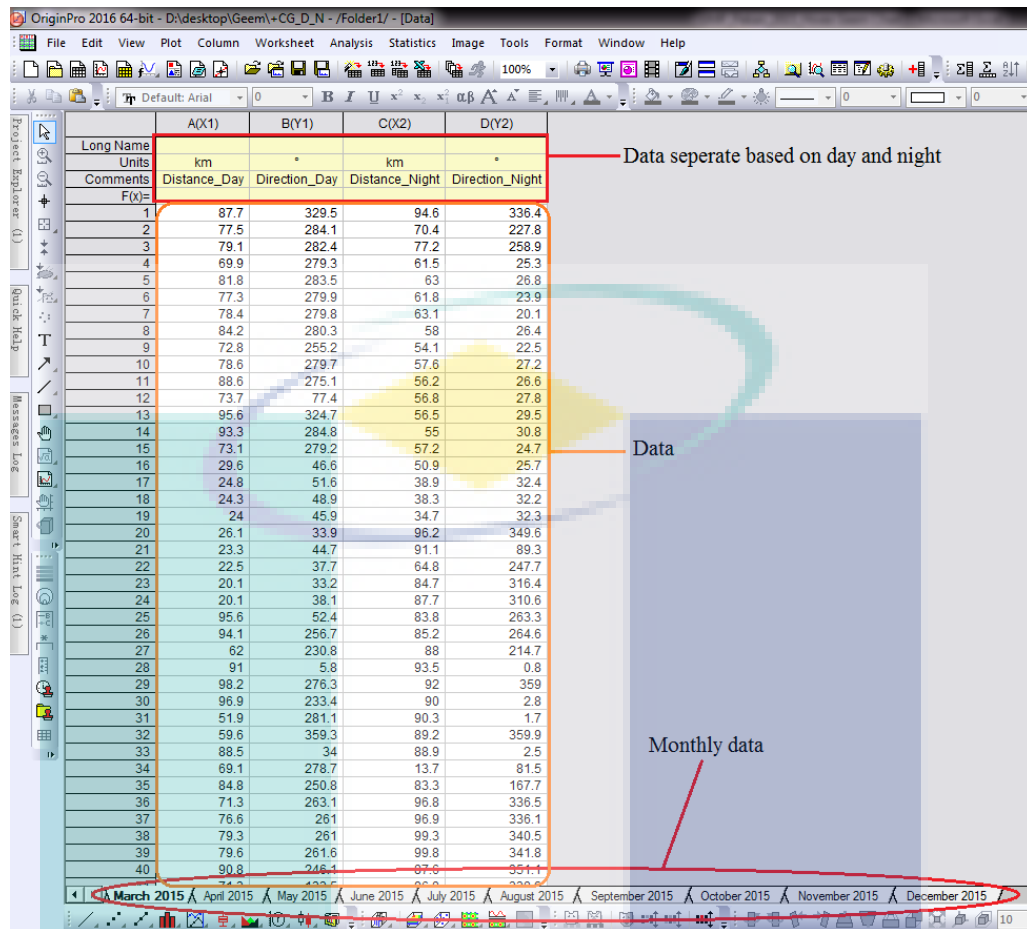


Figure 3.7 Origin Lab data booklet.

A system template was chosen from the plot tab as the sample to plot the lightning map. The PolarXrYTheta type was selected, as shown in Figure 3.9 and it was plot by clicking the “Plot” function. A lightning map was plotted successfully using Origin Lab. A discussion on +CG parent lightning is presented in the following Chapter.

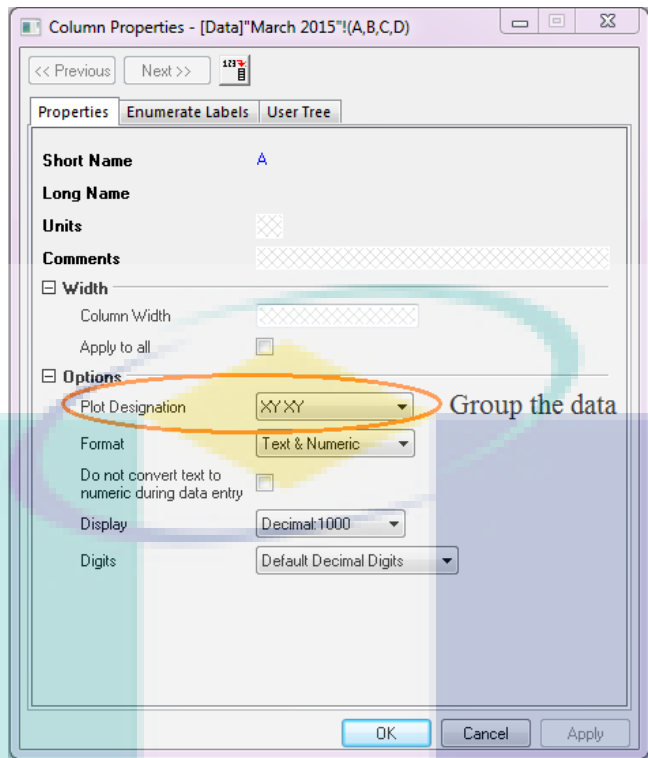


Figure 3.8 Column properties.

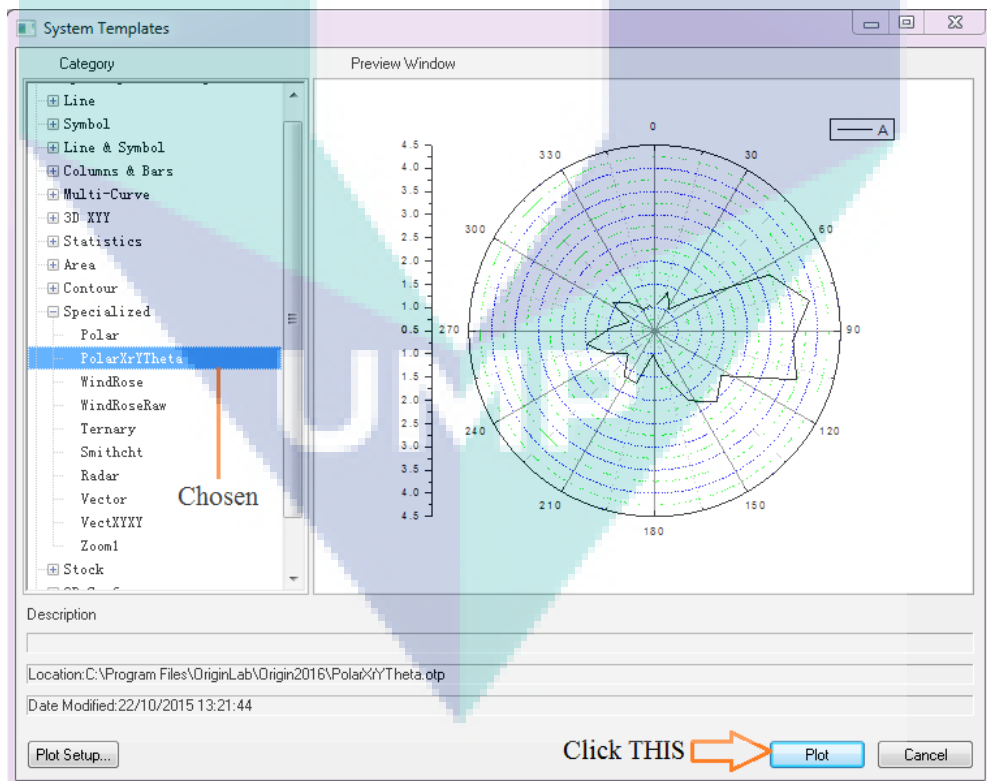


Figure 3.9 PolarXrYTheta type.

3.3 Image Capture

A highly sensitive camera model, Watec Ultimate 902H2, was chosen as the image acquisition device. The camera was set up at the Keysight Lab which is located at the second floor of Block 1, Faculty of Electrical and Electronics Engineering (FKEE), UMP Pekan campus. The camera is a monochrome camera frequently used in the past to capture natural phenomena such as meteor and full moon events. It was operated in video mode only during night time for the recording process. Only two techniques of fields of view (FOV) were used in the study, namely the wide-angle viewpoint and low-angle viewpoint, as discussed in the Chapter 2. After the video was captured by the camera, a Digital Video Recorder (DVR) acted as a bridge to transfer the video to the desktop where the save-mode operated automatically every 30 minutes. Furthermore, DVR converted the recorded analogue video into digital format and transferred it to a disk drive. Then, the KM player software was used to extract all the frames. Lastly, the results were displayed at the specific folder. This was needed to ensure that all the frames have been extracted one by one from the lightning event that had taken place to minimise the error of leftover. A block diagram of images captured and the camera setup panel is shown in Figure 3.10 and Figure 3.11 respectively.

The camera was set to shoot upwards at α° camera angle as explained in Figure 3.12. The calculation was made according to Kozak et al. (2014) by using the trigonometric method and explained further in Sub-topic 3.3.6 in detail. Then, the camera was focused on the direction where lightning events were occurring.

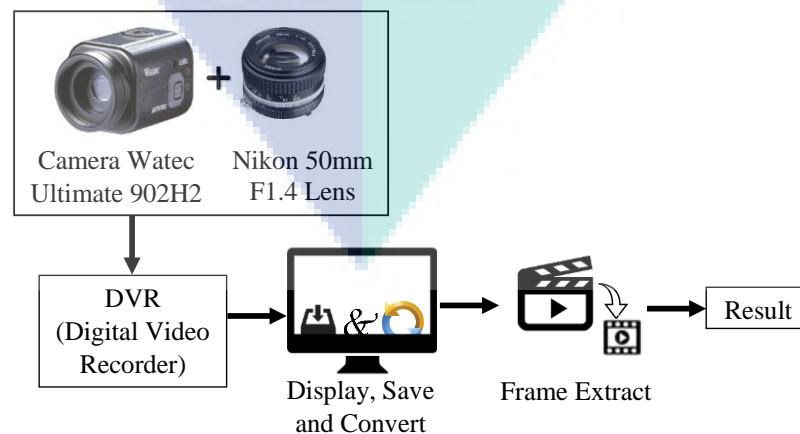


Figure 3.10 A block diagram of image captured.

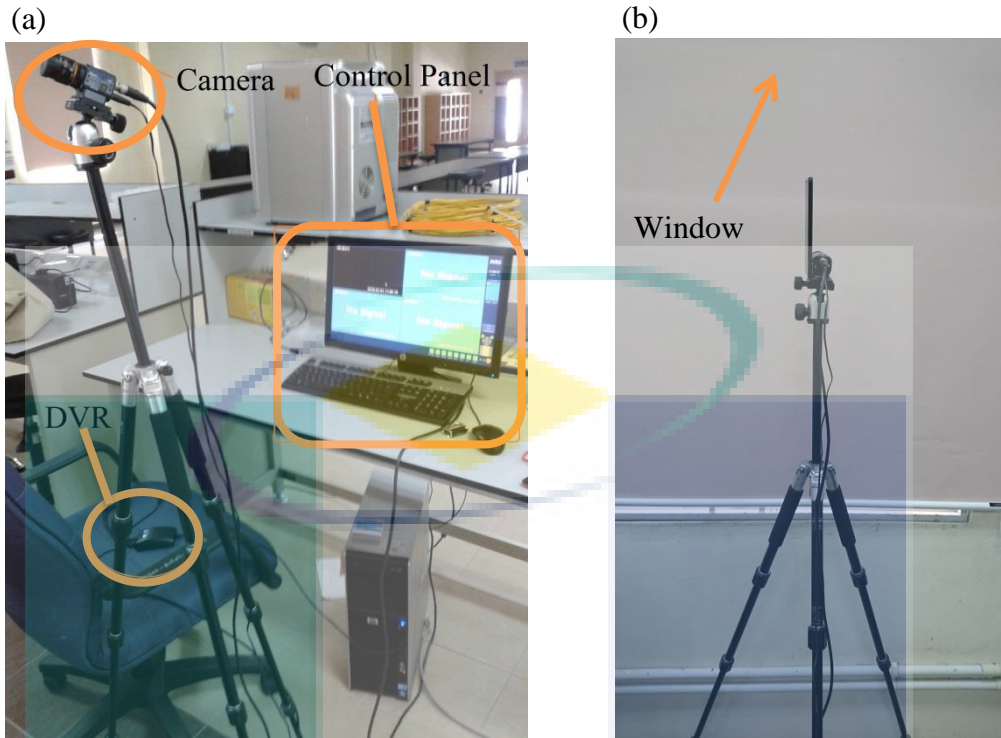


Figure 3.11 (a) Camera setup panel; (b) Camera locate beside window.

Table 3.1 Components used during the research.

Components	Length (m)	Quantity	Uses
BNC male connector	2	1	To connect camera and DVR.
Camera charger	2	1	To supply power to camera.

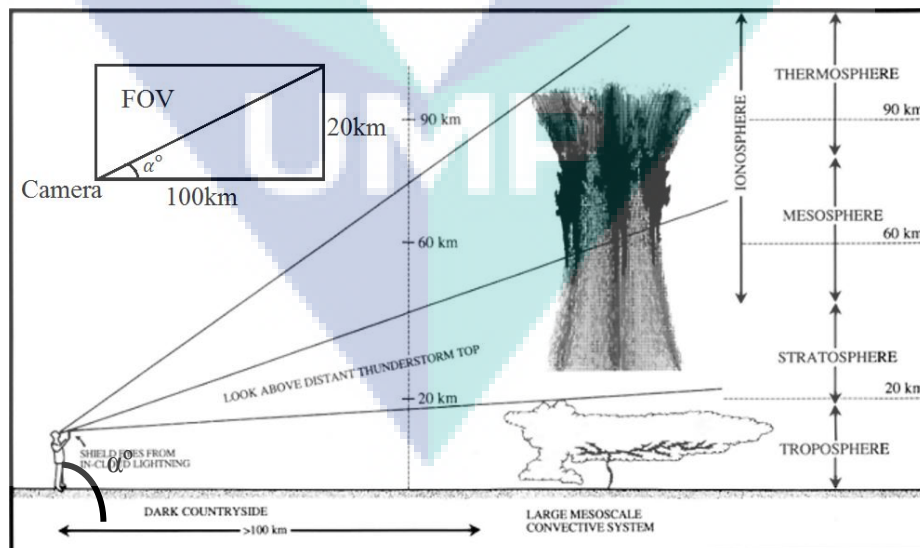


Figure 3.12 Explanation to capture a Sprite.

Source: Kozak et al. (2014).

3.3.1 Camera Lens

The Watec Ultimate 902H2 camera was coupled with Nikon 50 mm focal length with aperture f1.4 lens used to capture TLEs image. Then, the lens was replaced by Brinno Lens 24 mm to 70 mm focal length with aperture f1.4 lens in advance. Nikon lens can only focus at a specific area whereas Brinno Lens was able to control the adjustment and can focus on a more specific field of view. A better visual result was able to be produced by replacing a lens applicable to adjust its focal length. The user manual of Brinno Lens is attached in the Appendix section.

Firstly, the “zoom” screw was adjusted to capture a bigger or a smaller screen image using Brinno Lens. Next, the “aperture” screw adjusted to make sure that the amount of light intensity was acceptable as shown on the camera screen. Then, the “focus” screw was rotated to focus on the object. Lastly, the screws were tightened after each steps was done completely. Figure 3.13 showed Nikon lens and Brinno Lens used in this study.

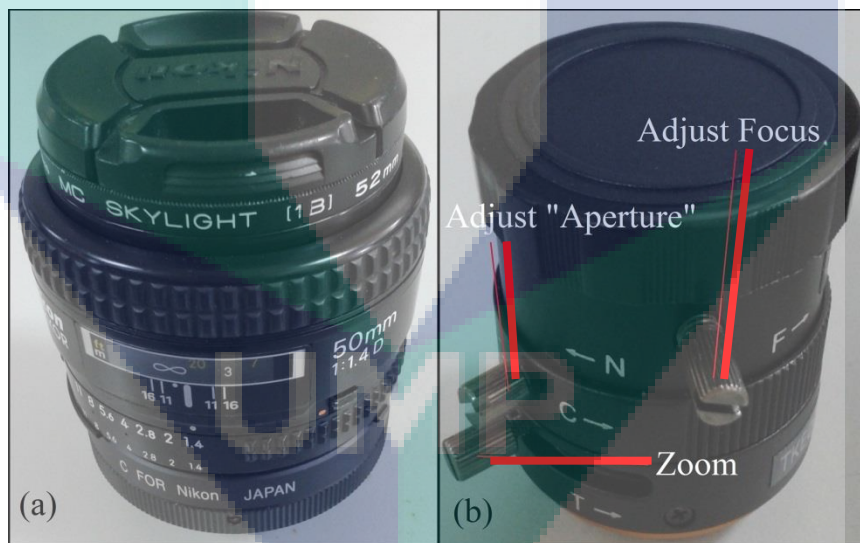


Figure 3.13 Two different of lens: (a) Nikon lens 50 mm focal length with aperture f1.4; (b) Brinno Lens 24 mm – 70 mm focal length with aperture f 1.4.

3.3.2 Digital Video Recorder (DVR)

High frame rate (frame per second – fps) relative to high resolutions ensures high definition frames were captured during the occurrence of TLEs. This feature was to ensure detail sequences of the event are captured and the nature of TLEs are

exposed. A digital video recorder (DVR) with high fps was chosen as the connector between the personal computer (PC) and the camera. It also controls the frames per seconds (fps) for the video recorded or image captured. In addition, the video recording was done in analogue mode. The recordings then needed to be transferred to the PC but the analogue type videos were difficult to transfer. Hence, the recordings were converted into digital mode in order to transfer it into the PC disk drive easily. However, the conversion decreased the resolution of the images. Three types of DVRs with different functions were used in the research. HD USB 2.0 DVR was used in the beginning, which was later replaced by the branded Jovision (JVS C300Q DVR) since the recorded file size of the HD USB 2.0 DVR videos were large and they need to be convert to .mp4 format after the recording. Lastly, JVS C300Q DVR was replaced by UU-DVR as JVS C300Q DVR has low resolution and low frame rate. In addition, results from JVS C300Q DVR were protected by the related authority, requiring a software named “JFilter” to be installed before reviewing the video by using KM player. The three types of DVRs are shown in Figure 3.14 and a clearer comparison between the three DVRs is made in Table 3.2. In addition, it was found that only the carrot Sprites events were captured during the tenure of the study and this finding is presented in Sub-topic 4.5.1.

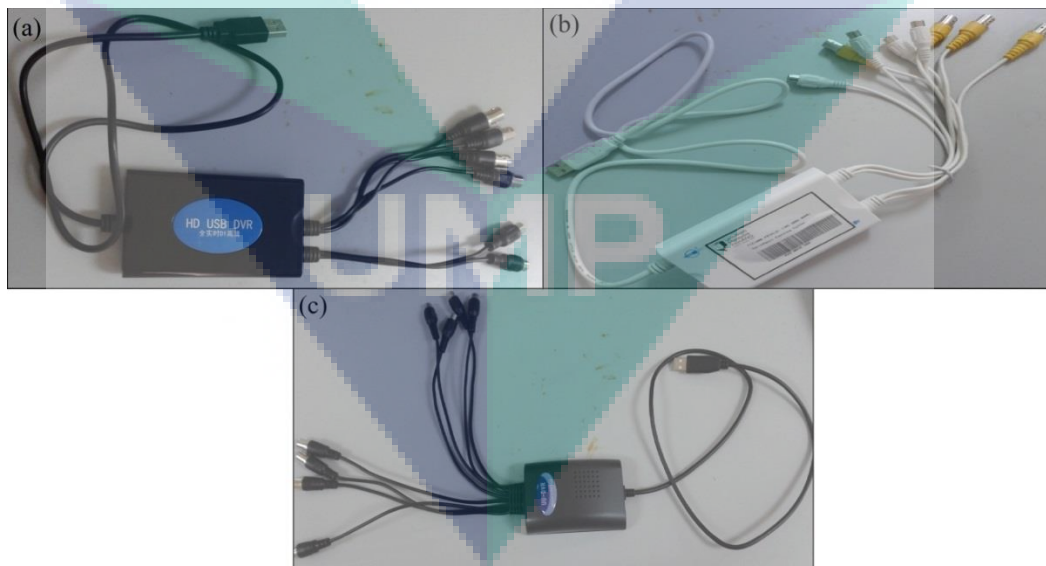


Figure 3.14 Three types of DVRs (a) HD USB 2.0 DVR; (b) Jovision (JVS C300Q DVR); (c) UU-DVR.

Table 3.2 Comparison of DVR.

Descriptions	HD USB 2.0 DVR	Jovision (JVS C300Q DVR)	UU-DVR
Format	PAL	PAL	PAL
Frame rate (fps)	25	12.5	25
File Type	.mp4	.sv4	.avi
Resolution	352 x 288	704 x 576	1920 x 1080

The three types of DVR have the same video system format, Phase Alternation by Line (PAL). The PAL recording system is commonly used in countries such as Malaysia, United Kingdom (UK), and Australia (Difflen, 2013).

HD USB 2.0 DVR has 25 fps and it records in .mp4 video format. Although the recorded image is clear, the file size is large and takes up the space to store the daily video. Meanwhile, JVS C300Q DVR has a clearer resolution at 704 x 576 compared to HD USB 2.0 DVR resolution which is only at 352 x 288. It records in .sv4 video format which is a unique format and requires a special application to be installed before the video can be viewed, as mentioned in the previous chapter. On the other hand, the use of JVS C300Q DVR was rejected for the observation in this study due to its lower fps (16 fps) compared to HD USB 2.0 DVR (25 fps) and UU-DVR (25 fps). UU-DVR contained the clearest resolution at 1920 x 1080 compared to HD USB 2.0 DVR and JVS C300Q DVR. It has 25 fps and records in .avi video format. In addition, .sv4 and .avi record in smaller file size than .mp4. For these reasons, UU-DVR was finally chosen as the connector to interface between PC and camera.

3.3.3 Video Record Control Panel

As stated in Chapter 2, there are several types of recording system that apply Phase Alternation by Line (PAL) system for the Malaysian region. The maximum fps of PAL system is only 25. However, it was found that the fps was controllable through the recording control panel. It was necessary to set the basic recording setup before the video recording. Firstly, the recording control panel and setting setup was opened through the “setting” tab as pointed out in Figure 3.15. In the setting page, the tab “System Setting” needed to be setup first by the control to save the location and video size. The video was set as saved in every 30 minutes. Figure 3.16 explains the setting details. After that, the “Video Setting” tab was selected to

determine the video format to be used and the fps value was then selected where the colour adjustment was ignored, as shown in Figure 3.17. Next, the control panel main page was referred and the number located at the right hand side was clicked on to start recording as pointed out in Figure 3.15. It was enabled by double-clicking the channel screen to enlarge the channel viewer. Figure 3.18 presents the viewer result. Lastly, the recording of video was continued and switched off at 6:30 am.



Figure 3.15 Recording control panel.

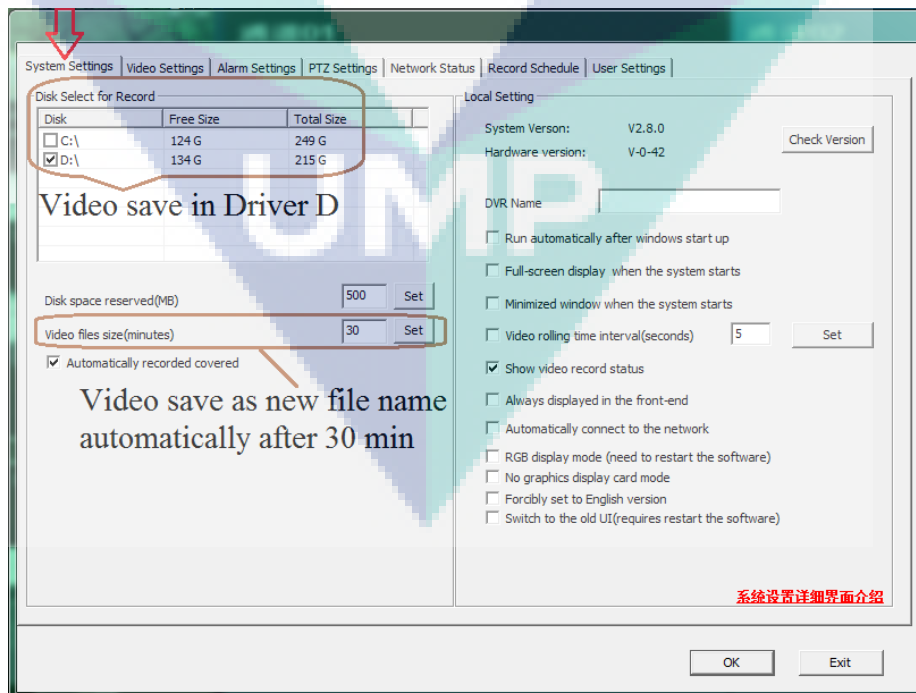


Figure 3.16 System setting.

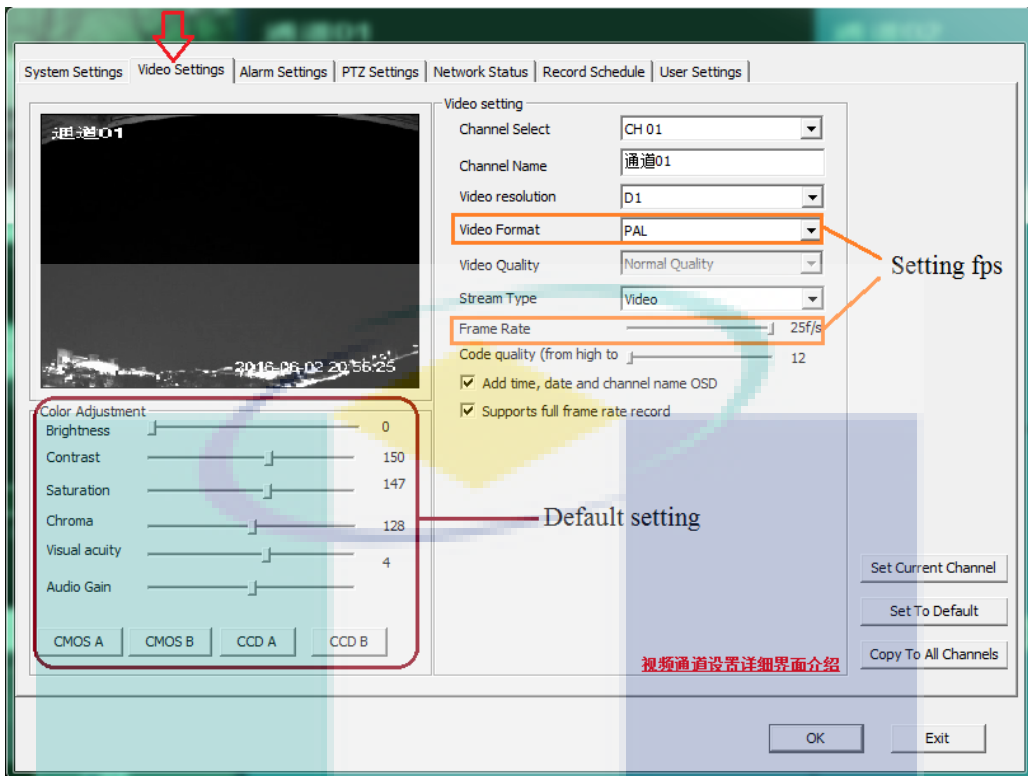


Figure 3.17 Video setting.



Figure 3.18 Channel 1 was enlarged by double-clicking the channel screen.

3.3.4 Frames Extraction

The videos were recorded under two types of video format, .avi and .sv4 using three different digital video recorders (DVR). The .avi type video format was recorded with HD USB 2.0 DVR and UU-DVR while .sv4 type video format was recorded with Jovision (JVS C300Q DVR). Before the extraction was done using

the KM player, the conversion of .avi video format for HD USB 2.0 DVR was needed. After the conversion from .avi format to .mp4 format, the fps increased. In addition, the video format conversion recorded by UU-DVR was not necessary as it was able to playback the videos using KM player easily, with high resolution. On the contrary, an extra software installer named “JFilter” needed to be installed to playback video format .sv4, as stated in the previous sub-topic.

All frames extracted from the video recorded in different formats continued to be processed by using the KM player. The function of frames extract was located at the KM player’s “Main Control” tab. The main control tab was invoked by “right clicking” the mouse at the video display screen. Then, the “Capture” option was chosen from the “Main Control” tab, after which another control tab was invoked. Lastly, a “Frame Extraction” control panel popped out by clicking “Frame Extract”. Figure 3.19 shows the steps to invoke “Frame Extraction”. It enabled setting and control frames extraction through the “Frame Extraction” control panel.

Firstly, the desired folder path that extracted the file to be saved was changed by clicking the “Open” button. Secondly, the image format that needed to be extracted was chosen. Image format “.bmp” was chosen in the project as showed in Figure 3.20. Thirdly, the method was selected with capture image only, as shown in Figure 3.21. Then, the number of frames was extracted continuously and all the images were kept in their original size after the extraction. Next, “Every Frame” button was checked in the “frames to extract column”. Lastly, “start” button was clicked to start the extraction. Both “Frame Extraction” control panel and the video display were ensured to be run at the same time as only then the frame extract can be carried out. The steps and selection process are displayed in Figure 3.22.

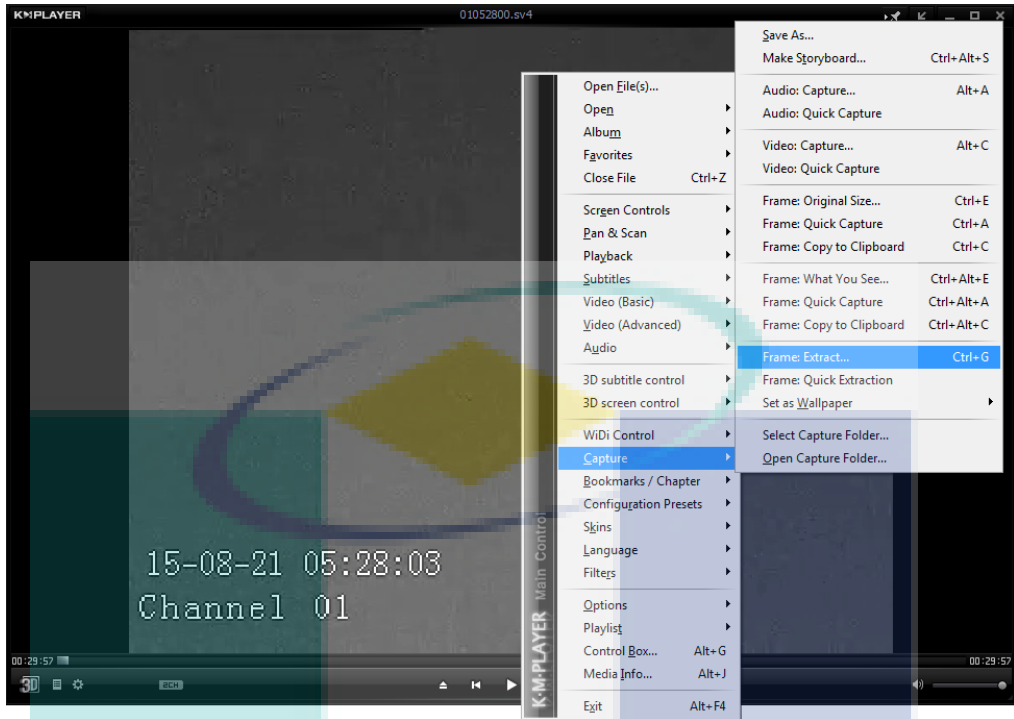


Figure 3.19 Steps to invoke “Frame Extraction”.

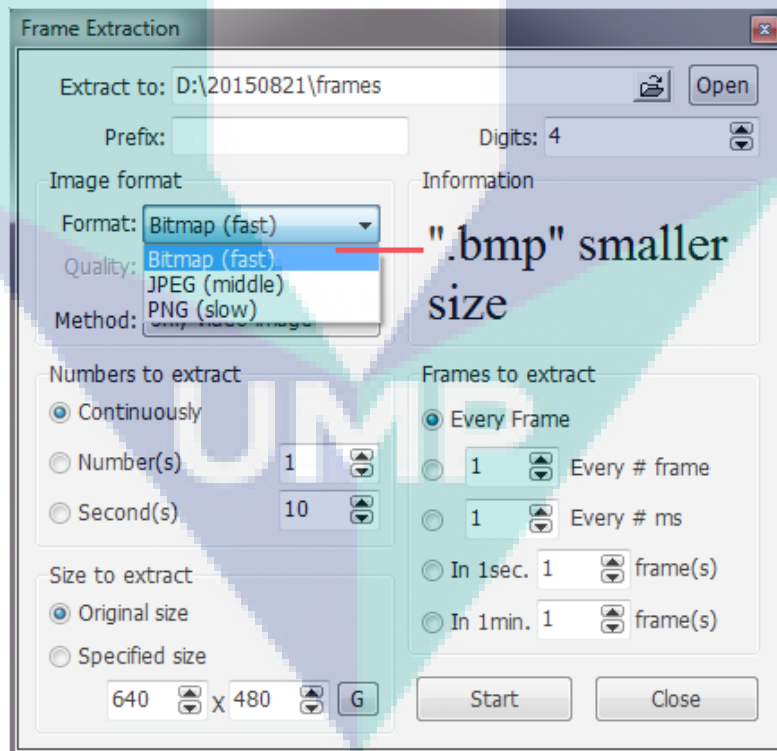


Figure 3.20 Format selection of image frames extracted.

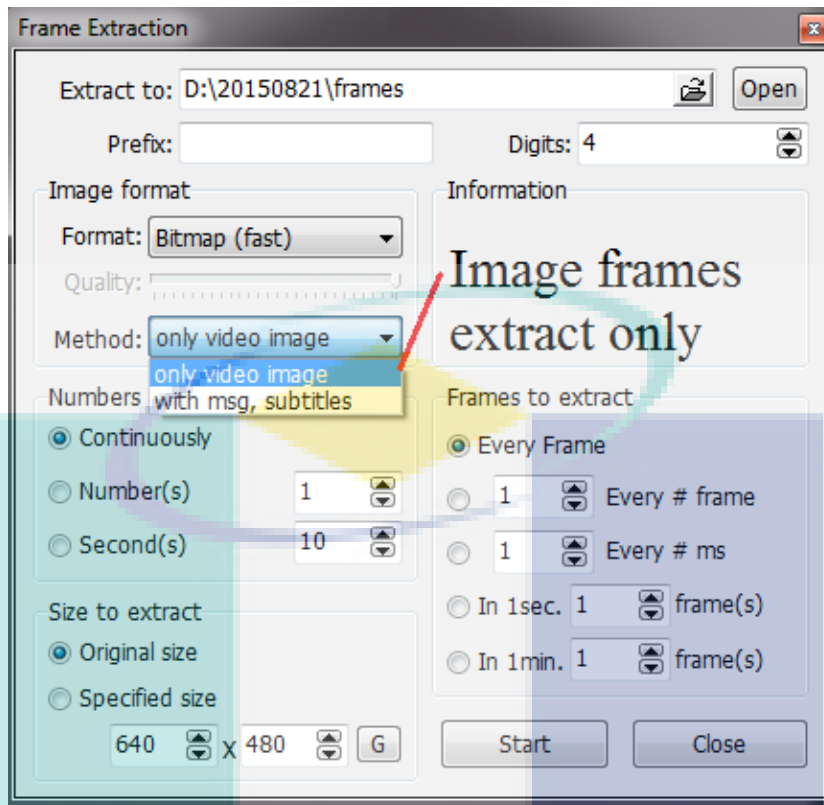


Figure 3.21 Method selection of image frames extracted.

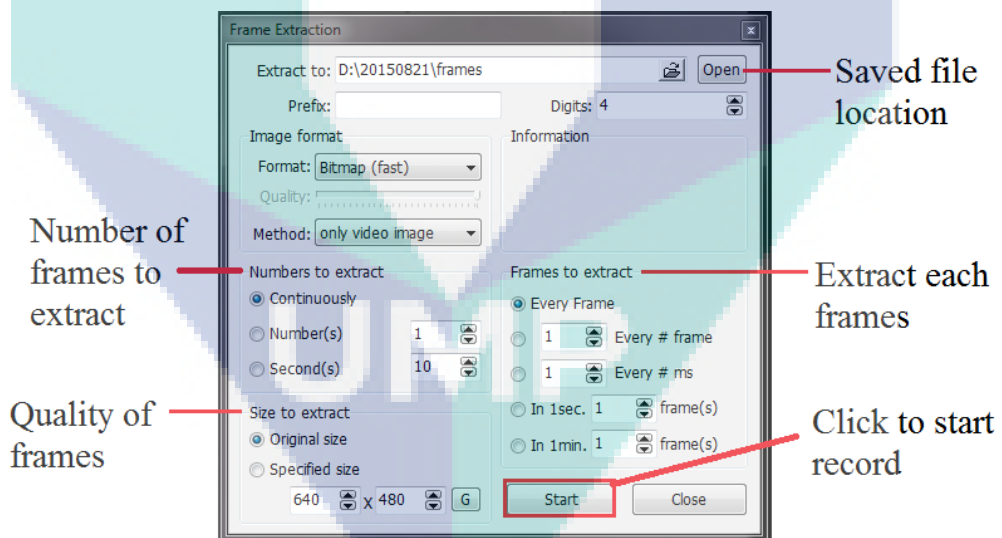


Figure 3.22 “Frame Extraction” setting and control panel.

3.3.5 Frames Rate Calculation

The formula to calculate time acquire for fps is shown in Equation 3.1 below:

$$\begin{aligned} \text{Frames per second (fps)} &= 25, & 3.1 \\ \text{Time acquire} &= 1/25 \\ &= \text{time acquire per frame} \\ &= 40 \text{ ms per frame} \end{aligned}$$

As a conclusion, each image frame was acquired 40 ms.

3.3.6 Angle of View (AOV) Calculation

The calculation of angle of view (AOV) was calculated by using Equation 2.1. A general condition was tabulated to initialise the condition for FOV calculation as in Table 3.3.

Table 3.3 Initial condition for FOV calculation.

Apparatus	Description
Camera sensor (Watec 902H2 = 1/2")	6.4 mm (horizontal) x 4.8 mm (vertically)
Nikon Lens	Focal length: 50 mm
Brinno Lens	Focal length: 24 mm to 70 mm

Nikon lens is a fixed focal length with 50 mm. On the other hand, Brinno lens is an adjustable lens with a focal length from 24 mm to 70 mm. Brinno lens has a wider view compared to Nikon lens. The calculated result is shown in Table 3.4.

Table 3.4 Angle of view with different lenses.

Lens	Angle of View (FOV), β
Nikon (50 mm)	7.3 °
Brinno (24 mm)	15.2 °
Brinno (70 mm)	5.2 °

Nikon lens has a limited AOV. It is capable of observing at 7.3 ° only. In contrast, Brinno lens has a larger AOV and its AOV capability is 5.2 ° to a maximum of AOV of 15.2 °. An illustrated FOV coverage for Nikon lens and Brinno lens is presented in Figure 3.23 and Figure 3.24 respectively.

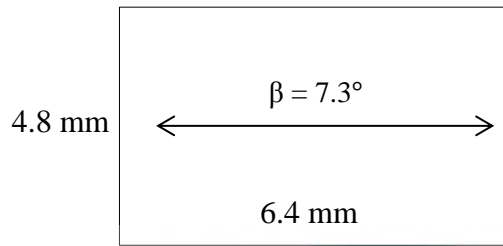


Figure 3.23 FOV coverage of Nikon lens.

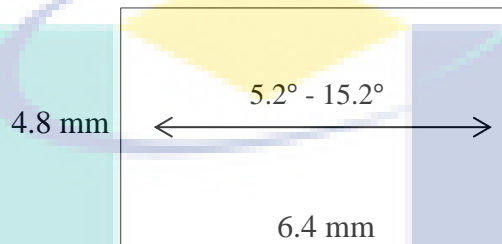


Figure 3.24 FOV coverage of Brinno lens.

The calculation has proven that the AOV for Nikon lens covered a viewer angle at approximately 7.3° while the AOV for Brinno lens covered a viewer angle of within 5.2° until 15.2° . Brinno lens covers a larger viewing field than Nikon lens.

3.3.7 Camera Setting Calculation (Degree)

Based on trigonometry theorems, tangent function was used to calculate the camera angle throughout the research. Equation 3.2 explains the tangent function. The minimum height of 20 km and maximum height of 70 km were chosen for this case where the distance was set at 100 km. The distance is the exact location of lightning. Exact location of lightning should be detected by using B-field antenna system.

$$\tan \alpha = \frac{\text{opposite}}{\text{adjacent}} \quad 3.2$$

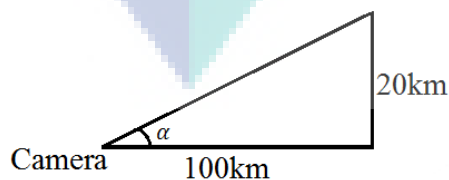


Figure 3.25 Camera condition.

The calculated result of the camera setting in degree is presented in Table 3.5.

Table 3.5 Camera setting's calculated result.

Height Condition (km)	Degree
20	11°
70	37°

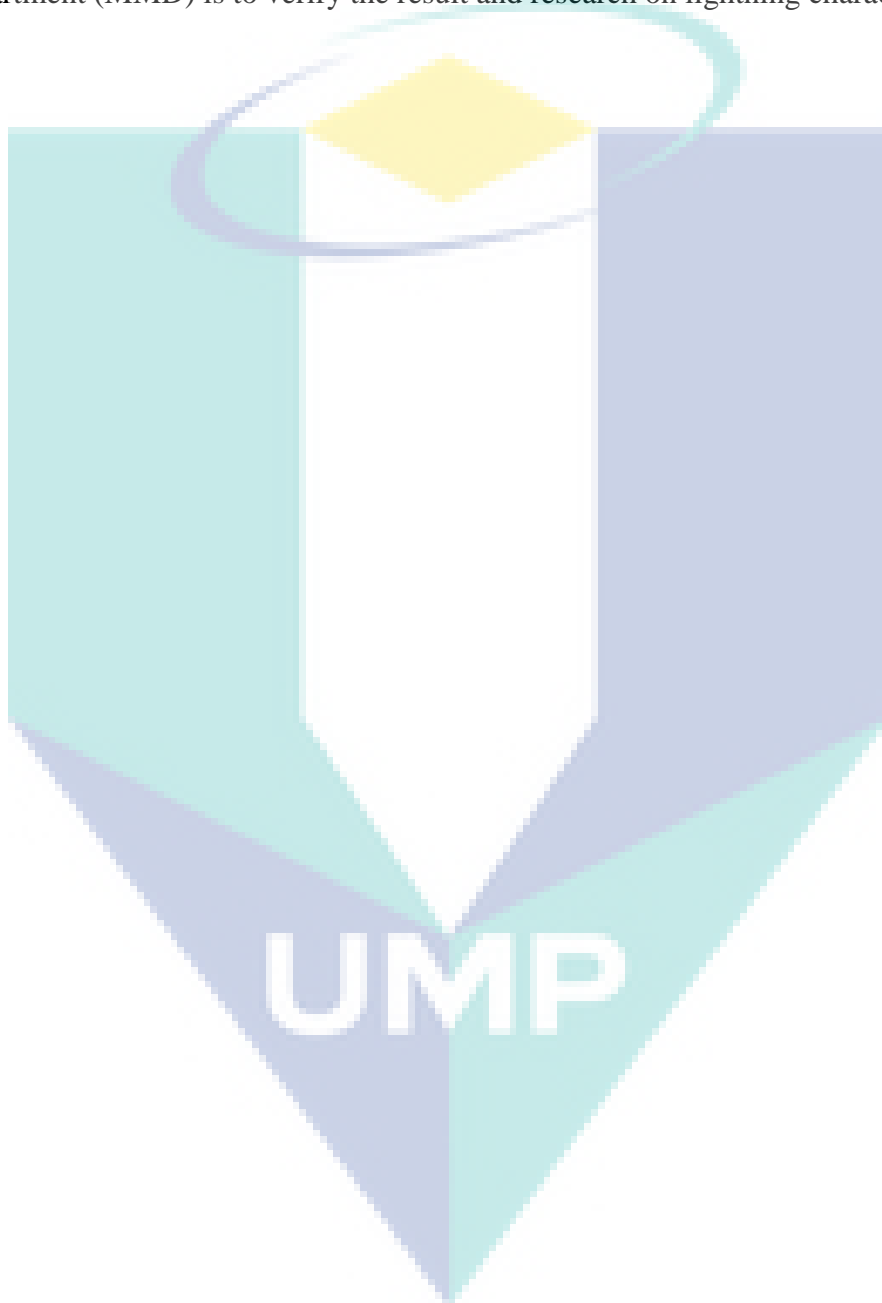
The calculated result of the camera setting in degree was set within the angle of 11° to 37° upward, directed from its point of origin. Figure 3.26 presents the camera setting before recordings began. The readings of the camera degree which was upward directed from its point of origin were noted down every time before the video start recording.



Figure 3.26 The setting of camera shooting upward at 11°

3.4 Summary

Throughout the chapter explained the apparatus used to capture lightning event and the procedure for panel setup. Camera, DVR, and software use to extract frame is explained though the chapter. Data obtained from Malaysian Meteorological Department (MMD) is to verify the result and research on lightning characteristics.



CHAPTER 4

RESULTS AND DISCUSSION

4.1 Introduction

This chapter presents the result of lightning map data collected by Malaysian Meteorological Department (MMD), and the TLEs images captured using the Watec Ultimate 902H2 camera.

The lightning map focused on positive cloud to ground (+CG) lightning only for the year 2015. The data was traced within a radius of 100 km where midpoint was set at Universiti Malaysia Pahang (UMP). It was able to track +CG parent lightning through the lightning map and the results were separated into day and night +CG lightning. Furthermore, a discussion covering most of the +CG events that had occurred within the area is also presented in this chapter.

A series of result was obtained based on the images captured though the images were not clearly visible. Therefore, the analysis was done based on the progress of the frames captured by the Watec camera. The frames were extracted from recorded video and the results are discussed throughout this chapter.

4.2 2015 Lightning Data Analysis from MMD

The following data was analysed according to the percentages of the occurrence of positive cloud to ground (+CG) lightning compared to negative cloud to ground (-CG) lightning for the lightning events in the year 2015. It mainly focused on +CG, especially the number of occurrences of +CG based on monthly and percentages during the day and night times. Furthermore, the highest and the lowest lightning intensity are also discussed in the following sub-topic

4.2.1 Occurrence of +CG Lightning and –CG Lightning from MMD

Lightning data for the year 2015 was analysed based on occurrences of +CG lightning and –CG lightning events by including the number of events that had taken place and the percentages within the radius of 100 km from UMP Pekan campus. A total lightning intensity of 2,602,823.30 kA was recorded in the year 2015. This showed that an average lightning intensity of 7,131.02 kA was recorded daily. The highest lightning intensity of +CG lightning achieved was 100.50 kA while the lowest lightning intensity achieved was 1.90 kA. On the contrary, the highest -CG lightning intensity recorded was up to 140 kA and the lowest lightning intensity was 1.80 kA. Table 4.1 shows the percentage and number of lightning events for the year 2015.

Table 4.1 Percentage of +CG lightning and –CG lightning for the year 2015.

Descriptions	Total Lightning Event	Percentage (%)
Lightning in year 2015	201,296	100.00
Occurrence of –CG lightning	157,200	78.09
Occurrence of +CG lightning	44,096	21.91

Based on the data collected by MMD, the total lightning events recorded within 100 km radius from the midpoint at UMP Pekan was 201,296. -CG lightning constituted 157,200 events or 78.09% while +CG lightning recorded 44,096 events or 21.91%. The result clearly showed that +CG lightning might has lower possibility to occur yet –CG lightning has the capability to be captured easily. This finding confirmed the claim that the percentage of +CG lightning are less than –CG lightning (Rakov and Uman, 2003); (Carey et al., 2003).

4.2.2 Monthly +CG Lightning Events

A bar chart in Figure 4.1 displays the number of +CG lightning for each month. It was found that +CG lightning events occurred most frequently in May with 9065 events, followed by July and August with 8531 and 8266 events respectively. The least number of +CG lightning event was found in February with only 15 events. The result indicated that +CG lightning occurred most frequently during the mid-year period, from May to September. According to Arnone et al. (2008), +CG lightning occurs more often during winter months however the four seasons climate does not exist in Malaysia due to its equatorial location. Instead,

Malaysia experiences rainy season at the end of the year and dry season at the beginning of the year. This indicates that rainy season does not affect the frequency of lightning since it was found to be occurring frequently during dry weather.

Furthermore, Malaysia experiences two types of Monsoon seasons: the Southwest monsoon season and Northeast monsoon season. The Southwest monsoon season spans from May until September while the Northeast monsoon starts from October and ends in March. The Northeast monsoon season brings more rainfall than the Southwest monsoon season (Zawiah et al., 2010). The data in Figure 4.1 shows that most of the +CG lightning in the study area occurred in the mid-year but not during the rainy season. Hence, the rainy season does not have much influence on the frequency of lightning events. The occurrence of lightning event is triggered by the electrostatic charged as previously claimed by Martin A. Uman (2008).

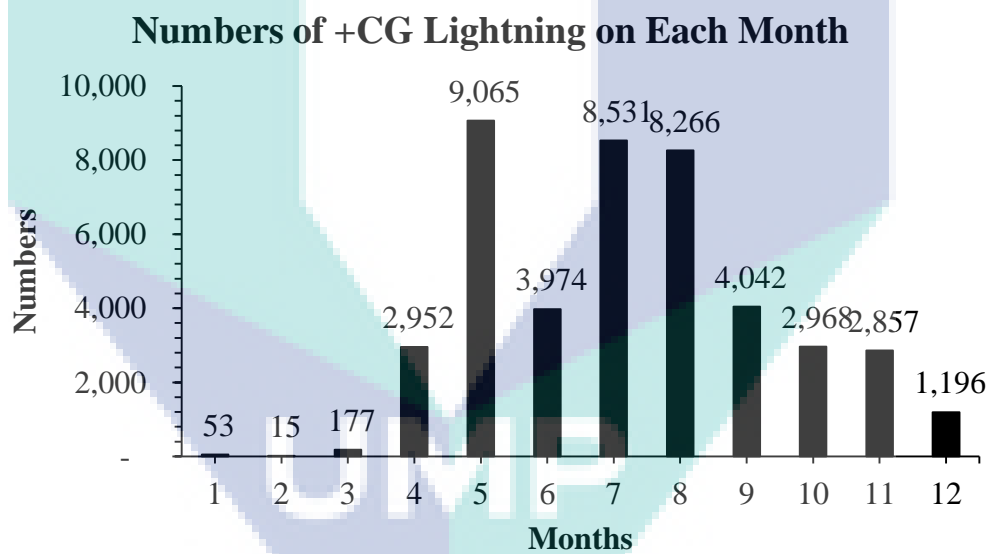


Figure 4.1 Number of +CG lightning for each month in 2015.

A group of data for rainfall events occurring within Pekan area was obtained from Pahang Department of Irrigation and Drainage. This data was used to find the link between the lightning events and rainfall quantity of the area. A combined line and bar chart in Figure 4.2 shows the comparison of rainfall quantity and numbers of lightning occurrence around Pekan area. It showed that the lightning events, including -CG lightning and +CG lightning were inversely proportional to the rainfall quantity. Huge quantities of rainfall were detected towards the end of the

year, starting from October 2015 to December 2015 which was during the Northeast Monsoon season. However, the total number of lightning events showed a decrease during the same period.

May 2015 had the highest lightning events with less rainfall. July 2015 showed the least amount of total rainfall, yet the total lightning events reached a higher rate. From the results' analysis of the real time data where the occurrences of lightning events were recorded, it was clearly proven that the frequency of lightning occurrence is not related to the amount of rainfall.

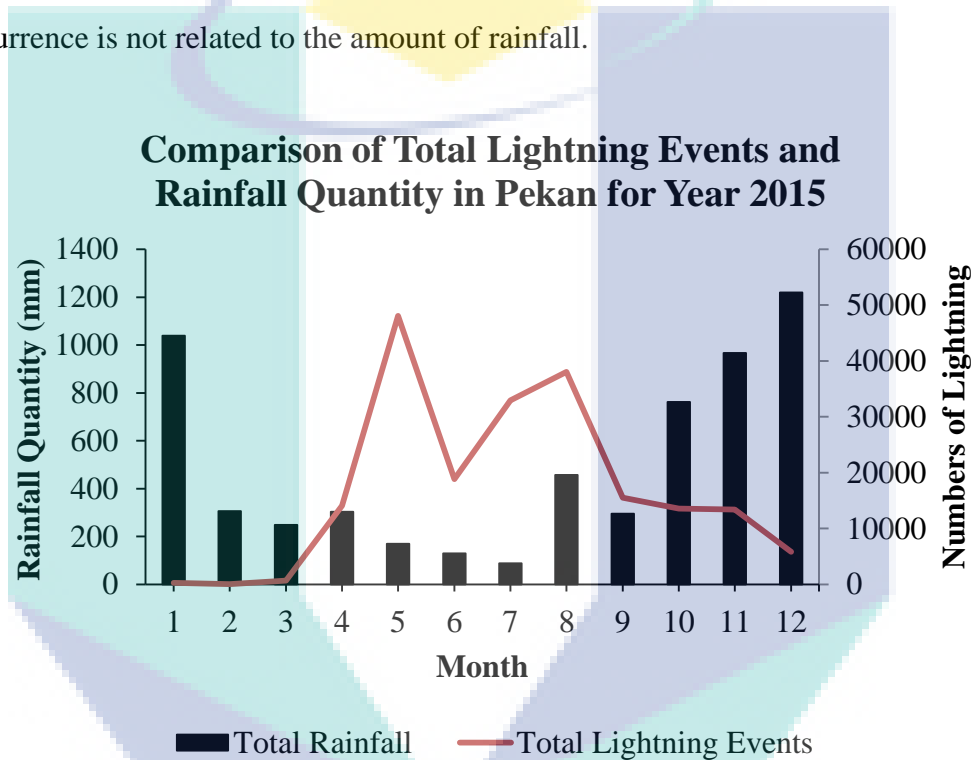


Figure 4.2 Comparison of total lightning events and rainfall quantity in Pekan in Year 2015.

Monthly percentage of +CG lightning events on day and night calculated based on the total number of +CG lightning from overall percentage. The equation as below:

$$\% \text{ of } +CG \text{ Lightning} = \frac{\text{No. of Lightning}}{\text{Total } +CG \text{ Lightning}} \times 21.91\% \quad 4.1$$

Table 4.2 Percentage of +CG lightning for day time and night-time in Pekan for 2015.

Month	Day (%)	Night (%)
1	0.02	0.01
2	0.00	0.01
3	0.06	0.03
4	1.11	0.36
5	2.68	1.83
6	1.11	0.86
7	1.52	2.72
8	1.24	2.86
9	0.76	1.25
10	0.58	0.89
11	0.63	0.79
12	0.30	0.30
Total	10.01	11.90

Although +CG lightning events occurred most intensely in May as shown in Figure 4.1, it was found that the +CG lightning events occurred the most at night in the months of July and August as shown in Table 4.2. The total percentage during day was 10.01% while at night was 11.90%. The result obviously shows that the majority of +CG lightning events occurred at night. The percentage of occurrences for +CG lightning events during night-time in August and July were 2.86% and 2.72% respectively in compared with -CG lightning, followed by May (1.83%) and September (1.25%). The least +CG lightning events at night was recorded in January and February which was 0.01%.

Figure 4.3 displays the percentage of +CG lightning for the day and night times in a graph. It can be seen clearly that +CG lightning events occurred frequently during the day in the first half of the year, from January to June. In the same way, +CG lightning events were more often at night from July to November. December almost had same quantity of +CG lightning events in day as well as night times. According to Serge Soula et al. (2009), Lyons et al. (2003), and Victor P. Pasko et al. (2012), Sprites produce a +CG lightning flashes when they occur. Hence, this research targeted +CG lightning events during night time during the second half of the year, especially during the months of July and August as these periods were found to be more suitable to capture the required data, as shown in Figure 4.3.

Percentages of +CG Lightning on Day and Night

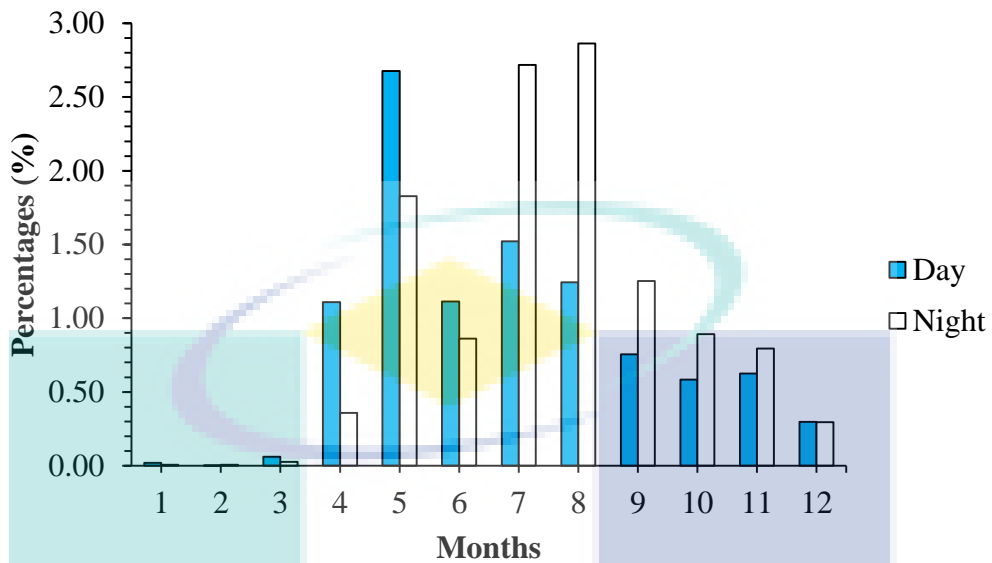


Figure 4.3 Percentages of +CG lightning in the day and night times.

4.3 Lightning Map Analysis for 2015

The lightning map result mainly focused on positive cloud to ground (+CG) lightning. The analysis were separated into two sections, namely the monthly day and night occurrences of +CG lightning and the yearly occurrences of +CG lightning. Duration for daytime and night-time was set to be within 7:00 am to 6:59 pm and 7:00 pm to 6:59 am respectively. Lightning events occurring within the specific time were considered as a group. In addition, the lightning direction was divided into eight groups: East, South, West, North, South-east, South-west, North-west, and North-east to differentiate the exact parent lightning of +CG lightning locations. Detailed information on the direction is shown in Figure 4.4.

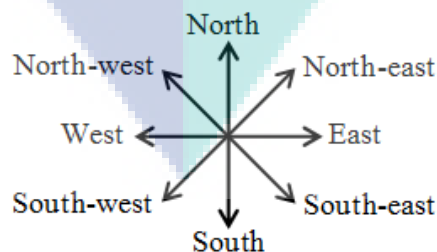


Figure 4.4 Vastu directions.

4.3.1 Day and Night Lightning Map for 2015

Day and night lightning maps were formed to detect the exact location of events of parent lightning for positive cloud to ground (+CG) lightning. It was divided into different groups based on the month – from January to December.

January recorded the least number of +CG lightning events as shown in Figure 4.5. +CG lightning happened between the directions of South (180°) and Southwest (225°) during daytime. However, they occurred between the directions of Southeast (135°) and South (180°) in the night-time. It was also found that a large quantity of the +CG lightning events occurred during daytime more than night-time.

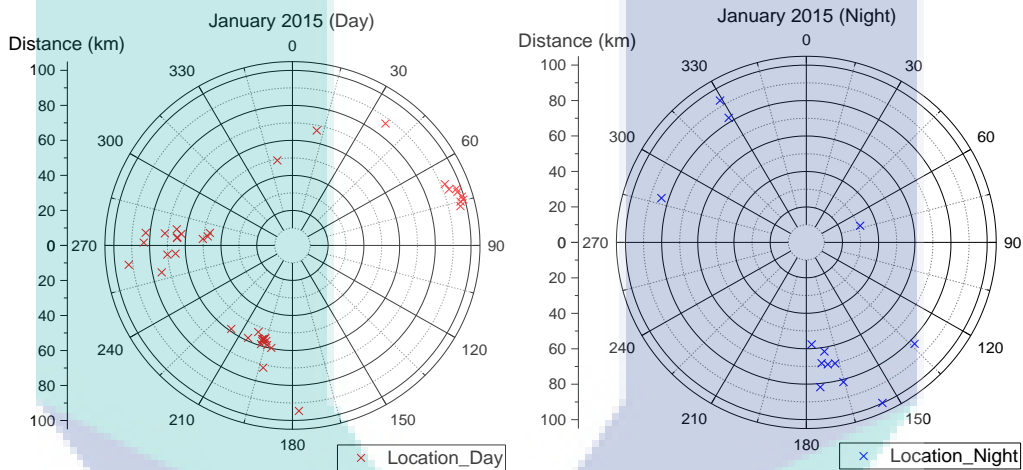


Figure 4.5 Day and night lightning map for January.

February experienced lesser +CG lightning events than January. There were only 15 events as pointed out in Figure 4.1, whereas Figure 4.6 clearly shows that the site experienced 15 +CG lightning events. It occurred between the directions of North (0°) and North-west (315°) during daytime and South-west (225°) and North-west (315°) during night-time.

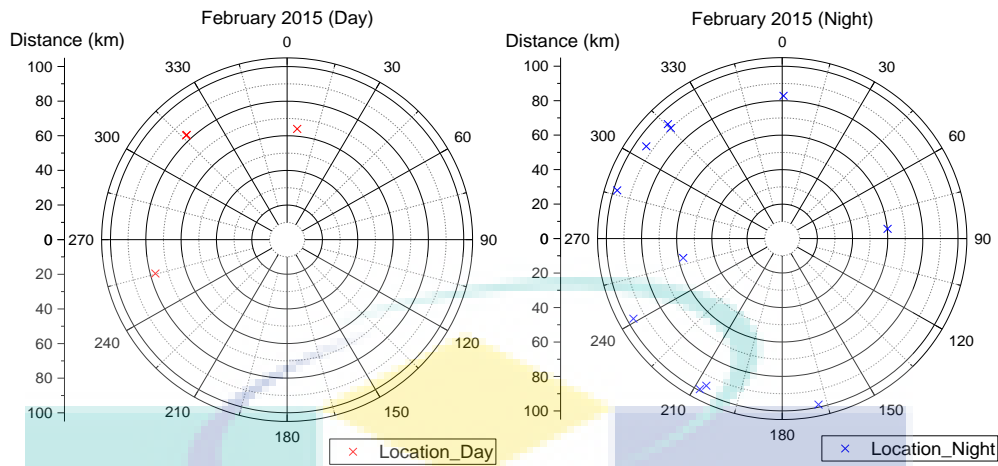


Figure 4.6 Day and night lightning map for February.

Most of the +CG lightning events occurred between the directions of South-west (225 °) and North-west (315 °) during the daytime and between North-west (315 °) and North-east (45 °) during the night-time in March. Details of the lightning locations are presented in Figure 4.7. It was also found that +CG lightning events occurred frequently during the daytime in March. March retained more +CG lightning events compared to January and February. January, February, and March can be grouped under the dry season with less rainfall during the months.

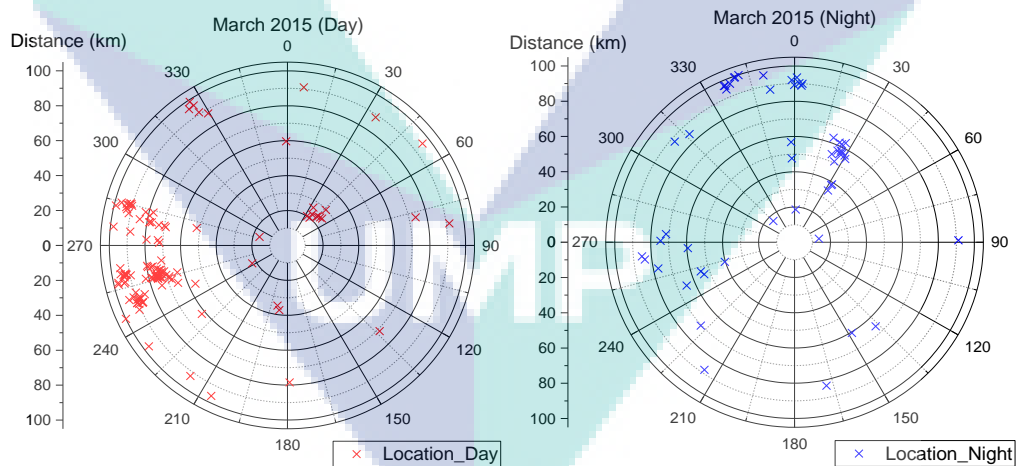


Figure 4.7 Day and night lightning map for March.

More lightning events occurred in April as compared to January, February, and March. This is due to the Southwest monsoon season that was bound to take over the dry season in the coming months. Most of the events that took place were near the western area, between South-west (225 °) and North-west (315 °) during the daytime. However, the events happened between the directions of North-west (315 °)

and East (90°) during night-time. The +CG lightning events mostly occurred during the daytime compared to the night-time. Figure 4.8 points out the location of +CG lightning events during the daytime and the night-time.

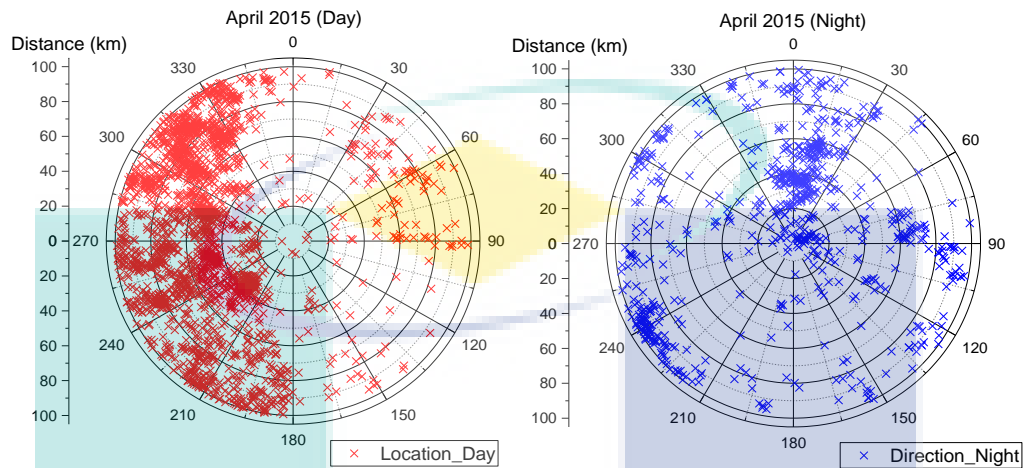


Figure 4.8 Day and night lightning map for April.

+CG lightning events in May occupied the West from the directions of South (180°) to West (270°) to North (0°) during daytime. In the same way, it covered areas between South-west (225°) and West (270°) during night-time. These show that +CG lightning occurred repeatedly during daytime as shown in Figure 4.9. Additionally, +CG lightning events increased dramatically in May compared with previous months. In summary, this may be caused by the approach of the Southwest monsoon season on the specific month whereby the rainfall during the daytime increased.

UMP

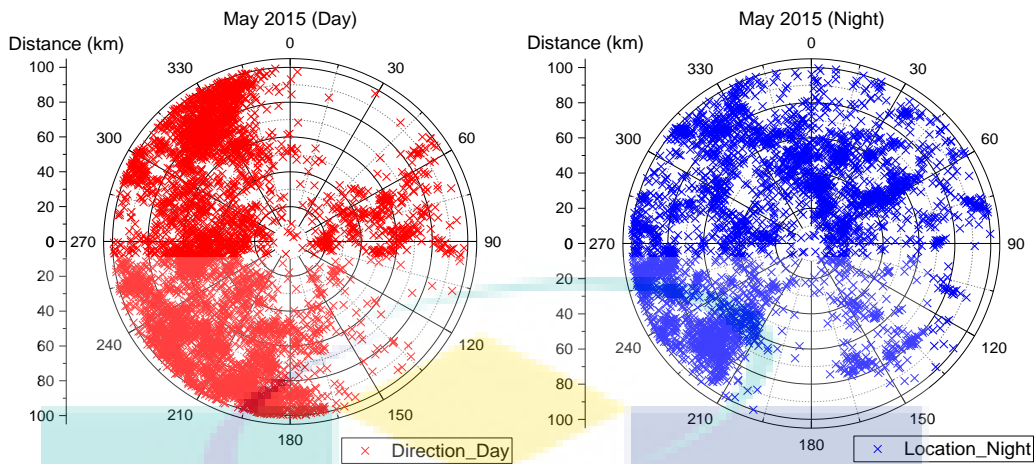


Figure 4.9 Day and night lightning map for May.

More +CG lightning events occurred in June during the daytime compared to the night-time as pointed out in Figure 4.10. +CG lightning in June was observed to have regularly occurred between South-west (225 °) and North-west (315 °) during the daytime. Nevertheless, it occurred in two directions: between South (180 °) and South-west (225 °), and between North (0 °) and North-east (45 °) during the night-time. The occurrences of +CG lightning events in June decreased compared to May.

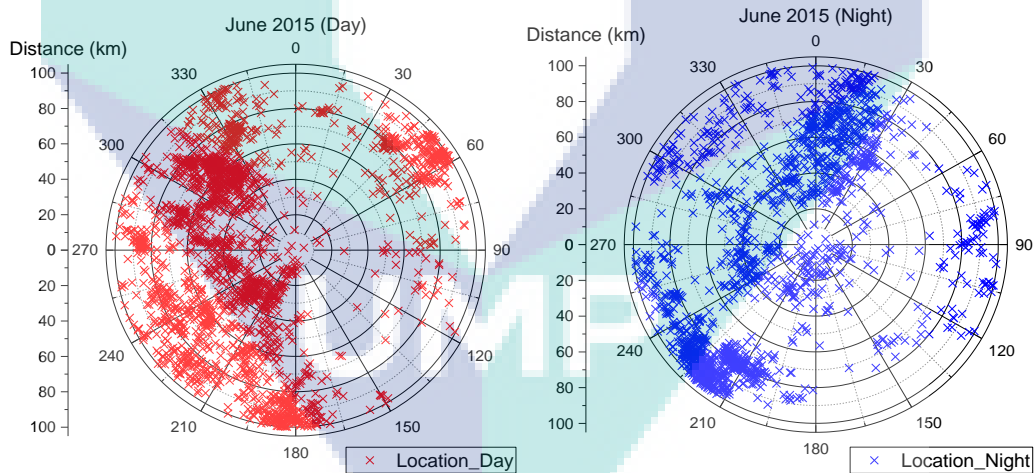


Figure 4.10 Day and night lightning map for June.

The +CG lightning events occurred more frequently during the night-time from July onwards as presented in Figure 4.11. It occurred frequently between South (180 °) and West (270 °) during the daytime and between North-west (315 °) and North-east (45 °) during the night-time. It was also found that July recorded the most +CG lightning events during the night-time compared to the previous month. To

conclude, July showed the potential for TLEs to be captured and the camera was set to be pointing to the directions between North-west (315 °) and North-east (45 °).

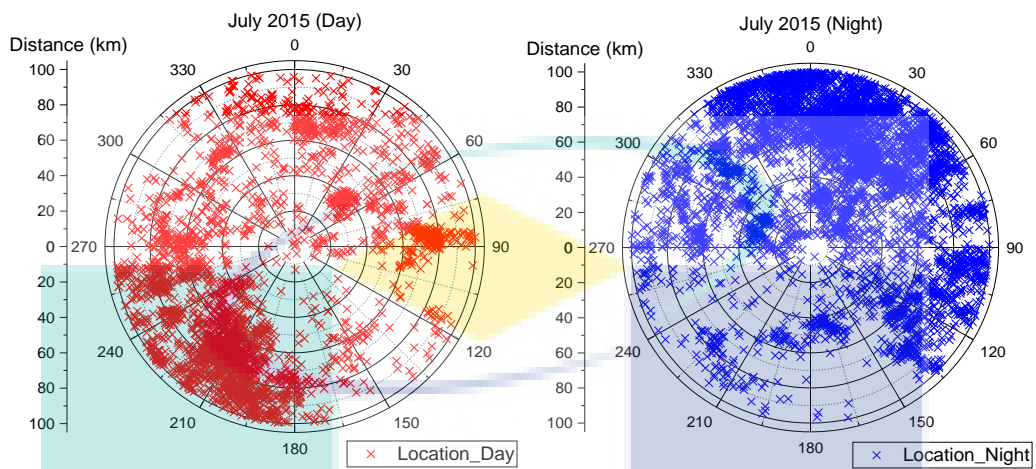


Figure 4.11 Day and night lightning map for July.

August occurred more +CG lightning events during night-time compared to daytime as observed from Figure 4.12. The lightning occurred repeatedly from directions South (180 °) to West (270 °) during daytime yet it repeatedly occurred from directions North-west (315 °) to East (90 °) during night-time. On the other hand, August experienced lesser lightning events on day while increased quantity of lightning events on night compared to July. In short, due to TLEs only can observe during night-time, hence, directions from North-west (315 °) to East (90 °) are suitable used to observe TLEs in August.

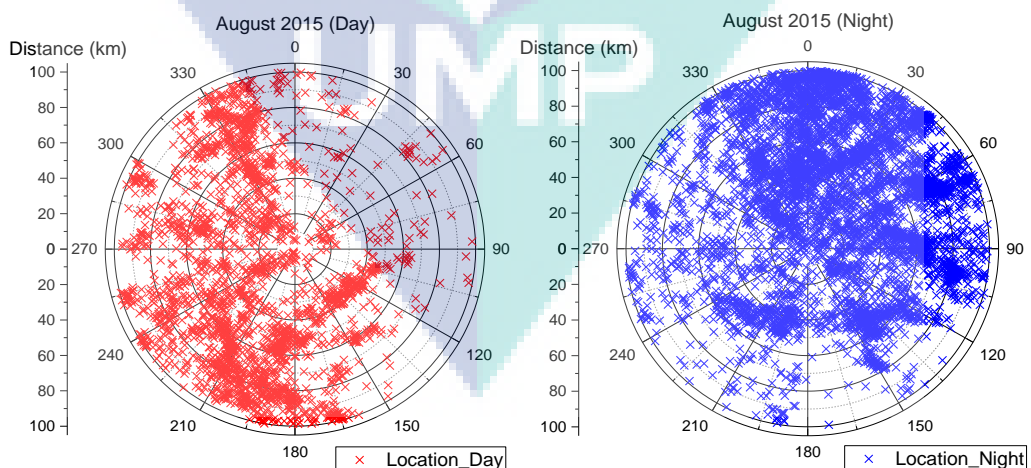


Figure 4.12 Day and night lightning map for August.

September experienced +CG lightning events as shown in Figure 4.13. It was found that +CG lightning events mostly covered the directions from North-west

(315°) to North (0°) and from North-east (45°) to East (90°) during the daytime. Similarly, it mostly occurred in the directions of North (0°) and North-east (45°) during the night-time. Moreover, +CG lightning events at night were more frequent than in the day. In comparison with previous months, especially July and August, September had lesser +CG lightning events in both the day and night times. This might be due to the end of the Southwest monsoon season in September. In brief, September was still found as a suitable month to observe TLEs due to the quantity of lightning events at night compared to the daytime.

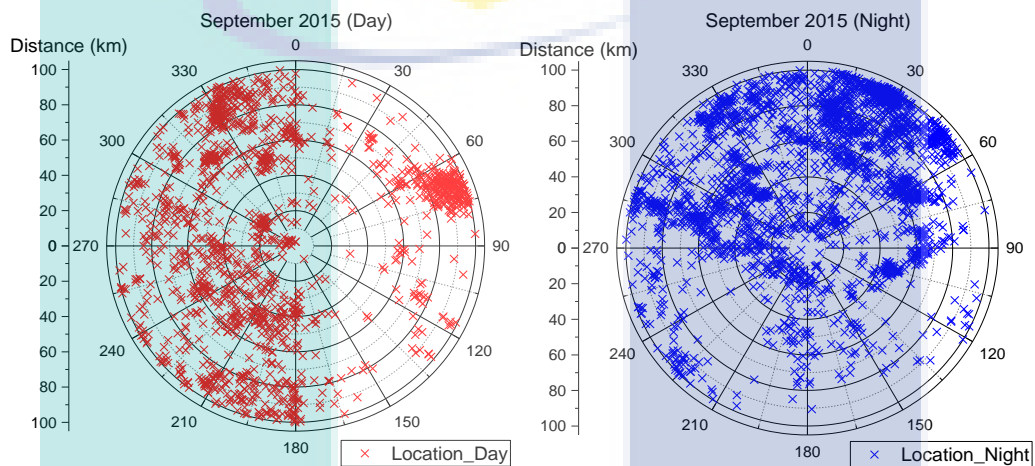


Figure 4.13 Day and night lightning map for September.

Lightning map for October is illustrated in Figure 4.14. The figure shows that the quantity of +CG lightning events decreased significantly compared to September. In October, +CG lightning events occurred between North-west (315°) and North (0°) during the daytime and between North-west (315°) to East (90°) during the night-time. Both +CG lightning conditions were not consistent and it may be due to the commencement of the Northeast monsoon season in October. Therefore, +CG lightning events in both the day and night times were mostly the same quantity. In summary, October can be considered as a suitable month to observe TLEs, yet the success of the observation decreased.

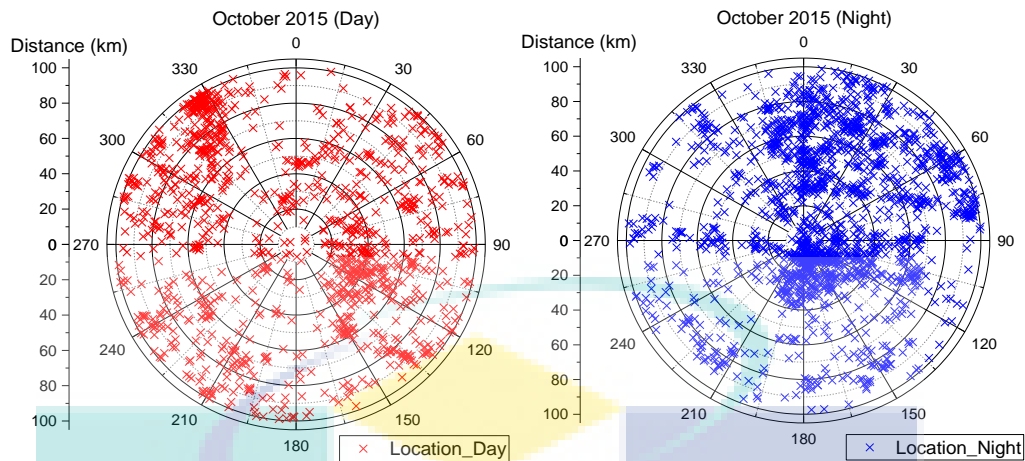


Figure 4.14 Day and night lightning map for October.

November experienced mostly similar quantity of +CG lightning events with October. The frequency of occurrence was fairly distributed for both the day and night times which as in November. However, they appeared in different locations. During the daytime, lightning events normally happened between South-west (225 °) and North-west (315 °) while lightning events occurred between North-west (315 °) and North-east (45 °) at night. November is the month that experiences the Northeast Monsoon season and the quantity of rainfall only increases, as stated by Zawiah et al. (2010). Thus, November showed a lesser possibility of occurrences of +CG lightning events compared to previous months. Figure 4.15 showed +CG lightning events in November 2015.

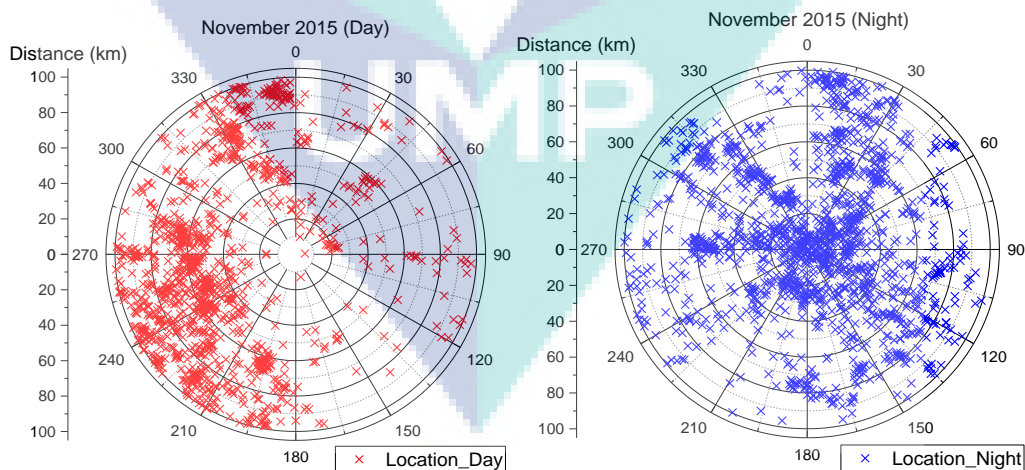


Figure 4.15 Day and night lightning map for November.

December recorded lesser +CG lightning events than November. Both day and night conditions were almost the same. The events occurred repeatedly in the

directions of South (180°) to South-west (225°) and North (0°) to North-east (45°) during the daytime. However, +CG lightning events occurred repeatedly in different directions during the night-time, between North-west (315°) and North-east (45°) and South-east (135°) and South (180°). The +CG lightning events decreased dramatically in December. Again, this might be due to Northeast Monsoon season with the increase in the rainfall conditions. In fact, December showed a low possibility to observe TLEs. Figure 4.16 indicates +CG lightning events in December 2015.

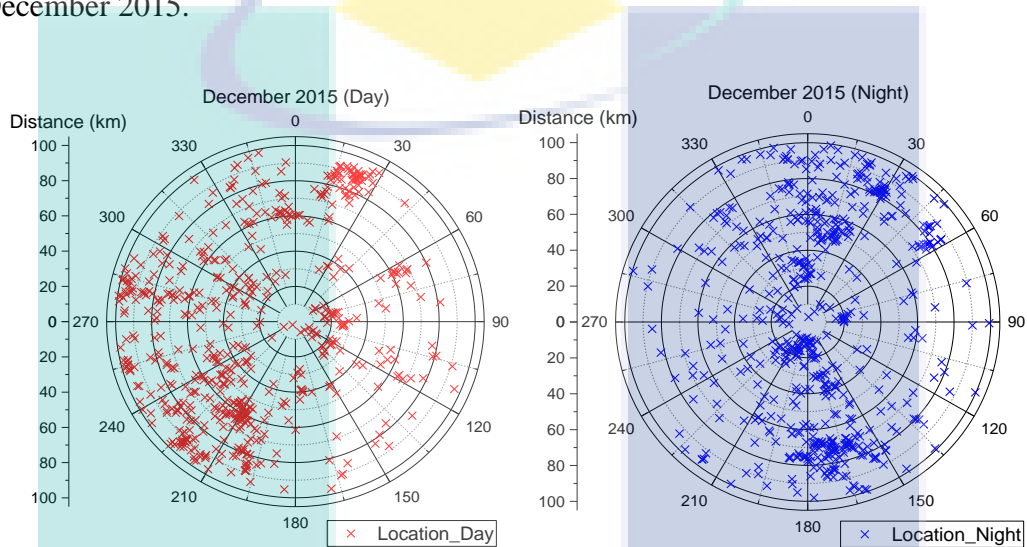


Figure 4.16 Day and night lightning map for December.

4.3.2 2015 Lightning Map Obtained from MMD Data

The daytime +CG lightning map for 2015 indicated that the lightning events happened around the western area of UMP Pekan campus frequently, as shown in Figure 4.17. It was also found that +CG lightning events occurred above the land's surface area more often than above the sea's surface as shown in Figure 4.17 and Figure 3.4 respectively. +CG lightning events during the daytime in 2015 also occurred near the seaside and above the sea's surface. Both conditions may have activated the occurrences of Gigantic Jets, Blue Jets, and Elves as reported by Chen et al. (2008).

+CG lightning events were also detected in the night-time, as illustrated in Figure 4.18 for the year 2015. The majority of +CG lightning events occurred around the North (0°) area from UMP Pekan campus. During the night-time, the quantity of +CG lightning were fairly detected on land surface, coastal surface, and

ocean surface. In summary, the camera was pointed toward the Northern (0°) zone from the campus location. Last but not least, the possibility occurrences of TLEs around UMP Pekan campus are deemed possible.

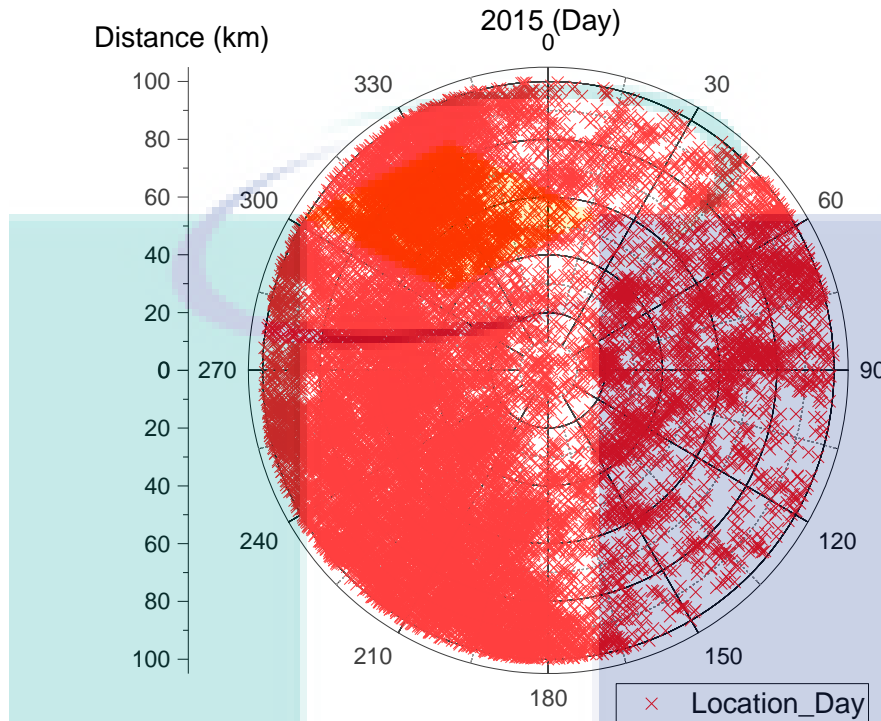


Figure 4.17 Daytime lightning map for 2015.

UMP

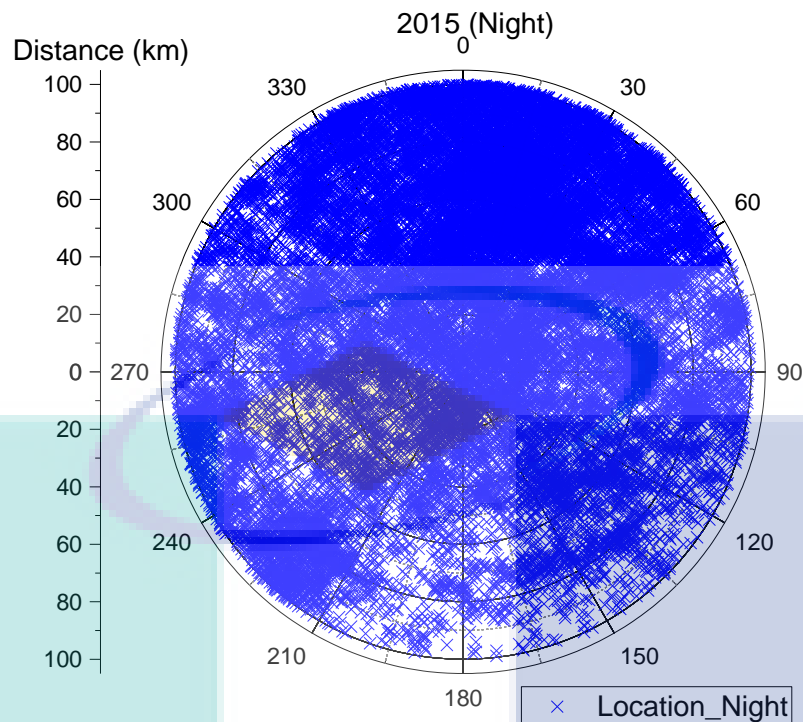


Figure 4.18 Night-time lightning map for 2015.

4.4 Image Capture Analysis

The image captured using the camera and the Digital Video Recorder (DVR) and the analysis are discussed in the following sub-topics.

4.4.1 Unknown Discharge Lightning Event

An unknown discharge lightning event was detected on 2nd July 2015 in the night time at 21:19 pm by using HD USB 2.0 DVR. Only the head of the unknown event was observable. The full view of the unknown event was not observable may be due to the condition of the clouds and the camera location on the ground. The evolution of an unknown event up to the discharge time of $t = 120$ ms above a thundercloud was filmed at 25 frames per second (fps) as shown in Figure 4.19. Before the unknown event was captured, there were 41 lightning events observed in the camera recording.

At the beginning of the recording, a lightning return stroke started to transport electrical charge to earth and the electric field produced had formed an event. The “head” of the unknown discharge lightning event observed appeared as a clot and was small in shape due to the panel set up location near to where the event

took place. The combination of bright “head” with a thin “hair” was similar to the result obtained by M. Hayakawa et al. (2012).

The unknown discharge lightning event began to discharge and shot down from the ionosphere at $t = 40$ ms. Then, the discharge was directed downward from the parent lightning flash at $t = 80$ ms. Lastly, the unknown discharge activity event disappeared at $t = 120$ ms. The lightning discharged process were similar to those stated by Martin A. Uman (2008). According to the fps calculation, the whole discharging process took approximately 160 ms. This finding is different with the result obtained by M. Hayakawa et al. (2012) whereby the duration of Sprite was approximately 5 s to 30 s. The unknown discharge lightning appeared after many clouds to ground (CG) lightning events had occurred and the current event was detected as +CG lightning discharged based on the observation. The finding is similar with Serge Soula et al. (2009), Lyons, et al. (2003), and V. P. Pasko et al.'s (2012) which reported Carrot Sprites have the characteristics with diameter less than 1 km, occurred at altitude from 20 km to 95 km, duration of occur is less than 16 ms or 5 s to 30 s, and it triggered by weak +CG produced. The unknown discharge lightning has the characteristics with diameter 0.37 km at altitude 24.3 km from earth surface. Duration of occur is approximately 160 ms. Hence, the unknown discharge lightning event most probably is a Carrot Sprite.

A localisation of the unknown discharge activity event is presented in Figure 4.20. The figure demonstrated unknown discharge lightning only during the night-time on 2nd July 2015 and it showed that most of the lightning events occurred between the directions of North-west and North-east, while the unknown discharge lightning event was detected in the directions of West (270 °) and North-west (315 °). The unknown discharge lightning event was observed in July.

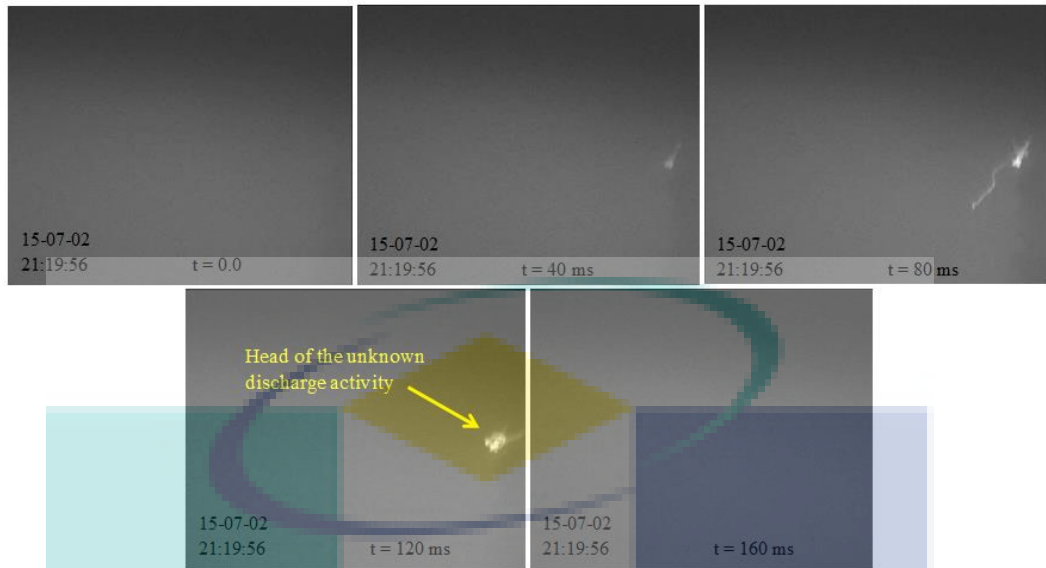


Figure 4.19 An unknown discharge activity event observed on 2nd July 2015 at 21:19 pm.

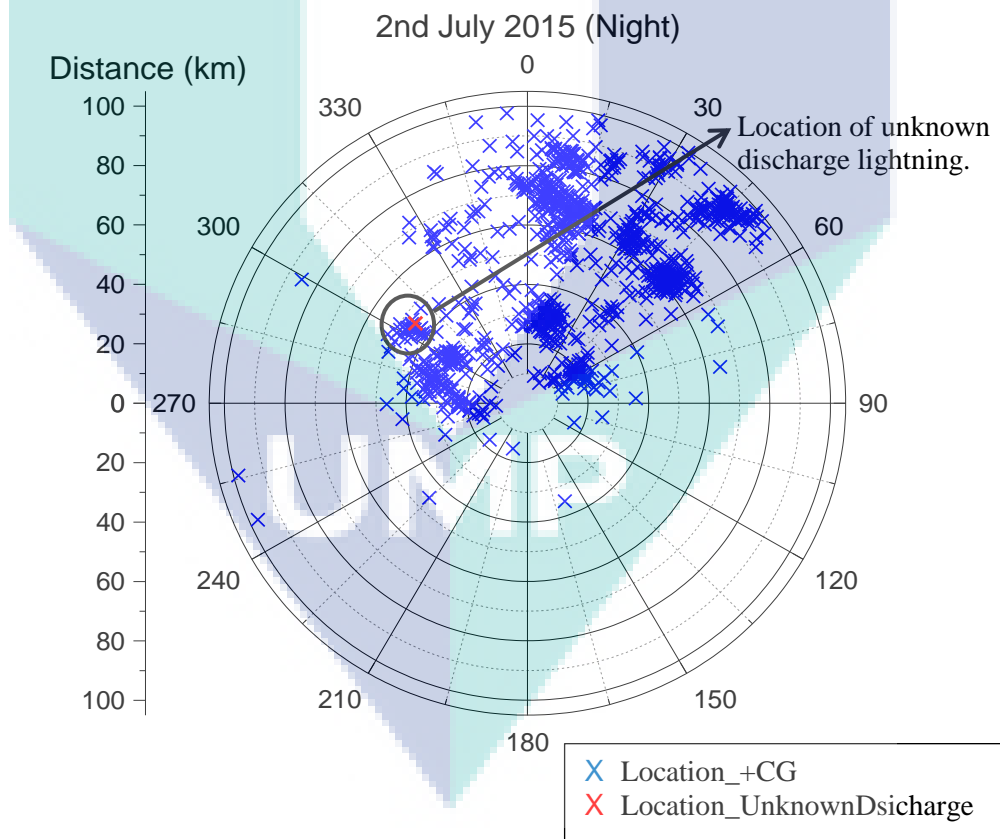


Figure 4.20 Location of unknown discharge lightning event in the lightning map.

4.4.2 Unknown Discharge Lightning Event Data Analysis

The time data presented in Figure 4.19 was compared with Malaysian Meteorological Department (MMD) to find out the details of unknown discharge lightning event. The data shown in Table 4.3 was extracted according to the time zone identified in Figure 4.19 and the lightning event was coordinated with the same lightning event that occurred on 2nd July 2015 during the night-time.

Table 4.3 Lightning event information.

Date	Time (MST)	Coordinate		Intensity (kA)	Lightning From Centre Point	
		Latitude (°N)	Longitude (°E)		Direction (°)	Distance (km)
2/7/2015	8:47:09 PM	3.789	103.077	-17.1	305.3	48.1
2/7/2015	8:52:14 PM	3.780	103.135	-17.4	309.3	42.3
2/7/2015	8:53:28 PM	3.782	103.134	-18.1	309.3	42.6
2/7/2015	8:53:29 PM	3.784	103.131	-12.2	309.3	42.9
2/7/2015	9:13:41 PM	3.782	103.096	-7.6	306.1	45.9
2/7/2015	9:16:08 PM	3.783	103.086	-11.9	305.4	47.0
2/7/2015	9:16:08 PM	3.785	103.084	-11.4	305.4	47.3
2/7/2015	9:16:08 PM	3.784	103.084	-9.8	305.4	47.2
2/7/2015	9:16:08 PM	3.789	103.090	-10.4	306.3	46.9
2/7/2015	9:19:50 PM	3.788	103.107	-12.1	307.7	45.4
2/7/2015	9:19:50 PM	3.780	103.098	+4.8	306.0	45.7
2/7/2015	9:19:50 PM	3.788	103.107	-10.0	307.6	45.3
2/7/2015	9:19:50 PM	3.782	103.103	-21.9	306.6	45.2
2/7/2015	9:24:04 PM	3.784	103.099	-4.4	306.5	45.8
2/7/2015	9:29:17 PM	3.787	103.094	-4.1	306.5	46.5
2/7/2015	9:35:23 PM	3.782	103.089	-11.2	305.5	46.6
2/7/2015	9:38:19 PM	3.781	103.055	-4.8	302.9	49.6

The unknown discharge lightning took place at latitude 3.78 °N and longitude 103.098 °E, as highlighted in Table 4.3. The location of the coordinate was defined well, namely between Sungai Tulang and Sungai Belat, Gambang, Pahang. It was located 45.7 km away from UMP Pekan Campus. The intensity represented the characteristics for each lightning events where negative (-) represents -CG lightning and positive (+) represents +CG lightning. Many -CG lightning events that occurred before as well as the only one +CG lightning event that occurred during the time before 9:19:50 pm. According to Sentman et al. (1995), a large peak current would be detected during the occurrences of Sprite with the corresponding instantaneous power of between 0.5 MW and 2.5 MW, whereas, a peak current of 4.8 kA was detected for the specific event of this observation. Hence, the possibility of the

unknown discharge lightning event to be Carrot Sprite is further strengthened. The lightning information in Table 4.3 showed that a thunderstorm began at 8:47:09 pm and ended at 9:38:19 pm. The thunderstorm ended with the occurrence a few –CG lightning after +CG lightning was triggered. This event is parallel to the statement reported by (Pawar and Kamra, 2004) that +CG lightning occurs during the last stage of thunderstorms.

The unknown discharge lightning occurred at altitude 24.3 km. This was calculated using the formula stated in Eq. (3.2). Camera angle pointed upward to the sky, α , was 28° and the value set before the theory of observation stated in Figure 3.12 was defined. The altitude result was different with the result concluded by Sentman et al. (1995) and V. P. Pasko et al. (1996) where Carrot Sprite can spread as high as 95 km. However, the Carrot Sprite like event observed in this research spread at the approximate altitude of 24.3 km.

4.4.3 Unknown Discharge Lightning Calculation

An initial condition was set up as described in the following subtopic to validate the method to find out the actual size of the unknown discharge lightning. In addition, the same method was applied to find out the actual size of the unknown discharge lightning in subtopic 4.5.3.2.

4.4.3.1 Initial Condition

An initial condition was tabulated in Table 4.4.

Table 4.4 Initial condition for image calculation.

Description	Condition
Camera lens, d_1	50 mm
Distance between camera and the object, d_2	200 cm, 300 cm, 400 cm, 500 cm, 600 cm, 700 cm, 800 cm, 900 cm, and 1000 cm
Height	0
Camera degree	0°
Object actual size	17.4 cm (H) x 14.4 cm (V)

An illustration of the camera setup is shown in Figure 4.21. As indicated in Figure 4.21, 50 mm focal length, d_1 , with d_2 at 200 cm were set for the actual FOV; hence, the ratio of distance between the camera sensor to the lens, d_1 and the lens to the object, d_2 , is 4 cm mm^{-1} as calculated in Equation 4.1. The ratio of d_1 and d_2 is

changeable by replacing different actual FOV, as shown in Table 4.4. Next, the camera sensor size is shown in Figure 4.22. This is to find out the actual object size that was displayed on the monitor by passing it through the camera sensor.

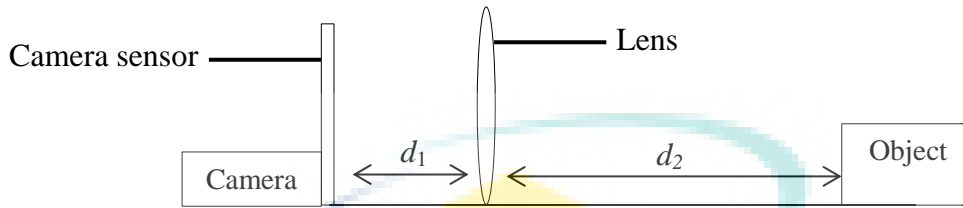


Figure 4.21 Illustration of the camera setup.

The ratio of the distance between the camera sensor to lens, d_1 and the lens to the object, d_2 , can be calculated as shown in Equation 4.1 below:

$$\begin{aligned}
 d_1 : d_2 & \\
 50 \text{ mm} : 200 \text{ cm} & \\
 1 \text{ mm} : 4 \text{ cm} & \\
 1 : 4 \text{ cm mm}^{-1} &
 \end{aligned}
 \tag{4.1}$$

4.8 mm
(c_2)

6.4 mm (c_1)

Figure 4.22 Camera sensor size.

Figure 4.23 show the actual object size displayed on the monitor screen. The full frame pixel of the image is 720 pixels (H) and 576 pixels (V) while the object covered 246 pixels (H) and 224 pixels (V) of the full frame image. The actual object size was able to be calculated by multiplying the actual object size on the camera and the field ratio.

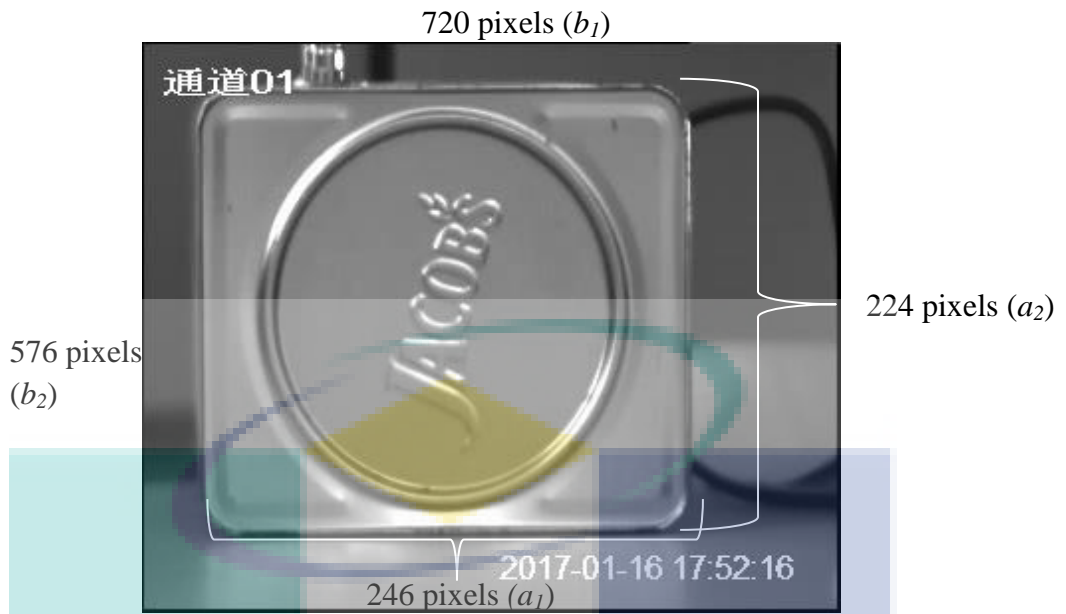


Figure 4.23 Actual object size displayed on the monitor screen with distance, d_2 from camera.

Equation 4.2, Equation 4.3, and Equation 4.4 were used to calculate the actual object size for horizontal (H) and vertical (V). Equation 4.2 shows the ratio of the object size on the screen in pixel b_1 or b_2 , and full frame in pixel a_1 or a_2 .

$$a_1 : b_1 \text{ or } a_2 : b_2 \quad 4.2$$

where,

a_1 = horizontal object size on screen in pixel;

a_2 = vertical object size on screen in pixel;

b_1 = horizontal full frame in pixel;

b_2 = vertical full frame in pixel.

Equation 4.3 used to calculate the actual object size on camera sensor.

$$\text{Actual object size on camera sensor} = \text{ratio of object size on screen in pixel, } b_1 \text{ or } b_2, \text{ and full frame in pixel x camera sensor size } (c_1 \text{ or } c_2) \quad 4.3$$

where,

c_1 = horizontal camera sensor size;

c_2 = vertical camera sensor size.

Equation 4.4 used to calculate the actual size.

$$\text{Actual size} = \text{Actual object size on camera sensor} \times \text{Ratio of distance between camera sensor to lens and lens to object} \quad 4.4$$

The calculated actual size was tabulated in Table 4.5. The actual horizontal and vertical for the object found was 17.4 cm (H) and 14.4 cm (V) respectively.

Table 4.5 Calculated horizontal and vertical size in cm.

d_2 (cm)	Horizontal size (cm)	Vertical size (cm)
200	8.7	7.5
300	8.7	7.5
400	8.6	7.5
500	8.8	7.4
600	8.6	7.5
700	8.7	7.5
800	8.7	7.6
900	8.5	7.5
1000	8.7	7.3

The average value for horizontal size (H) was 8.70 cm and average value for vertical size (V) was 7.50 cm. However, the real size of the object was 17.40 cm (H) and 14.40 cm (V). This clearly shows that calculated horizontal size is twice as smaller than the actual size and calculated vertical size is 1.92 smaller than actual size. This is due to the data lost during the conversion of video from analogue into digital type. To summarise, it is necessary to multiply twice the horizontal value and 1.92 for vertical value for the calculation of the unknown discharge lightning, as indicated in the following sub-topic.

4.4.3.2 Actual Size Calculation

A calculation carried out to identify the actual size of the unknown discharge lightning is presented in this sub-topic. Figure 4.24 demonstrates the location of the unknown discharge activity while Figure 4.25 demonstrates the camera lens and actual field. Furthermore, Figure 4.26 presents the actual view of +CG lightning event from the PC monitor.

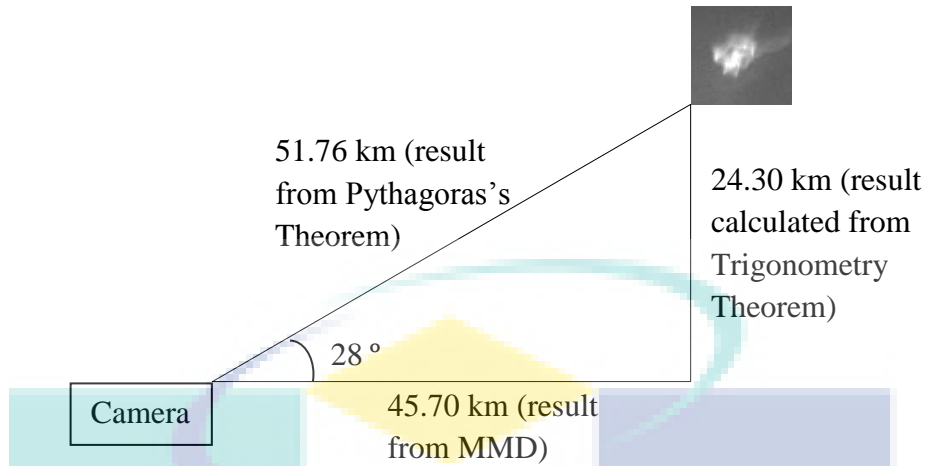


Figure 4.24 Demonstrated location of the unknown discharge lightning.

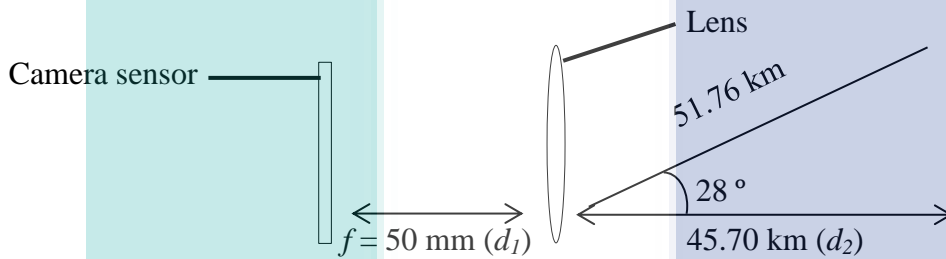


Figure 4.25 Demonstrated camera lens and the actual field.

The 50 mm focal length is the distance between camera sensor to lens, d_1 , and lens to object, d_2 is 45.70 km. By referring to Equation 4.1, the ratio of distance between camera sensor to lens, d_1 and lens to object, d_2 , was identified as 0.914 km mm^{-1} .

The full frame pixel of the image was 720 pixels (H) and 576 pixels (V) while the unknown discharge lightning covered only 23 pixels (H) and 22 pixels (V). An actual size calculation was calculated using Equation 4.2, Equation 4.3, and Equation 4.4.

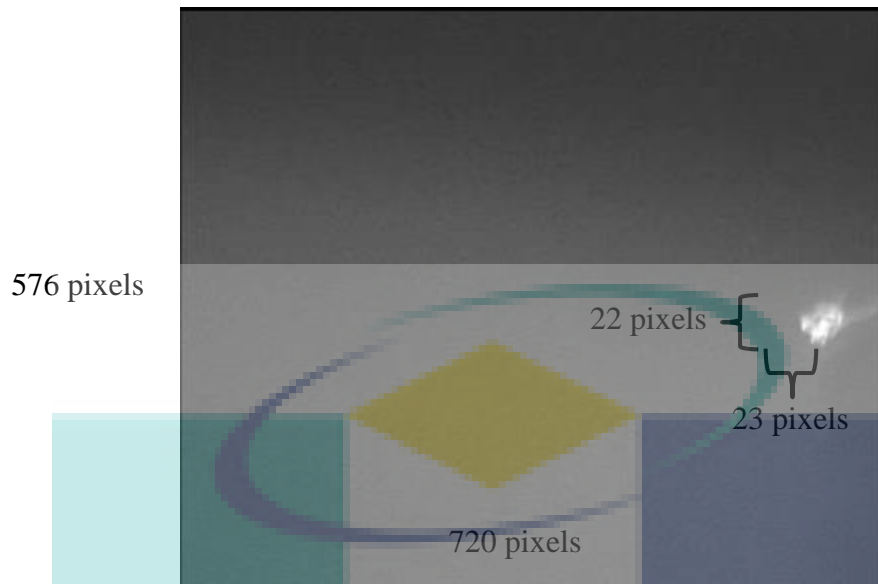


Figure 4.26 Actual view of the +CG lightning event from the PC monitor.

The calculated result as tabulated in Table 4.6.

Table 4.6 Calculated size of the unknown discharge lightning.

Unknown discharge lightning	
Horizontal size (km)	0.37
Vertical size (km)	0.32

Since 0.37 km represents horizontal size. In conclusion, the diameter of unknown discharge lightning is 0.37 km.

4.4.4 Horizon Distance

A calculation of the horizon distance is shown in this subtopic to find out the actual altitude distance from the ground. Figure 4.27 describes the condition of the unknown discharge lightning on the horizon distance where d_0 represents distance from camera to the event taken place which is 45.7 km, R_{earth} represents earth's radius which is 6371 km, α_1 represents the angle of camera shooting upward to the event which is 28° , and h_1 represents horizon distance.

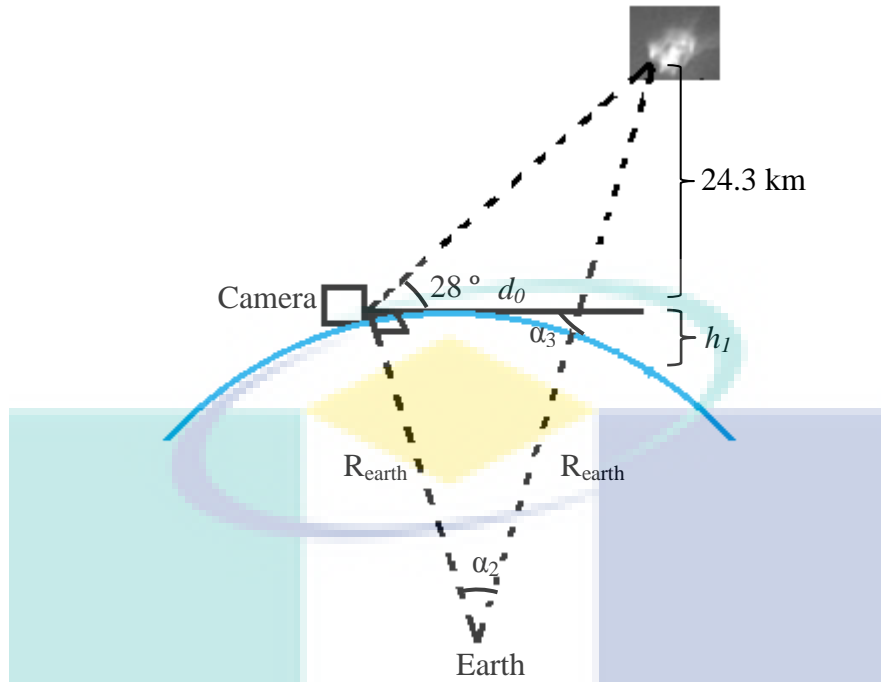


Figure 4.27 Condition of the unknown discharge lightning on the horizon distance.

Equation 4.5 is the Trigonometry Theorem used to find the horizon distance,

h_1 .

$$\tan \alpha_3 = \frac{R_{earth}}{d_0} \quad 4.5$$

$$\tan \alpha_3 = \frac{6371km}{45.7km}$$

$$\alpha_3 = \tan^{-1} 139.41$$

$$= 89.59^\circ$$

Equation 4.6 is to find the angle, α_2 . For a triangle = 180° , hence,

$$\alpha_2 = 180^\circ - 90^\circ - \alpha_3 \quad 4.6$$

$$\alpha_2 = 180^\circ - 90^\circ - 89.59^\circ$$

$$\alpha_2 = 0.41^\circ$$

Equation 4.7 is to find horizon distance, h_1 .

$$\cos \alpha_2 = \frac{R_{earth}}{h_1 + R_{earth}} \quad 4.7$$

$$\cos 0.41^\circ = \frac{6371km}{h_1 + 6371km}$$

$$h_1 = 0.1639 \text{ km}$$

$$h_1 = 163.9 \text{ m}$$

Since the height from the horizon line to the earth surface is small compared to the horizon line to the object, it was deemed negligible. In short, the height of the object is 24.3 km from earth surface.

4.5 Summary

As a summary, chapter 4 explained the result of the finding. Result proven using some calculation especially to find out the size of the unknown discharge lightning event. Data obtained from Malaysian Meteorological Department (MMD) used to determine the exact location of the unknown discharge lightning. Data from MMD prove the relationship between rainfall and lightning event. In short, result explained in details and specific throughout chapter 4.

UMP

CHAPTER 5

CONCLUSION AND RECOMMENDATION

5.1 Conclusion

According to the result obtained from Malaysian Meteorological Department (MMD), the occurrence of positive cloud to ground (+CG) lightning showed a minor percentage which is 21.91% compared to the occurrence of negative cloud to ground (-CG) lightning which was reported at 78.09% from the overall lightning events in the country. The analysis indicated that +CG lightning occurred more frequently at night from July until November during the period of the study. Based on this, nights in the month of July seem to indicate the highest possibility to observe TLEs. November on the other hand has been shown to experience lesser +CG lightning events than July even though the Monsoon season had a huge influence in November. However, the findings show that Monsoon season is not related to lightning event. It only influences the rainfall quantity. An occurrence of lightning event is influenced by the collision of positive and negative static charges. Furthermore, the +CG lightning mostly occurred in the northern area from UMP Pekan as revealed in the yearly lightning map. Hence, the camera should be point to the north direction. In addition, +CG lightning occurs due to the connection of downward-moving positively charged step leaders and the ground which causes a return stroke to occur.

An unknown discharge lightning event was detected at an approximate altitude height of 24.3 km with the intensity of 4.8 kA. The unknown event had taken place at directions of West (270 °) to North-west (315 °) or between Sungai Tulang and Sungai Belat, Gambang, Pahang. It was located 45.7 km from UMP Pekan Campus. The unknown event was compared with the Carrot Sprite

characteristics. The compared result has shown that both had a diameter of less than 1 km and occurred due to a weak +CG flashes produced. The altitude height of the unknown discharge lightning event also ranged from 20 km to 95 km. In a conclusion, the unknown discharge lightning is possibly a Carrot Sprite.

5.2 Recommendation

The camera control and monitoring system can become more effective and simple in future research by adding a few features and functions. The following are possible improvements that can be applied:

- a. Replace the Digital Video Recorder (DVR) to a higher frame rate (fps) feature. The frame rate must at least 100 fps or higher.
- b. Apply online control system to monitor the camera status and observe the sky's condition anytime.
- c. Implement software that can extract frames from the video which contains the lightning event directly.
- d. Use a digital single-lens reflex (DSLR) to observe TLEs, namely by focusing more on their physical characteristics such as colour.

REFERENCES

- Arnone, E., Berg, P., Arnold, N.F., Christiansen, B., Thejll, P., 2008. An Estimate Of The Impact Of Transient Luminous Events On The Atmospheric Temperature. *Adv. Geosci.* 37–43.
- Bailey, M.A., 2010. Investigating Characteristics of Lightning-Induced Transient Luminous Events Over South America. Utah State University.
- Barrington-Leigh, C.P., Inan, U.S., Stanley, M., 2001. Identification of sprites and elves with intensified video and broadband array photometry. *J. Geophys. Res.* 106, 1741.
- Barrington- Leigh, C.P., Inan, U.S., 1999. Elves triggered by positive and negative lightning discharges. *Geophys. Res. Lett.* 26, 683.
- Blaes, P.R., Marshall, R.A., Inan, U.S., 2014. Return Stroke Speed of Cloud-to-Ground Lightning Estimated from Elve Hole Radii. *Geophys. Res. Lett.* 9182–9187.
- Carey, L.D., Rutledge, S.A., Petersen, W.A., 2003. The Relationship between Severe Storm Reports and Cloud-to-Ground Lightning Polarity in the Contiguous United States from 1989 to 1998. *Mon. Weather Rev.* 131, 1211–1228.
- Chen, A.B., Kuo, C.L., Lee, Y.J., Su, H.T., Hsu, R.R., Chern, J.L., Frey, H.U., Mende, S.B., Takahashi, Y., Fukunishi, H., Chang, Y.S., Liu, T.Y., Lee, L.C., 2008. Global distributions and occurrence rates of transient luminous events. *J. Geophys. Res. Sp. Phys.* 113, 1–8.
- Corsetino, M., 2013. Canon EOS 6D Digital Field Guide, Digital Field Guide. Wiley.
- Cummer, S. a., Jaugey, N., Li, J., Lyons, W. a., Nelson, T.E., Gerken, E. a., 2006. Submillisecond Imaging of Sprite Development and Structure. *Geophys. Res. Lett.* 33, L04104.
- Dan Robinson, 1995. How Cloud-to-Ground Lightning Works.
- David Neumeyer (Ed.), 2014. The Oxford Handbook of Film Music Studies. Oxford University Press USA, New York.
- Diffen, 2013. NTSC vs PAL - Difference and Comparison | Diffen. URL http://www.diffen.com/difference/NTSC_vs_PAL (accessed 5.9.16).

- E. M. Wescott, Sentman, D.D., M. J. Heavner, D. L. Hampton, 1998. Observations of “Columniform” Sprites. *J. Atmos. Solar-Terrestrial Phys.* 733–740.
- E.M. Wescott, D.D. Sentman, H.C. Stenbaek-Nielsen, P. Huet, Heavner, M.J. and D.R.M., 2001. New Evidence For The Brightness And Ionization Of Blue Starters And Blue Jets. *J. Geophys. Res.* 106, 549–554.
- Ebert, U., 2012. Thunderstorms As Electron Accelerators And The Discharge Zoo Above The Clouds. *escampig2012.ist.utl.pt* 10–11.
- Ernest McCollough, 1893. *Industry: A Monthly Magazine Devoted to Science, Engineering and Mechanic Arts.*
- Franz, R.C., Nemzek, R.J., Winckler, J.R., 1990. Television Image of a Large Upward Electrical Discharge Above a Thunderstorm System, *Science* (New York, N.Y.). New York.
- Fukunishi, H., Takahashi, Y., Kubota, M., Sakanoi, K., Inan, U.S., Lyons, W. a., 1996. Elves: Lightning- induced transient luminous events in the lower ionosphere. *Geophys. Res. Lett.* 23, 2157.
- Galstian, T. V, 2013. *Smart Mini-Cameras.* Taylor & Francis.
- Haldoupis, C., Amvrosiadi, N., Cotts, B.R.T., van der Velde, O. a, Chanrion, O., Neubert, T., 2010. More evidence for a one-to-one correlation between Sprites and Early VLF perturbations. *J. Geophys. Res. Phys.* 115, n/a.
- Jing, Y., GuiLi, F., 2014. A Gigantic Jet Event over a Summer Storm in China, in: 2014 International Conference on Lightning Protection (ICLP). pp. 1138–1140.
- Kim, H., Jung, J., Paik, J., 2016. Fisheye Lens Camera Based Surveillance System for Wide Field of View Monitoring. *Opt. - Int. J. Light Electron Opt.* 127, 5636–5646.
- Kozak, L. V, Odzimek, A., Volvach, a E., Ivchenko, V.M., Kozak, P.M., Lapchuk, V.P., 2014. Observation and Analysis of Transient Luminous Events in the Earth’s Atmosphere, in: 2014 24nd Int. Crimean Conference “Microwave & Telecommunication Technology” (CriMiCo’2014). Russia, pp. 1087–1088.
- Krehbiel, P.R., Riouset, J. a., Pasko, V.P., Thomas, R.J., Rison, W., Stanley, M. a., Edens, H.E., 2008. Upward Electrical Discharges From Thunderstorms. *Nat. Geosci.* 1, 233–237.

- Lang, T.J., Lyons, W. a., Rutledge, S. a., Meyer, J.D., MacGorman, D.R., Cummer, S. a., 2010. Transient Luminous Events above Two Mesoscale Convective Systems: Storm Structure and Evolution. *J. Geophys. Res.* 115, A00E22.
- Luque, A., Ebert, U., 2010. Lightning above the clouds. *Europhys. News* 41, 19–22.
- Lyons, W. a., Nelson, T.E., Armstrong, R. a., Pasko, V.P., Stanley, M. a., 2003a. Upward Electrical Discharges from Thunderstorm Tops. *Bull. Am. Meteorol. Soc.* 84, 445–454.
- Lyons, W. a., Nelson, T.E., Williams, E.R., Cummer, S. a., Stanley, M. a., 2003b. Characteristics Of Sprite-Producing Positive Cloud-To-Ground Lightning During The 19 July 2000 STEPS Mesoscale Convective Systems. *Mon. Weather Rev.* 131, 2417–2427.
- M. Hayakawa, Y. Hobara, T. Suzuki, 2012. Lightning Effect in the Mesosphere and Ionosphere, in: Cooray, V. (Ed.), *Lightning Electromagnetics*. Institution of Engineering and Technology, London, pp. 611–646.
- Martin A. Uman, 2008. *The Art and Science of Lightning Protect*. Cambridge University Press.
- Martin A. Uman, 1972. Everything You Always Wanted To Know About Lightning But Were Afraid To Ask. *Saturday Rev.* 36–41.
- Mende, S.B., Rairden, R.L., Swenson, G.R., Lyons, W.A., 1995. Sprite spectra; N 2 1 PG band identification. *Geophys. Res. Lett.* 22, 2633–2636.
- National Lightning Safety Institute (NLSI), 1988. World Lightning Activity [WWW Document]. URL http://www.lightningsafety.com/nlsi_info/world-lightning-activity.html (accessed 10.5.14).
- Newsome, R.T., Inan, U.S., 2010. Free-running ground-based photometric array imaging of transient luminous events. *J. Geophys. Res.* 115, A00E41.
- Pasko, V.P., 2010. Recent Advances In Theory Of Transient Luminous Events. *J. Geophys. Res.* 115, A00E35.
- Pasko, V.P., Inan, U.S., Bell, T.F., 1996. Sprites as Luminous Columns of Ionization Produced by Quasi- electrostatic Thundercloud Fields. *Geophys. Res. Lett.* 23, 649–652.
- Pasko, V.P., Stanley, M.A., Mathews, J.D., Inan, U.S., Wood, T.G., 2002. Electrical Discharge From A Thundercloud Top To The Lower Ionosphere. *Nature* 416, 152–154.

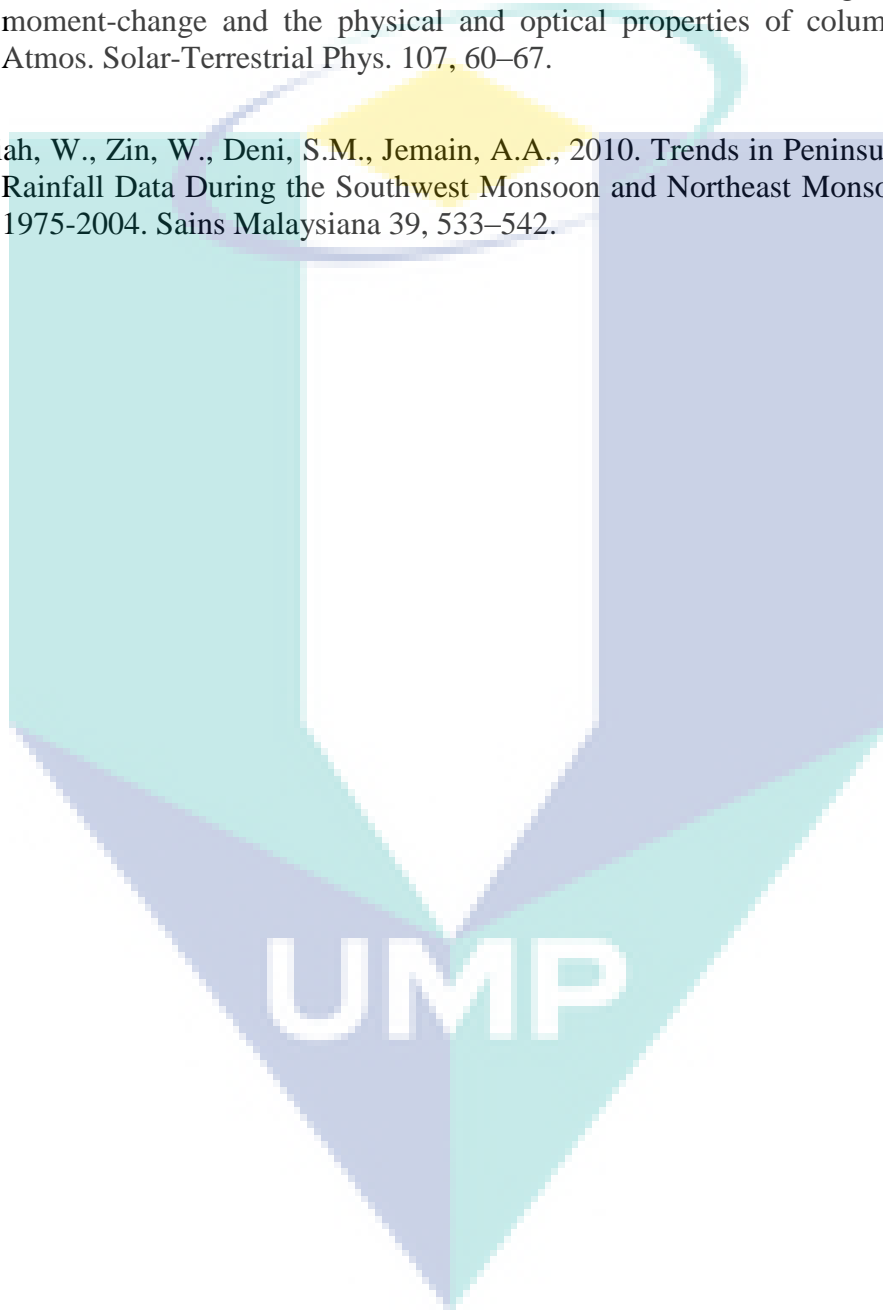
- Pasko, V.P., Yair, Y., Kuo, C.-L., 2012. Lightning Related Transient Luminous Events at High Altitude in the Earth's Atmosphere: Phenomenology, Mechanisms and Effects, *Space Science Reviews*.
- Passas, M., Madiedo, J.M., Gordillo-Vázquez, F.J., 2016. High Resolution Spectroscopy of an Orionid Meteor from 700 to 800 nm. *Icarus* 266, 134–141.
- Passas, M., Sánchez, J., Luque, A., Gordillo-vázquez, F.J., 2014. Transient Upper Atmospheric Plasmas : Sprites and Halos. *IEEE Trans. Plasma Sci.* 1–2.
- Pawar, S.D., Kamra, A.K., 2004. Evolution of Lightning and the Possible Initiation/Triggering of Lightning Discharges by the Lower Positive Charge Center in an Isolated Thundercloud in the Tropics. *J. Geophys. Res.* 109, 1–12.
- Pettegrew, B.P., Market, P.S., Holle, R.L., Demetriades, N.W.S., 2003. Analysis of cloud and cloud-to-ground lightning in winter precipitation.
- Pillman, B., 2010. Camera Exposure Determination Based on a Psychometric Quality Model, in: 2010 IEEE Workshop On Signal Processing Systems. *IEEE*, pp. 339–344.
- Rakov, V.A., 2007. Lightning Return Stroke Speed. *J. Light. Res.* 1, 80–89.
- Rakov, V.A., Uman, M.A., 2003. *Lightning: Physics and Effects*. Cambridge University Press.
- Robert Hirsch, 2012. *Light and Lens: Photography in the Age*, 2nd ed. Focal Press.
- Rocha, R.M.L., Diniz, J.H., Carvalho, a M., Filho, a C., 1999. Cloud-to-ground lightning in southeastern Brazil in 1993.
- Sentman, D.D., Wescott, E.M., Osborne, D.L., Hampton, D.L., Heavner, M.J., 1995a. Preliminary results from the Sprites94 Aircraft Campaign: 1. Red sprites. *Geophys. Res. Lett.* 22, 1205–1208.
- Sentman, D.D., Wescott, E.M., Osborne, D.L., Hampton, D.L., Heavner, M.J., 1995b. Preliminary Results from the Sprites94 Aircraft Campaign: 2. Blue Jets. *Geophys. Res. Lett.* 22, 1205–1208.
- Singh, R., K. Maurya, A., Veenadhari, B., R., S., Gokani, S.A., Cohen, M.B., Chanrion, O., Neubert, T., 2014. First observations of transient luminous events in Indian sub-continent. *Curr. Sci.* 107, 1107–1108.

- Soula, S., Iacovella, F., van der Velde, O., Montanya J., Füllekrug, M., Farges, T., Bór, J., Georgis, J.-F., NaitAmor, S., Martin, J.-M., 2014. Multi-instrumental Analysis of Large Sprite Events and Their Producing Storm in Southern France. *Atmos. Res.* 135–136, 415–431.
- Soula, S., van der Velde, O., Montanya, J., 2012. Optical Observations and Conditions of Production of Transient Luminous Events (Sprites, Elves, Gigantic Jets), in: 1st TEA - IS Summer School. Spain.
- Soula, S., van der Velde, O., Montanya J., Neubert, T., Chanrion, O., Ganot, M., 2009. Analysis Of Thunderstorm And Lightning Activity Associated With Sprites Observed During The EuroSprite Campaigns: Two Case Studies. *Atmos. Res.* 91, 514–528.
- Su, H.T., Hsu, R.R., Chen, a B., Wang, Y.C., Hsiao, W.S., Lai, W.C., Lee, L.C., Sato, M., Fukunishi, H., 2003. Gigantic Jets Between A Thundercloud And The Ionosphere. *Nature* 423, 974–976.
- Suzuki, T., Hayakawa, M., Hobara, Y., Kusunoki, K., 2011. Summer Thunderstorm Associated With Cluster Of Blue Jets And Starters In Japan. *Nssl.Noaa.Gov* 15–20.
- Uman, M.A., 1994. Natural Lightning. *IEEE Transactions Ind. Appl.* 30, 785–790.
- van der Velde, O., 2008. EuroSprite: Winter Sprites and Elves Over the Bay of Biscay. *EuroSprites*.
- Wescott, E.M., Sentman, D.D., Heavner, M.J., Hampton, D.L., Osborne, D.L., Vaughan, O.H., 1996. Blue Starters: Brief Upward Discharges From An Intense Arkansas Thunderstorm. *Geophys. Res. Lett.* 23, 2153–2156.
- Wescott, E.M., Sentman, D.D., Heavner, M.J., Hampton, D.L., Vaughan, O.H., 1998. Blue Jets: Their Relationship To Lightning And Very Large Hailfall, And Their Physical Mechanisms For Their Production. *J. Atmos. Solar-Terrestrial Phys.* 60, 713–724.
- Williams, E.R., 1987. The Electrification of Thunderstorms. *Sci. Am.* 259, 88–99.
- Wood, L., 2004. NTSC, PAL, and SECAM Overview, in: *Video Demystified. A Handbook for the Digital Engineer (Demystifying Technology)*. Germany, pp. 247–373.
- Yair, Y., Price, C., Israelevich, P., Devir, A., Ziv, B., 2004. New Observations of Transient Luminous Events from the Space Shuttle during the MEIDEX. *EMC'04/Sendai 4E2-1*, 917–920.

Yair, Y., Rubanenko, L., Mezuman, K., Elhalel, G., Pariente, M., Glickman-Pariente, M., Ziv, B., Takahashi, Y., Inoue, T., 2013. New Color Images Of Transient Luminous Events From Dedicated Observations On The International Space Station. *J. Atmos. Solar-Terrestrial Phys.* 102, 140–147.

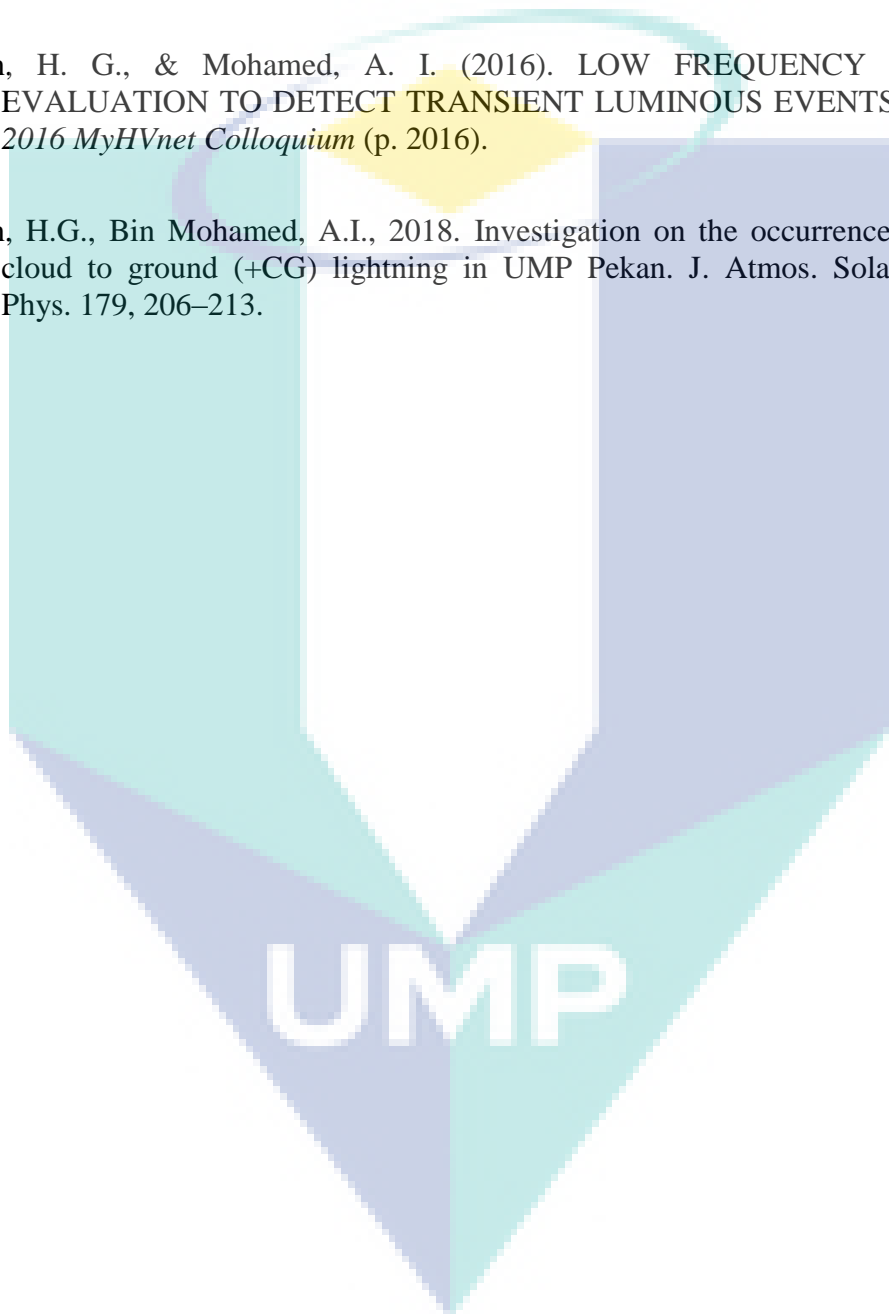
Yaniv, R., Yair, Y., Price, C., Bór, J., Sato, M., Hobara, Y., Cummer, S., Li, J., Devir, A., 2014. Ground-based observations of the relations between lightning charge-moment-change and the physical and optical properties of column sprites. *J. Atmos. Solar-Terrestrial Phys.* 107, 60–67.

Zawiah, W., Zin, W., Deni, S.M., Jemain, A.A., 2010. Trends in Peninsular Malaysia Rainfall Data During the Southwest Monsoon and Northeast Monsoon Seasons: 1975-2004. *Sains Malaysiana* 39, 533–542.



APPENDIX A
LIST OF PUBLICATION

- Chan, H. G., Jadin, M. S., & Mohamed, A. I. (2015). OBSERVATION OF TRANSIENT LUMINOUS EVENTS (TLEs) IN PEKAN. *ARPN Journal of Engineering and Applied Sciences*, 10(22), 10716–10721.
- Chan, H. G., & Mohamed, A. I. (2016). LOW FREQUENCY ANTENNA EVALUATION TO DETECT TRANSIENT LUMINOUS EVENTS (TLEs). In *2016 MyHVnet Colloquium* (p. 2016).
- Chan, H.G., Bin Mohamed, A.I., 2018. Investigation on the occurrence of positive cloud to ground (+CG) lightning in UMP Pekan. *J. Atmos. Solar-Terrestrial Phys.* 179, 206–213.



**APPENDIX B
TECHNICAL DATA SHEET**



WAT-902H 2 / 3 ULTIMATE

SPECIFICATIONS

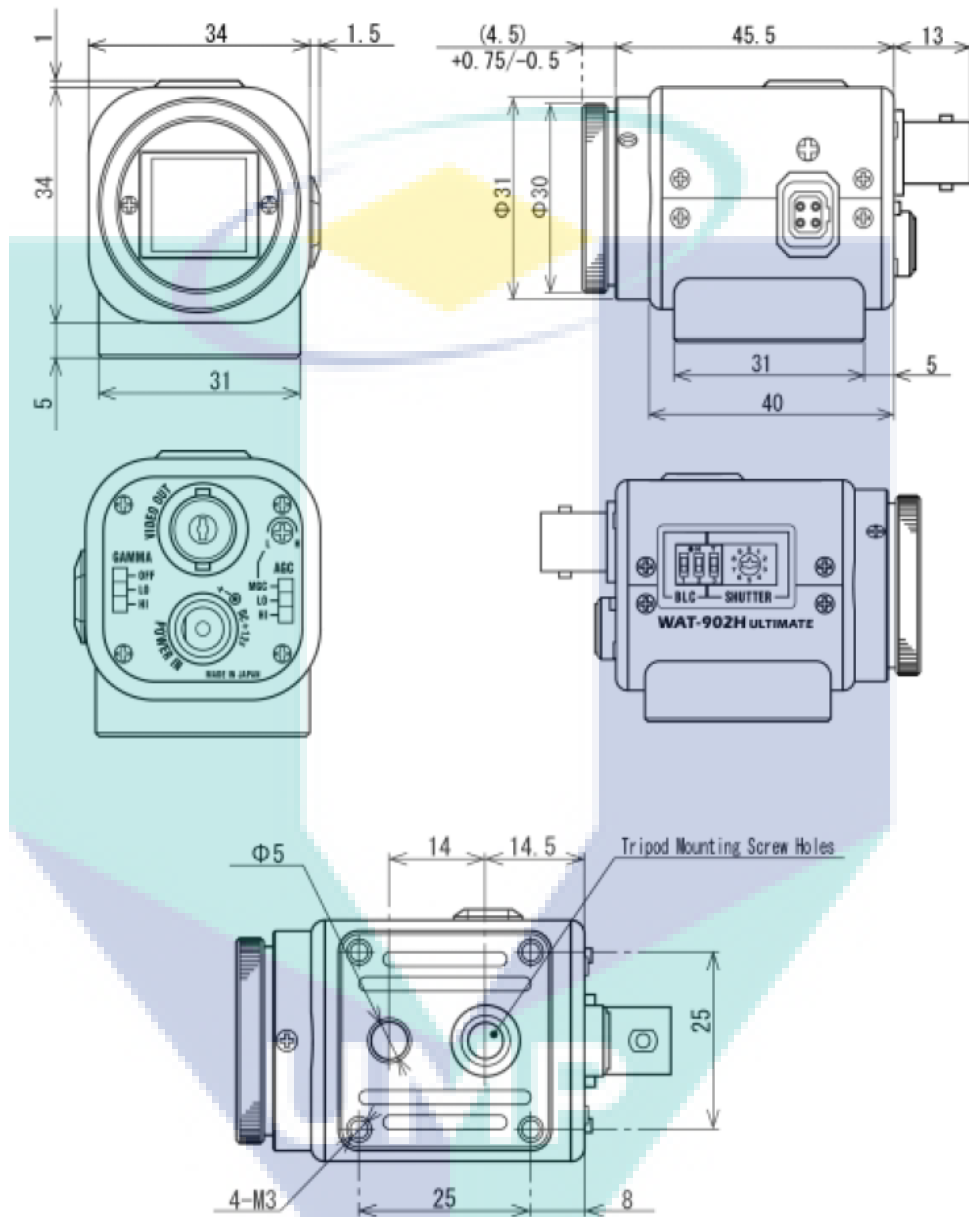
Model	WAT-902H2 ULTIMATE (EIA)	WAT-902H2 ULTIMATE (CCIR)
Pick-up element	1/2" interline transfer CCD image sensor	
Number of total pixels	811(H) × 508(V)	795(H) × 596(V)
Number of effective pixels	768(H) × 494(V)	752(H) × 582(V)
Unit cell size	8.4um(H) × 9.8um(V)	8.6um(H) × 8.3um(V)
Shutter speeds	EI1: 1/60 sec. - 1/100000 sec. EI2: 1/100 sec. - 1/100000 sec. FL: 1/100 sec. OFF: 1/60 sec.	EI1: 1/50 sec. - 1/100000 sec. EI2: 1/120 sec. - 1/100000 sec. FL: 1/120 sec. FL: 1/50 sec.
	1/250, 1/500, 1/1000, 1/2000, 1/5000, 1/10000, 1/100000 sec.	
Minimum illumination	0.0001 lx. F1.4	

Model	WAT-902H3 ULTIMATE (EIA)	WAT-902H3 ULTIMATE (CCIR)
Pick-up element	1/3" interline transfer CCD image sensor	
Number of total pixels	811(H) × 508(V)	795(H) × 596(V)
Number of effective pixels	768(H) × 494(V)	752(H) × 582(V)
Unit cell size	6.35um(H) × 7.40um(V)	6.50um(H) × 6.25um(V)
Shutter speeds	EI1: 1/60 sec. - 1/100000 sec. EI2: 1/100 sec. - 1/100000 sec. FL: 1/100 sec. OFF: 1/60 sec.	EI: 1/50 sec. - 1/100,000 sec. EI2: 1/120 sec. - 1/100000 sec. FL: 1/120 sec. FL: 1/50 sec.
	1/250, 1/500, 1/1000, 1/2000, 1/5000, 1/10000, 1/100000 sec.	
Minimum illumination	0.0002 lx. F1.4	

Common specifications	
Synchronizing system	Internal sync.
Video output	1Vp-p, 75ohms, unbalanced
Resolution (H)	570TVL (Center)
SN ratio	More than 50dB (AGC OFF)
AGC	①HI: 5-60dB ②LO: 5-32dB ③MGC(5-60dB)
Back light compensation	①OFF(Default) ②Center ③Lower ④Center + lower
Gamma correction	①HI ($\gamma \approx 0.35$) ②LO ($\gamma \approx 0.45$) ③OFF ($\gamma \approx 1$)
Power supply	DC12V ± 10%
Power consumption	1.32W (110mA)
Operating temperature	-10°C - +40°C
Storage temperature	-30°C - +70°C
Dimensions(W×H×L)	35.5 × 40 × 63 (mm)
Weight	approx. 98g

Design and specifications are subject to change without notice.

DIMENSIONS (mm)



Technical Specification Data Sheet

The Nikon logo is displayed in a bold, black, sans-serif font. It is positioned below a yellow rectangular graphic that features several white diagonal lines radiating from the top-left corner, creating a sense of motion or light rays.

Model: Nikon AF Nikkor 50 mm f/1.4 D	
Focal Length	50 mm
Maximum Aperture	f/1.4
Minimum Aperture	f/16
Lens Construction	7 elements in 6 groups
Picture Angle	46° [31° 30' with Nikon digital Cameras (Nikon DX format)]
Closest Focusing Distance	0.45 m / 1.5 ft.
Maximum Reproduction Ratio	1/6.8
No. of Diaphragm Blades	7
Filter / Attachment Size	52 mm
Diameter x Length (extension for lens mount)	Approximately 64.5 x 42.5 mm or 2.5 x 1.7 in.
Weight	Approximately 230 g / 8.1 oz.
Supplies Accessories	52 mm Snap-on front lens cap

Features:

1. f/1.4 high-speed normal lens.
2. Compact and lightweight.
3. Provides high-contrast image even with maximum aperture.
4. Ideal for travel and full-length portraits in available light.

Lens Construction:



Source:

http://imaging.nikon.com/lineup/lens/singlefocal/normal/af_50mmf_14d/

Technical Specification Data Sheet

brinno
brilliant innovation



BCS 24-70

Brinno Lens
24-70mm F1.4

User Manual

brinno

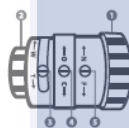
1. Package contents



- ① Brinno Lens 24-70 mm F1.4 (BCS 24-70) x 1
- ② Lens Bag x 1
- ③ IR Filter x 1
- ④ IR Filter case x 1
- ⑤ User manual x 1

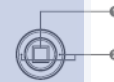
2. Parts of device

Brinno Lens



- ① Top cover
- ② Bottom cover
- ③ Zoom
- ④ Aperture
- ⑤ Focus

IR Filter



- ① Glass
- ② Driving Holes

3. Installation

3-1 To remove the current lens kit(BCS 019) from TLC200 Pro



a. Turn TLC200 Pro face down to the floor to protect against dust getting on the sensor. **b.** Rotate counter-clockwise to unlock the BCS 019.

3-2 To Install IR Filter on TLC200 Pro



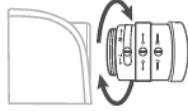
a. Rotate lens upwards, then place the IR filter horizontally. **b.** Screw in IR filter with fingers. **c.** Insert the screwdriver* from TLC200 Pro into one of the driving holes, turn clockwise until tight.

* For more information, please refer to the TLC200 Pro manual page 5(Package Content).

⚠ IR Filter works with BCS 019, BCS 18-55 and BCS 24-70. It's recommended to keep IR Filter on TLC200 Pro.

3. Installation

3-3 To Install Brinno Lens (BCS 24-70) on TLC200 Pro

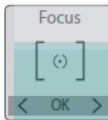


Remove the bottom lens cover and turn the BCS 24-70 clockwise to install the lens on the TLC 200 Pro.



Be careful when using different lens, the TLC200 Pro may tip over due to the gravity center shift especially without batteries.

4. Focus Adjustment



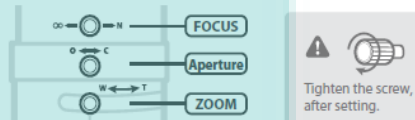
Adjust the lens focus

Go to the "Focus" menu (Time Lapse Camera TLC200 Pro), see the enlarge preview screen. Rotate the lens to focus object.



For more information, please refer to TLC200 Pro manual page 16.

Manully set up



5. Specification

MODEL	BCS 24-70
MOUNT TYPE	CS-mount
FOCAL LENGTH	24-70 mm
APERTURE	F1.4 ~ 2.4
ANGLE OF VIEW	94 ~ 38°
FOCUS DISTANCE	Tele 1cm ~ ∞ Wide 10cm ~ ∞
SIZE	Ø32x40 mm
WEIGHT	61 g

To Insure Long Term Use



DUST



FINGERPRINT



Avoid to storing the lens in high-temperature, high-humidity locations.

Thank you for purchasing Brinno Time Lapse Camera Accessories!

If you have any questions or problems setting up your Brinno TimeLapse Camera please contact the sales staff where you purchased our product or email us at Brinno Incorporated directly: customerservice@brinno.com

brinno
brilliant innovation

7F, No.75, Zhou Zi St., Taipei City 11493, Taiwan
Phone:+886-2-8751-0306 Fax:+886-2-8751-0549
customerservice@brinno.com

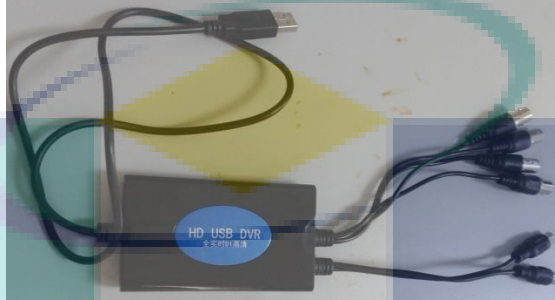
301-0065-00 (EN A1)

Source: https://www.bhphotovideo.com/c/product/1021210-REG/brinno_bcs_24_70_cs_24_70mm_f_1_4_lens.html

UMP

Technical Specification Data Sheet

USB DVR



Model: HD USB 2.0	
Video Input	4 channels
Audio Input	2 channels
Video Standard	PAL / NTSC
Resolution	352 x 288 / 704 x 576
Maximum Frame Rate per Channel	25 fps (PAL) / 30 fps (NTSC)
Data Format	MPEG4
Screen set	Resolution 1024 x 768
Colour Quality	16 bits / 32 bits
USB Port	2.0

UMP

Technical Specification Data Sheet



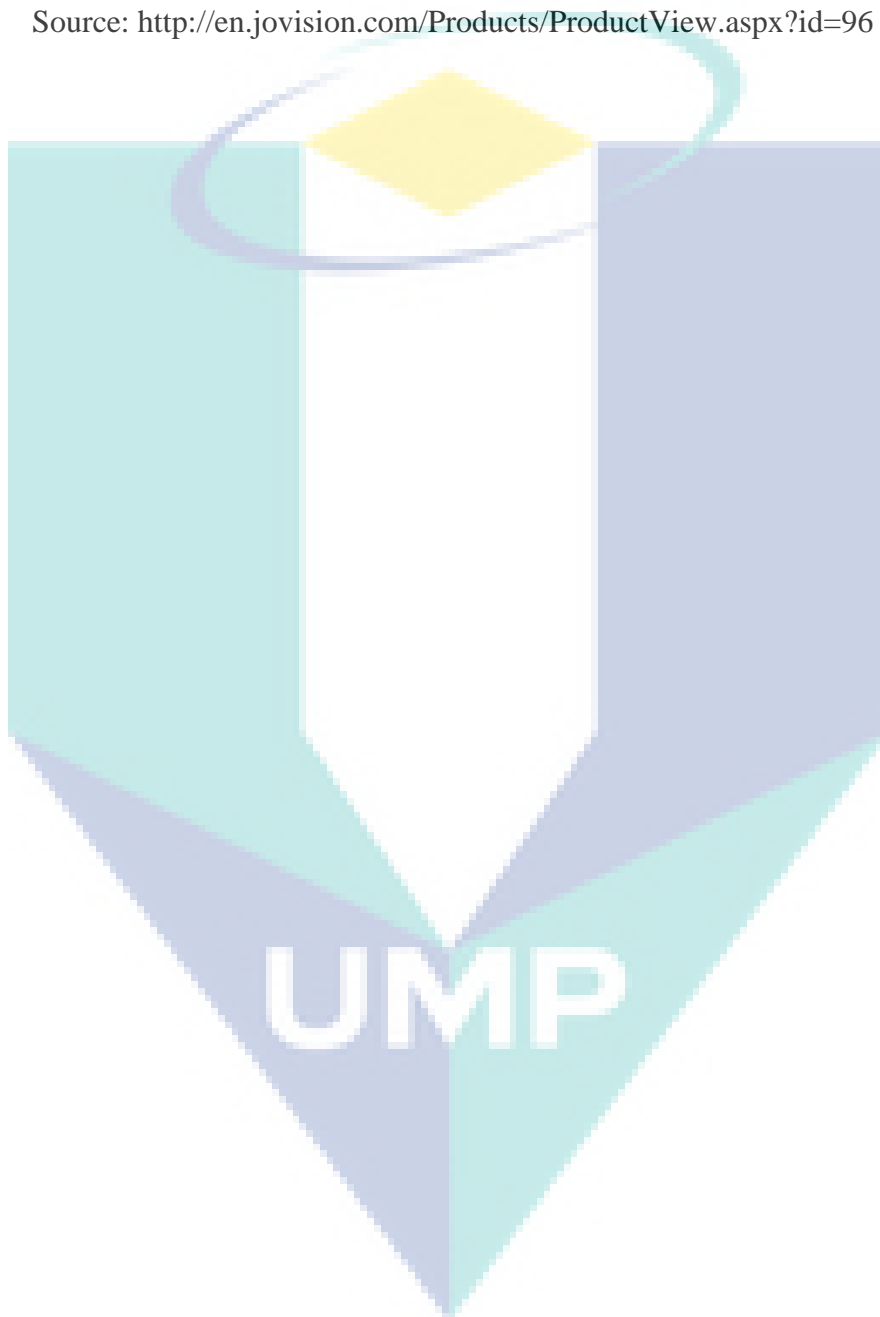
Model: JVS-C300Q	
Video Input	4 channels
Audio Input	4 channels
Video Standard	PAL / NTSC
Video Compression	H.264
Previewing Resolution	4 channel: PAL (D1: 704*576 WD1: 960*576) NTSC (D1: 640*480 WD1: 960*480)
Playback Resolution	4 channel: PAL (D1: 704*576 WD1: 960*576) NTSC (D1: 640*480 WD1: 960*480)
Previewing fps	4 channel: PAL:12.5 fps / NTSC: 15 fps
Playback fps	4 channel: PAL:12.5 fps / NTSC: 15 fps
Compression Bit Rate	16K~2Mbps adjustable
Sampling Capacity	10 bit
Power Consumption	Less than 3W
Video Input Interface	BNC port
Audio Input Interface	RCA port
USB DVR Interface	USB port

Features:

1. With functions of Privacy Masking, Motion Detection, E-mail alert, etc.
2. Supports remote view through IE.
3. Supports CV, CC, WebCC for remote view
4. Supports iPhone, iPad, Android Phone, etc.
5. Previewing resolution WD1 or D1 and compression resolution can be WD1, D1, WCIF, or CIF.
6. Video preview applied the DirectDraw technology and video compression standard is H.264.
7. Applies the newly developed CloudSEE transmission platform.
8. Adopts new coding and decoding technology with excellent performance.

9. Using the newly designed UI (User Interface).
10. Applies USB 2.0 interface, and compatible to various PC and laptop.
11. Supports PAL and NTSC.
12. With function of Dual-stream.

Source: <http://en.jovision.com/Products/ProductView.aspx?id=96>



Technical Specification Data Sheet



Model: Easy USB DVR (UU)	
Video / Audio Channel	4 channels video & 4 channels audio
Video Format	PAL / NTSC
Audio Format	4-CH
Data Format	H.264
Network Support	TCP / IP, UPNP
Frame Rate	4-CH 100 fps (PAL) / 120 fps (NTSC)
Resolution	Maximum 1920 x 1080 pixel
Support Music Format	MP3, WMA, AAC, WAV, OGG, AC3, DDP, TrueHD, DTS, HD, FLAC, APE
Support Media Format	MPEG, TS, VOB, ISO, ASF, FLV, DAT, MPG, AVI, WMV, MKV, MOV, RM, RMVB
Support Decoder Format	HD MPEG 1/2/4, H.264, HD AVC/VC-1, RM/RMVB, Xvid/DivX3/4/5/6, RealVideo 8/9/10
Support Photo Format	HD JPEG, BMP, GIF, PNG, TIFF
Mobile Terminal Support	iPhone, iPad, Android
Web Support	IE browser remote surveillance

Features:

1. 100% new and high quality.
2. Very convenient and practical.
3. Support Windows 7, Windows XP.
4. Specially developed for the USB interface.
5. Supports 4-channel real-time video input.
6. Elegant black appearance and small volume, and easy to carry.
7. Suitable for monitoring small systems or using a notebook computer to conduct monitoring.

Source: <http://www.ebay.com/itm/4CH-USB-2-0-DVR-Security-Video-Audio-Recorder-H-264-Camera-System-Capture-Card-/351467711258?hash=item51d51bab1a:g:XFIAAOSwjVVVudSV>